Ca^{2+}-signalling-based Molecular Communication Systems Towards Nanomedicine Development

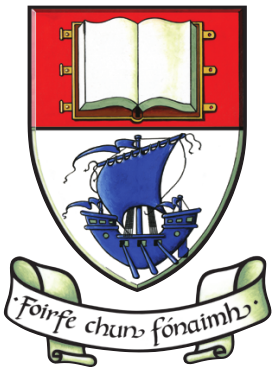

Michael Taynnan Barros, M.Sc.

School of Science and Computing

Waterford Institute of Technology

This dissertation is submitted for the degree of

Doctor of Philosophy

Supervisors: Dr. Sasitharan BALASUBRAMANIAM
Dr. Brendan JENNINGS

May 2016

Contents

Declaration

I hereby certify that this material, which I now submit for assessment on the programme of study leading to the award of Doctor of Philosophy, is entirely my own work and has not been taken from the work of others save to the extent that such work has been cited and acknowledged within the text of my work.

Signed:..... ID: 20056918

Ca^{2+}-signalling-based Molecular Communication Systems Towards Nanomedicine Development

M. T. Barros

Abstract

Nanomedicine is an attempt to revolutionize current methods for diagnosing, treating and preventing diseases that integrates fields such as molecular biology, biotechnology as well as nanotechnology. One envisioned application is sensing and actuation capabilities at the molecular scale using nano scale devices, namely nanomachines. While numerous examples of these applications have been tested *in vivo*, the real deployments are far from reality. This is mainly due to limitations in controlling as well as monitoring their performance. At the same time, the miniature scale of nanomachines means their computational capabilities are also limited. However, integrating communication and networking functionalities can provide new opportunities for sensing and actuation applications of nanomachines. One form of communication that has been recently appointed to realise this vision is Molecular Communication. Many natural molecular communication systems are found inside the human body. The current challenge is to utilise these natural systems to create artificial biocompatible communication networks that can interconnect multiple nanomachines. Such nanonetworks can represent a new type of communication network that can also be connected to the Internet, enabling fine granular sensing deep inside the organs and tissues inside the human body. This new vision is defined as the *Internet of Bio-Nano Things* (*IoBNT*).

The focus of this thesis is on developing artificial molecular communication systems for cellular tissues inside the human body. A model and analysis of a Ca^{2+}-signalling-based molecular communication system for embedded nanomachines is proposed. A mathematical framework was developed for 3D tissues of different types of cells that communicate using Ca^{2+}-signalling, where this framework integrates the gap junction behaviour as well as

the physiological properties that can affect the communication behaviour. The framework analyses the end-to-end capacity, molecular delay, as well as molecular gain for the different types of tissues. Since cellular tissues are flexible body, the communication process is also modelled considering deformation and structural changes. The thesis also presents communication protocols from wireless communication networks applied to the Ca^{2+}-signalling-based molecular communication system. This includes development of protocols, where channel impairments such as noise and poor information capacity were overcome using communication-by-silence theory in order to improve the end-to-end data rate for "On-Off Keying" modulation. The thesis also focuses on applications of the Ca^{2+}-signalling-based molecular communication system. Firstly, a channel state detection/inference technique that provides information about the current cellular tissue conditions was designed, termed Molecular Nanonetwork Inference Process. The inference process utilizes a simple machine learning algorithm to learn and infer various metrics including the types of deformation, estimated locations of the nanomachines, as well as the concentration of Ca^{2+} ions used by the transmitters. The second application is based on modelling the tripartite synapse, and focuses particularly on astrocyte cells using Ca^{2+}-signalling to communicate and provide upkeep to the neuronal networks. A feed-forward feedback control technique has been proposed to control synaptic quality in the tripartite synapses molecular communication channel, and this includes regulating the quantity of Ca^{2+} concentration within the cytosol in order to prevent any dangerous levels that can lead to diseases. At the same time, the feed-forward feedback control model is also used for molecular communication systems in order to prevent excessive noise within the channel, while maintaining decent data rate performance.

Creating artificial communication systems that are embedded into the tissue, can lead to new forms of *smart tissues* that play a major role for future IoBNT vision.

I dedicate this to myself!
For facing all my fears,
and reaching my dream!
Well done mate!

"Achievement of your happiness
is the only moral purpose of your life,
and that happiness, not pain or
mindless self-indulgence, is the proof of
your moral integrity, since it is the
proof and the result of your loyalty to
the achievement of your values." Ayn Rand

Acknowledgment

First I would like to thank the people who made this thesis possible...

I have a deep gratitude and appreciation for both of my supervisors, for teaching me research "stuff" that transcended my life! Your passion and your vision, Sasi, has aligned with my ambition and pushed me to bring out the best in me. Your hard work ethics and perfectionism has taught me that high level skill set is mainly achieved by hard work and persistence, talent is useless if no action is taken. Brendan, your critical thinking and precision has taught me that high level of research is only reached with maturity. You have to take a step back to move two steps forward. Such valuable lessons are more important than any technical advice because it shaped my core, my mindset... a teaching that won't ever be lost! I consider both of you my lifetime friends!

I thank my beloved family. Marinaldo, Jussara, Larrisa and Nana, you were with me at all times!

I thank my crazy friends. Radhika, Stepan, Mandy, Gareth, Kriti, Conor, Aaron and many others that made my Waterford journey a lot more pleasant! And you are always welcome to be my company!

Many thanks to all my TSSG colleagues, for the immeasurable help, for the laughs, and for the advices. TSSG is a great place to work that I was blessed to be part of it during these years.

Nobody should be scared of sad or disappointing moments, because they are the closet to a certain better next day. I came across *Real Social Dynamics* at the worst moment in my PhD. I have no words to describe the work that Tyler (Owen Cook) and his crew has made on my life. The impact of your life teaching in my life enabled me to be on the path towards the person I always wanted to be, but somehow I prevented myself from going for it. Thanks for your love towards the world!

Inspiration plays a big role in my life, and there are always people that I look up to. So, thanks for the inspiration: George Cantor, Nicola Tesla, Michael Faraday, Isaac Newton, Marie Curie, Alan Turing and Claude Shannon.

Music is also a big part of my life, and during these 4 years I was always listening to a bunch of bands, so I need to praise the work from: Gojira, Metallica, Megadeth, U2, As I Lay Dying, Tremonti, Alter Bridge, Two Doors Cinema Club, The Killers, Arctic Monkey, Killswitch Engage and many others...

"So here we go, heroes or ghosts..."

List of Figures

List of Tables

Chapter 1

Introduction

Communication is an inherent function that has evolved with humans and is a major driving factor for numerous natural processes that has led to world development that stands today. For example, cognitive-based communication systems have enabled constant human development, from speech to written and voice communication, and most recently, multi-perceptual communication. These advancements are shaping our times of the information era, where our lives are embedded deep into the communication environment that we live. This has played a major role in numerous fields such as healthcare, where Information and Communication Technology (ICT) have been proposed to enable more efficient diagnosis, treatment and prevention of diseases. However, the current communication systems infrastructure for healthcare monitoring fails in providing accurate medical information leading to poor decision making. A new communication paradigm has recently been proposed aiming to achieve high levels of accuracy by providing medical information at the molecular level. This new paradigm is termed **Molecular Communication**, and is expected to transform medicine, in particular nanomedicine, as well as the healthcare industry.

Molecular communication systems have always existed naturally both within the human body as well as the environment. Biologists have developed mathematical and statistical tools for modelling and analysing such systems for more than 100 years. The knowledge

obtained from those studies have enabled scientific evolution towards using biological systems, e.g., living organisms or derivatives thereof, to create a wide range of innovative products. This field is called biotechnology, and runs in parallel with other interdisciplinary fields, such as bioengineering and biomedical engineering. The field of nanotechnology has taken biotechnology to the next level. Limitations in diagnosis, treatment and prevention of diseases are being eliminated by the usage of nanomaterials and nanoparticles [1][2][3]. As an example, *Co-polymer poly(lactic-co-glycolic acid)* (*PLGA*) has been developed for many years and has been approved by the *US Food and Drug Administration* (FDA) for the use in drug delivery, diagnostics and other clinical applications including cardiovascular disease and cancer treatment, as well as vaccine and tissue engineering. This research area is known as **nanomedicine**, and a complete transformation in medicine is expected in the near future.

Nevertheless, the access and control of biological systems at the molecular level is a great challenge. Nanotechnology alongside with nanomedicine alone is not capable of providing a complete solution. Limitations in modern nanotechnology are in providing a value chain solution that can see technology be realised in practical nanomedicine. For example, researchers have proposed the development of miniature devices, either biological or synthetic, that can not only measure molecular information but actuate upon it, namely *nanomachines*. These embedded nanomachines although can perform certain functionalities, are very limited due to their computational capabilities. However, integrating communication and networking capabilities for information exchange locally and globally inside the human body will further enhance their potential applications, and provide an avenue towards deploying them for practical use. Molecular Communication has appeared as the ideal enabler for that, and its role in information exchange between nanomachines at the nano/molecular scales will allow nanomedicine [3] to reach its potentiality.

The **Internet of Bio-Nano Things**, is a vision where a huge network of nanomachines will communicate with each other and/or an external gateway for providing nanomedicine

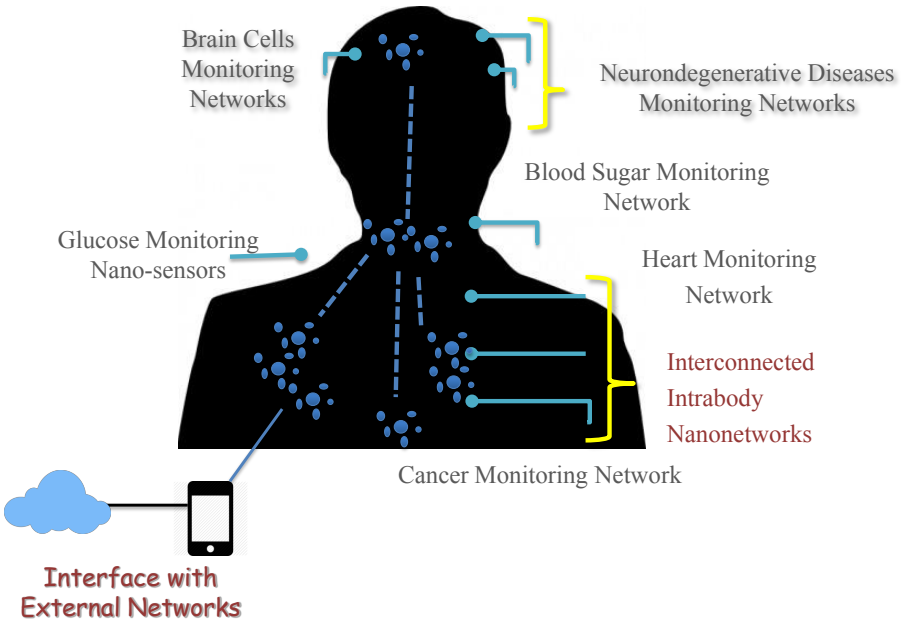

Fig. 1.1 IoBNT scenario and connection of different nanonetworks inside the human body. This vision will enable numerous application as described in the figure.

envisioned functionalities, including: real-time monitoring, fast actuation at the molecular level, fast disease treatment, intelligent drug delivery, tissue engineering and many others. The envisioned scenario is presented in Figure 1.1, and consists of many networks within the human body that will be responsible for different medical tasks, including: neurodegenerative diseases, heart, cancer and glucose monitoring. The presented vision is going to be based on an interdisciplinary research field involving molecular communication, biotechnology and nanomedicine. Healthcare is a major industry for the modern society, and evidently any research in that topic has the potential impact to affect millions of people and generate large revenue for a number of industries. Based on this, IoBNT can bring along new forms of real-time health monitoring and response resulting in improved life quality and expectancy.

Currently such technology is only at the early stage of development and many challenges are faced by the community. Two major challenges are classified: IoBNT theory development and IoBNT realization. A plurality of molecular communication systems exists inside the human body, many of which have not been fully understood or modelled; those which are

modelled have limited analysis on their full functional behaviour. A complete IoBNT theory development is still on its way, and it is very important for addressing the next challenge, which is IoBNT realization. This challenge lies in the development of nanomachines and its interoperability within the human body. At the same time the capabilities of engineering information transfer between these nanomachines to suit various applications remains to be investigated before a full IoBNT solution can be realised.

1.1 Path towards using molecular communication in nanomedicine

As previously introduced, molecular communication enables information transmission at the molecular/nano scales. This will allow future nanomachines that have communication capabilities to perform more complex tasks cooperatively as well as providing connections between different types of *nanonetworks*. This is the central vision for the foundation of IoBNT. The long term vision of IoBNT is to have nanonetworks inside the human body working cooperatively using the envisioned communication platform, and connect to the cloud to provide a new form of fine granular personal health monitoring solution [4][5][6].

Since the birth of this new field, three main backbone nanonetworks were defined: nervous nanonetwork, cardiovascular nanonetwork and also endocrine nanonetwork. These networks were identified as long range molecular communication systems within the human body.

The nervous nanonetwork provides a communication infrastructure based on the neural-spike signalling. This relies on the natural neuronal nanonetwork inside the human body, which consists of the central nervous network and the peripheral nervous network. Differently, cardiovascular nanonetwork is based on the circulatory system for transmitting information

through the blood cells. Finally, the endocrine network relies on the glands that emit hormones as part of their communication process.

Although the modelling of these long range molecular communication have been studied extensively, they are not sufficient for the development of IoBNT. A major requirement is integrating short range molecular communication that will connect to the ends of the long range molecular communication [7]. However, short range nanonetworks still need intense research work especially due to their complex behaviour at the molecular scale. For example, communication systems inside the cellular tissues enable short range communication between the cells, but there are no solutions that address how they can be integrated to long range.

Capitalizing on the need for short-range nanonetworks communication systems, and in parallel, aiming to provide novel healthcare applications, the focus on this thesis in on developing molecular communication systems and their protocols within cellular tissues. In the next subsections, the definition of a molecular communication system as well as state-of-the-art review, challenges, limitations and objectives of the research work will be presented.

1.1.1 Generic Model of a Molecular Communication Systems

Molecular communication systems are the primary choice to perform communication between nanomachines within biological environments. Nanomachines are defined as biological or synthetic entities capable of performing limited computation, sensing and/or actuation at the nanoscale [8]. They have the size of a macromolecule ($100\mu m$). Few approaches are currently being proposed for the design of nanomachines [8]. However, its realization is not practical at the current level of available technology [5].

A generic model for a molecular communication system is defined in Fig. 1.2. Based on the telecommunication system model, it has five components: encoding, transmission, propagation, reception and decoding. These components are organized into three main

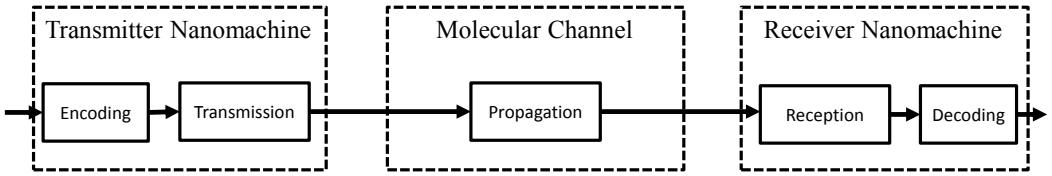

Fig. 1.2 Communication system based on a transmitter nanomachine, a molecular channel and a receiver nanomachine. The transmitter nanomachine is responsible for encoding and transmission of information. The molecular channel is responsible for propagating the information molecules. Finally, the receiver nanomachine is responsible for receiving and decoding the information.

blocks: a transmitter nanomachine, a molecular channel and a receiver nanomachine. These three blocks are further explored in the following subsections.

1.1.1.1 Transmitter Nanomachine

The transmitter nanomachine (or source nanomachine) is responsible for encoding information into molecules and releasing it to the environment. There exists many different encoding approaches and they rely on the properties of the cells. As an example, the commonly used approach is the concentration modulation technique, in which information is encoded into the concentration of specific molecules that are released into the channel.

1.1.1.2 Molecular Channel

The molecular channel is the medium in which information molecules propagate from a transmitter nanomachine to a receiver nanomachine. The propagation process can be performed in two different ways:

1. *Passively:* Information molecules are propagated solely based on the characteristics of the medium. One form of this molecular channel is the diffusion process, and an example is Ca^{2+} signalling. This form of communication is the focus of this thesis.

2. *Actively:* This form of molecular channel involves an agent/organism that picks up the information molecules from the transmitter nanomachine and delivers it to the receiver nanomachine. Examples include: bacteria and nanomotors.

1.1.1.3 Receiver Nanomachine

The receiver nanomachine (or destination nanomachine) is responsible for capturing the information molecules and also decoding its information. Capturing information molecules is dependent on the molecular channel and can possibly have different approaches. The most common approach is based on chemical reactions that are produced by the binding process of the molecules to the surface of the receiver nanomachine. The binding process also leads to decoding, since the interpretation of information will result from the chemical reaction between the molecules and receptors on the surface.

1.2 State-of-the-art review

In the following, the state-of-the-art review on current molecular communication systems that have been proposed by the communication engineering research community is presented. The following systems are discussed: diffusion, bacterial and nanomotors molecular communication systems. The state-of-the-art review in Ca^{2+} signalling molecular communication system is presented in Chapter 2 .

1.2.1 Diffusion-based Molecular Communication

Diffusion-based molecular communication system is one of the first proposed models for molecular communication. The model relies on Brownian motion of molecules in free space, and the research have concentrated on studying the noise within the channel, modulation techniques, as well as detection of molecules at the receivers.

The first end-to-end model for diffusion-based molecular communication was first introduced by Pierobon and Akyildiz [9]. A complete mathematical framework was presented for the transmitter nanomachine that emits information molecules in free space, the molecular channel where the molecules diffuse and the binding process of the molecules at the receiver nanomachine. The performance of the single-link communication system was analysed in terms of normalized gain and channel group delay, which enabled a mechanism to quantify how slow and poor the communication gain is. This is followed by more extensive analysis found in Llaster et al. [10][11], in which the molecular concentration was varied over the channel and the group delay was measured.

Llaster et al. also extensively analysed an optimal pulse shape for minimizing bit error rate in [12]. The authors found that using the optimal pulse shape was needed to minimize the error resulting from the noise within the channel. The channel in this case is the diffusion of molecules that hang within the environment, interfering with the subsequent bits that are transmitted. This was followed by a proposal of detection techniques for pulse shapes based on amplitude and energy of the received molecules [13]. More effective detection techniques were proposed by Lin and colleagues [14], based on an asynchronous threshold method for performance improvement. Modulation and detection research in molecular communication are important for the design of receivers, which has been extensively studied in [15][16][17]. Those studies provided a great variety of mathematical analysis on coding, detection and modulation specifically for receiver design.

More communication performance metrics were applied to diffusion-based molecular communication system for analysing noise and error. Firstly, Pierobon et al. developed mathematical models for interpreting noise in the molecular communication channel in [18] and [19]. More recently, they have analysed interference in such communication channel based on power spectral density techniques [20]. This evaluation work has led researchers to investigate error performance, such as the approach based on pulse-based modulation

proposed by [21]. Finally, since channel condition information is important for transmission performance and optimization, Noel et al. provided a mathematical framework for such performance enhancing tools [22]. This technique estimates channel parameters when the transmitter nanomachine is sending a constant flow of molecules.

Channel capacity has also been investigated by Pierobon and Akyildiz in [23] and [24]. They have developed a closed form mathematical expression for the information capacity while taking into account memory and noise characteristics of the system. An information capacity expression was obtained by combining functions of the diffusion coefficient, the temperature, the transmitter–receiver distance, the bandwidth of the transmitted signal, and the average transmitted power. Results showed that a few kbps can be reached within a distance range of tenth of micrometer and for an average transmitted power around 1 pW.

Even though such modelling and performance analysis have been made, one of the major limitation is that the proposed molecular communication system is only limited to a single-link. In order to realise a full networking solution that uses molecular communication that can be useful for nanomedicine applications, multi-links diffusion-based molecular communication system has to be intensely investigated. Ahmadzade recently started with a technique for relaying information in a two-link diffusion-based molecular communication system [25].

1.2.2 Bacteria-based Molecular Communication

Bacteria are widespread within the environment as well as internally within the human body. While there are negative aspects of bacteria, such as infections they can cause, they are essentially needed to provide a stable environment as part of the natural ecosystem. In the realms of molecular communication, there have been proposals made for using bacteria.

Bacteria-based molecular communication system was first introduced by Cobo and Akyildiz [26]. They proposed an idea to encode information into the plasmid and embedding

this into the bacteria. The bacteria will then actively swim towards the receiver nanomachine to deliver the encoded information. Although their motility process is based on random walk, bacteria are guided by the process of chemotaxis to reach a destination point. This is achieved when a chemoattractant substance is released by the receiver. The authors have developed an end-to-end model for a single-link molecular communication model and analysed the delay, throughput and capacity.

In the same direction, Lio and Balasubramaniam [27] have shown that using bacteria conjugation (which is the transfer of DNA molecules from one bacteria to another) can result in routing based on a network of nanomachines that relay chemoattractants from the receiver. Also in [28], they have shown how this mechanism is used to achieve multi-link communication using bacteria-based molecular communication system.

Since then, researchers working on this topic have taken two directions. In the first direction, communication analysis of this system is being currently investigated based on modelling and performance evaluation of their delivery performance (e.g., first passage time as well as delay distribution). In the second direction, researchers are concentrating on applying this communication system for biological applications.

Recently, researchers developed a closed-form mathematical expression for bacterial nanonetwork [29]. This is followed by modelling signal transduction for amplitude-based pulse modulation [30] and collision analysis [31]. From the perspective of medium access protocols, Krishnaswamy and Sivakumar have developed a source addressing mechanism [32]. However, these work is based on using molecules emitted from bacterial population (also known as the process of quorum sensing), rather than the microbes delivering plasmids to a destination point.

A new communication approach that uses periods of silence was proposed in [33][34] by Krishnaswamy et al. for molecule based communication using bacterial population. Synchronized clocks are assumed to be in the transmitter and receiver nanomachines that can

count the values that are transmitted. Based on the clock counting, information is encoded into periods of silence between the start and stop pulses. This technique increases the data rate for super slow bacterial nanonetworks, and has been a source of inspiration for a technique that is also proposed in this thesis.

Applications for this type of communication were proposed for biological processes. Lo and Wei concentrated their efforts in developing an autonomous control for molecular communication in a population of bacteria [35]. This was achieved by a biological controller that is able to change bacteria concentration based on the environmental conditions. Also, researchers were able to develop a target tracking system using cooperative bacteria [36][37][38]. In this application, engineered bacteria transmits repellents to search for a target, and upon discovery of the target, will emit attractants to call the other microbes towards that location.

1.2.3 Microfluidic-based Molecular Communication

Recently an entire research topic has been devoted to microfluidic communication systems, where the flow of information is established through propagation of fluids along a miniature channel. In this model, the transmitter and receiver chambers are interconnected via a microfluidic channel in a microchip. Such molecular communication system has the advantage of using fluidic medium to transport information along a guided channel.

Microfluid-based molecular communication system was first introduced and modelled by Bicen et al. [39][40][41], where the chip was used to allow population of bacteria to emit molecules for communication. They investigated and modelled many communication aspects, including: gain, attenuation, interference and capacity. Wirdatmadja et al. [42] investigated this communication system looking at the achievable data rate performance for OOK shift keying with communication-by-silence. In this communication process, the information is transmitted through air bubbles that are pushed under pressure through the aqueous channel.

Through the communication-by-silence process, the only air bubbles required are two bits, which are the start and stop bits, where the information is conveyed through the counting process at the receiver.

1.2.4 Nanomotors-based Molecular Communication

Nanomotors are molecular/nano scales elements found in the cells, where they mobilize by walking on actin filament skeleton. The walking process is achieved by converting ATP energy that enables the walking process. They can be divided into biological (e.g., kinesin motor) or synthetic systems (e.g., carbon nanotube nanomotor). The nanomotors generally carry information molecules with them which are propagated by the active movement along the microtubule filament. Even though this is a very limited type of molecular communication system that is found within the cell, its importance is to provide communication between the nucleus and the outer membrane. Researchers have been proposing different approaches to model and realise this form of communication system.

Moore et al. [43] and [44], have proposed modelling this form of biological movement for molecular communication. This intracellular communication is from the mobilisation of vesicles in the nucleus, which are transported to the cellular membrane by kinesin motors. The authors also found that from the movement of the molecular motors, the actin filament networks can be re-arranged leading to a self-organization process [45]. More recently, Chahibi and Balasingham [46] have analytically modelled this form of molecular communication system in terms of delay and attenuation.

1.2.5 Applications for Molecular Communication

Molecular communication has gained attention from engineers and life science researchers for the potential flexibility and integration with biological systems for medical applications. Mainly, four applications were investigated that have pushed the field of molecular communi-

cation research towards the spotlight, namely: nanomedicine, intelligent drug delivery and Internet of Bio-NanoThings.

1.2.5.1 Nanomedicine

Monitoring and adapting disease treatment and diagnosis at the molecular level are revolutionizing nanomedicine. Molecular communication is going to play an important role in this field, where the communication between nanomachines will support the execution of nano/molecular scales monitoring. Felicetti et al. reviewed the challenges and prospects of molecular communication in nanomedicine, showing a variety of ideas for both diagnosis and treatment [47].

Disease detection and personalised diagnosis using molecular communication can bring real-time monitoring in the human tissues. Studying abnormalities in cell-cell communication is an idea for disease detection and personalised diagnosis of patients at a fine granular scale. Detection of such abnormalities can be performed using telecommunication tools with low complexity and, therefore, resulting in easier approaches for implementation.

Molecular communication is going to also bring the treatment of diseases to another level of effectiveness. Felicetti et al. argued that communication of active nanorobots in the human body has the potential to improve efficiency in: drug delivery, immune system activation, tissue engineering and nano surgery. However, the envisioned applications are not yet properly studied and intense research effort is needed in all the listed topics.

1.2.5.2 Intelligent Drug Delivery

The most studied application of molecular communication is intelligent drug delivery systems developed by Chahibi et al. [48][49][50][51]. Using molecular communication principles, drug delivery can enhance its performance of reaching the target by utilising telecommunication theories, such as routing. The rate of drug delivery and its propagation patterns

can be modelled, therefore, allowing adjustments and improvements to the dosage accuracy. Specifically, Chahibi et al. focused on modelling the circulatory system in the blood stream. Depending on the place that the drug molecules are inserted in the body, the rate and propagation will be optimum in a specific point of the body. They also worked with antibody-mediated drug delivery systems, in which small molecules (antibodies) that propagate in the body and bind selectively to their corresponding receptors (antigens) expressed at the surface of the diseased cells. This technique is one of the most encouraging therapeutic solutions for treating several diseases such as cancer.

1.2.5.3 Internet of Bio-NanoThings

Lastly, the Internet of Bio-NanoThings (IoNT), introduced by [52], is a perfect example of the potential technology that can result from nano communication research. In this vision, the nanomachines can be connected to each other and then onto an external computing entity such as the cloud. In the vision of IoBNT [53], the cells are engineered through synthetic biology, enabling them to have properties similar to a typical Internet of Thing (IoT) device. The authors discussed how artificial cells can be created to network between heterogeneous molecular nanonetworks, which in turn can be connected to a bio-cyber interface that links to an external device outside the body (e.g., mobile phone). Numerous envisioned applications of IoBNT includes: military, healthcare, security as well as nanomedicine.

1.3 Research scope and objectives of the thesis

The aim of the research in this thesis is to investigate how molecular communication system for nanomachines can be embedded into human cellular tissues. However, the design of such system is quite challenging due to the natural body's characteristics and homoeostasis requirements to provide stability. The system needs to maintain regular body's functions as well as rejection or modifications to the internal immune system. Therefore, a reasonable

choice in developing such a communication system is to use the already existing signalling processes that are found within the cellular tissues. One of the most important natural signalling mechanisms inside cellular tissues is Ca^{2+} signalling [54][55]. The referred system is going to be the baseline for the design of Ca^{2+}-signalling-based molecular communication system, which is the focus of this thesis. The limitations and challenges of this form of molecular communication system will be addressed as follows:

1. **Developing a representative communication model:** Natural communication/signalling processes are hard to model, and this is further amplified when trying to develop an artificial communication system. The main issue lies in the stochastic nature of this signalling process that involves both intra and intercellular signalling mechanism between the cells.

2. **Developing communication protocols:** In order to advance the field of molecular communication, as well as develop new research solutions to achieve networking capabilities between multiple nanomachines, new protocols will need to be incorporated. However, the design of the protocols must consider the stochastic and uncertain communication behaviour between the cells described above, as well as the limited computational capabilities of the nanomachines.

1.3.1 Objectives

Since validation and realization of the proposed Ca^{2+}-signalling-based molecular communication system are currently not practical, the focus of this thesis is in developing a theoretical model. This relies on expanding the existing models to capture both the stochastic behaviour of Ca^{2+}-signalling and the physiological implications that can limit the performance of the communication system embedded into cellular tissues. Taking this into account, the thesis is going to extensively analyse and propose the molecular communication model

based on utilising known telecommunication and information technology theories that will be applied to the Ca^{2+} signalling process. By developing this framework for creating a Ca^{2+}-signalling-based molecular communication system will lead towards new application within the field of nanomedicine. In the following section, the objectives will be defined into research questions detailing the challenges in this thesis work.

1.4 Research Questions

Ca^{2+} signalling within cells has been studied and investigated in molecular biology for more than 20 years. This form of communication is one of the most abundant signalling modes found in the body and is responsible for many regulatory mechanisms since its communication failures are linked to numerous diseases [54][56]. This adds to the motivation of developing a molecular communication system using this form of signalling for embedded nanomachines inside the cellular tissue. Therefore, the focus of this thesis is in fully developing and analysing a theoretical framework for *Ca^{2+}-signalling-based Molecular Communication for Cellular Tissues*, and is formalized through the following hypothesis:

"Nanomachines, either artificially eletronically designed (e.g., chips inside a cell) or synthetically engineered, can be embedded into cellular tissues and perform communication using Ca^{2+} signalling."

The system can be visualized in Fig. 1.3. A transmitter nanomachine is capable of encoding digital information with Ca^{2+} concentration as well as modulating it. Ca^{2+} ions are then diffused into the molecular channel, which is characterized by the intracellular and intercellular signalling processes between the cells. At the receiver nanomachine, the arrived Ca^{2+} concentration is demodulated and decoded. As described earlier, due to the inherent stochastic behaviour of this signalling process[57][58], a noisy communication channel is expected.

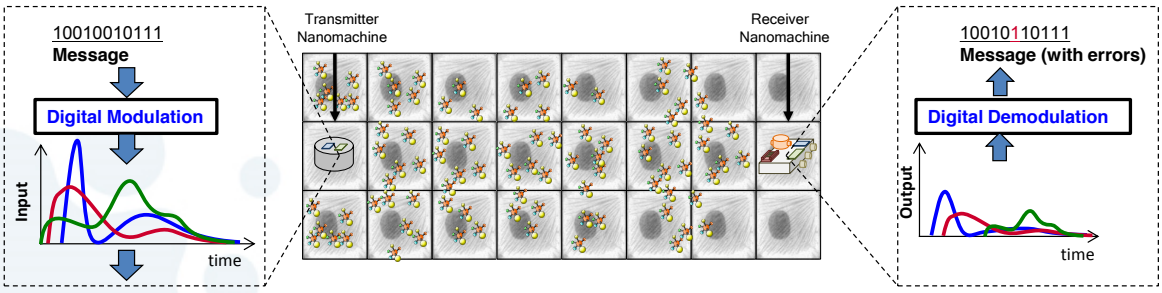

Fig. 1.3 Ca^{2+}-signalling-based molecular communication for cellular tissues. A transmitter nanomachine releases encoded information using modulated Ca^{2+} concentration, which is propagated through the molecular channel. The received signals contains errors that are due to the noisy characteristics of the molecular channel.

Telecommunication and information technology tools are going to be used for the performance analysis, based on the guidelines in [59]. The basic guideline is to define the emission, propagation and reception processes. The emission process is basically the encoding of a message by a transmitter nanomachine. The message is then transmitted through a channel, which in this case is a tissue. The received information is then decoded to a message by the receiver. The thesis will present representative communication models as well as protocols for Ca^{2+} signalling within the tissue for a number of different cell types, and this will be the basis for the framework.

Five research questions were defined for the development of Ca^{2+}-signalling-based Molecular Communication for cellular tissues, and they are listed as follows:

1. **First Research Question (RQ1) -** *What type of molecular communication system model can be developed for Ca^{2+} signalling in a cellular tissue?*

   This question addresses the modelling of the molecular communication system for Ca^{2+} signalling in a cellular tissue. Ca^{2+} signalling is basically modelled with ordinary differential equations with stochastic solvers [60][57][61][62; 63]. Although solutions have been proposed for transmitting digital bits based on Ca^{2+} signalling, the proposed models are incomplete due to unrealistic cellular tissue properties, which do not

consider stochastic behaviour of gap junctions, different types of cellular tissues and their physiological properties [60; 99; 102; 104].

2. **Second Research Question (RQ2) -** *How can the physiological shapes or gap junctions' behaviour from different cells that communicate using Ca^{2+} signalling affect information capacity, molecular delay, molecular gain and noise?*

   Biological systems undergoes different physiological processes over time that might cause issues to the communication system, and in particular when the objective is to artificially stimulate Ca^{2+} ions to transmit bits. The design of a molecular communication system for cellular tissues needs to incorporate tissue properties and overcome any negative impact on the performance. A specific property that needs to be incorporated are the cell shapes. As an example, epithelial tissues have square-shaped cells, blood cells have a circular shape and muscular cells have an elliptical shape. Diffusion in cellular tissues depends on the shape of the cells since this impacts on the Ca^{2+} propagation velocity as well as direction. At the same time, the intercellular signalling based on the gap junctions closing/opening behaviour also has to be considered (gap junctions are connections between adjacent cells in the tissues). Since cells in the human body are naturally soft structures, they can go through shape changes (e.g., movements or collisions). The study of the cellular tissue deformation has, therefore, significant importance in impacting the communication performance.

   Each of these properties will be need to be analyzed from the perspective of channel capacity, noise and gain, as well as the end-to-end delay.

3. **Third Research Question (RQ3) -** *Based on the excessive noise found in the Ca^{2+}-signalling-based molecular communication system, what new types of modulation and transmission protocols can be developed?*

Limitation of Ca^{2+}-signalling-based molecular communication systems is in the inherent noise that affects the capacity [5]. The investigation on noise in Ca^{2+} signalling channel [64] is a result from the stimulation of ions when information are transmitted. The noise will be further amplified when the tissue undergoes deformation. This issue needs to be addressed with the design of new types of modulation and transmission protocol that may currently be available in conventional wireless networks.

4. **Fourth Research Question (RQ4) -** *Can the current cellular tissue state (e.g., deformation) be detected? If so, what can be done with such information?*

   Detecting and inferring cellular tissue properties is an attractive tool that can be used in designing new applications that use Ca^{2+} signalling communication as well as diagnose diseases that can emerge from the tissue [65]. By inferring the current state of the tissue, the protocols can also utilise this information to adapt in order to improve the communication system performance.

5. **Fifth Research Question (RQ5) -** *Can the cytosolic Ca^{2+} concentration be controlled? and what are the applications of the control model?*

   The Ca^{2+} signalling, as described above, can result in excessive noise due to variations in the concentrations during intra and intercellular signalling. This noise effect can occur naturally resulting in diseases (e.g., neurodegenerative diseases), or artificially when applied to molecular communication. In the latter case, molecular communication that use Ca^{2+} are required to stimulate extra quantity of ions to convey information, which can lead to stress on the cells. Therefore, design of protocols must consider the effects that variations on Ca^{2+} concentration can have on the human body.

1.5 Document Organization

The rest of the thesis is organized as follows. Chapter 2 presents background information about Ca^{2+} signalling and the characterization of Ca^{2+} signalling in the human body. The research contribution summary is presented in Chapter 3. The research papers containing the contribution of this thesis are found in Chapters 4 to 8. A discussion about the insights obtained with the research work in this thesis is presented in Chapter 9. Finally, conclusion and future work are presented in Chapter 10.

Chapter 2

Ca^{2+} Signalling

Ca^{2+} signalling is a natural mechanism that transmits ions at short distances between interconnected cells within a tissue. This form of communication can be found in a variety of cells, providing various physiological and regulatory purposes (e.g., cell growth, proliferation and fertilization, muscle contraction, neuronal communication, cellular motility and differentiation), provoked by IP_3 stimulation, hormonal or neurotransmitter signals. The Ca^{2+} signalling can travel small to medium distances (over several hundred micrometers) by means of molecular diffusion, propagating across the extracellular space and gap junction of the neighbouring cells. This powerful biological signalling has brought the attention of nanonetworks and molecular communication researchers as one form of communication and networking between nanomachines.

There are numerous reviews on Ca^{2+} physiology in the literature [66]: in 2003 an entire issue of Nature Reviews was devoted to the subject and contains reviews of Ca^{2+} homeostasis [54], extracellular Ca^{2+} sensing [67], Ca^{2+} signalling during embryogenesis [68], the Ca^{2+}-apoptosis link [69], and the regulation of cardiac contractility by Ca^{2+} [70]. Other useful reviews for fundamentals of Ca^{2+} signalling are [71] and [72].

This chapter presents background information on Ca^{2+} signalling for the complete understanding of the work presented in this thesis. The chapter will start with a description

on how the Ca^{2+} signalling behaves internally in the cell (*intracellular signalling*) and, this is followed by how the waves are propagated to other cells and eventually to the whole tissue (*intercellular signalling*).

2.1 Intracellular Ca^{2+} Signalling

Intracellular Ca^{2+} signalling is a natural regulatory process inside human cells that leads to numerous physiological regulations. A number of chemical reactions and their magnitude are responsible for maintaining Ca^{2+} concentration within the cytosol, as well as producing oscillation effects and wave propagation. Ca^{2+} signalling is dependent on the IP_3 [1], and its relationship is important for the communication purpose.

Intracellular Ca^{2+} signalling occurs in the following way: by stimulating the IP_3 the Ca^{2+} signals are released (*Stimulation*). At the same time, the released IP_3 also indirectly controls the influx of Ca^{2+} ions to the endoplasmic reticulum and its storage in the cytosolic area (*Storage*). Besides the stimulation process, certain cellular components are also capable of self-generating Ca^{2+} ions (*Amplification*). Finally, exchange of Ca^{2+} ions is conducted in two ways: cell-cell communication (*Diffusion*) and aleatory exchange of Ca^{2+} to the extracellular space (*Release*) [61]. This process can be visualized in Fig. 2.1.

Ca^{2+} signalling has been studied first by the biological community, which aimed to observe how the cellular evolutionary process communicates. Goldbeter et al. [61] modelled the Ca^{2+} signalling oscillations in the cytosol inside the cell. They presented a number of ordinary differential equations that accurately describe the relationships inside the cell responsible for the Ca^{2+} production, storage and release. They also presented a method to stimulate the Ca^{2+} release at higher frequencies through protein phospohrylation, which is considered a method for frequency encoding for Ca^{2+} signals. This work is further extended

[1] Inositol 1,4,5-trisphosphate (IP_3) is a secondary message molecule that travels through the cytosol and stimulates the release of Ca^{2+} from the endoplasmic reticulum to the cytosol.

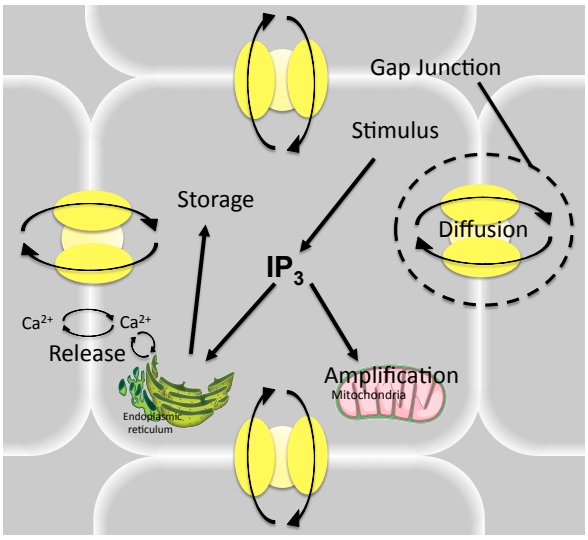

Fig. 2.1 The stages of the Ca^{2+} signalling process: (1) The process starts from the stimulation and extracellular leakage of Ca^{2+} ions into the cytosol. (2) Transport the Ca^{2+} ions from the cellular store (or cytosolic space) to the endoplasmic reticulum. (3) Release of Ca^{2+} ions from the endoplasmic reticulum into the cytosol, where the release will also include the leakage of Ca^{2+} ions (4). Lastly, (5) the Ca^{2+} ions are transported from the cytosol to the extracellular space.

by Berridge et al. [73] which has extended the analysis of modulating information through Ca^{2+} signals fully developing the theory for AM and FM encoding. Some systems proprieties of Ca^{2+} signalling were also investigated under a spatial and temporal analysis in Berrigde et al. [74]. They concluded that this system might have different spatial and temporal dynamics, because slow cellular responses are controlled by intracellular Ca^{2+} signals and faster cellular responses are controlled by high Ca^{2+} localized spikes. Other works that analyses the process of Ca^{2+} oscillations, regulations and dynamics, are from Tsien et al. [75] and Berrigde et al. [54].

2.2 Intercellular Ca^{2+} Signalling

Intercellular Ca^{2+} signalling is central to development and various regulatory purposes (e.g., cell growth and proliferation, fertilization, muscle contraction, neuronal transmission, cellular

motility and differentiation), and is initiated by IP_3 stimulation, or through hormonal or neurotransmitter signalling. This biological communication platform is found in a variety of cell types, including: *glial or astrocytes* [76][77], *neurons* [78], *ephitelium* [79][80], *endothelium* [81], *smooth muscle* [82], *cardiomyocytes* [83], *hepatocytes* [84], *osteocytes* [85], *chondrocytes* [86], *kidney* [87], *mammary gland* [88], *mast* [89], *pancreatic* [90], and *keratinocytes* [91].

Cells are soft structures that present different shapes and can undergo deformation. The deformation of a cell can affect the performance of Ca^{2+} signalling, in particular communication that is performed through diffusion of molecules inside the cellular tissue. Masselter and Speck [92] investigate how tissue deformation spatially modulates *angiogenic* and *angiogenesis* signals. This is due to the physical forces applied to the developing tissues. For example, during vascular development, the deformation caused by such forces has a huge impact on the Ca^{2+} signalling and the overall behaviour of the cell. This challenge is also explored in the thesis.

Chemical synapses depend on a structure that connect the cytosol of two adjacent cells, namely the *Gap Junctions*. Once opened, gap junctions allow Ca^{2+} ions to flow from one cell to another. Further description on the gap junctions is found in the next section.

2.3 Gap Junction

In intercellular communication, Ca^{2+} ions are propagated through cellular tissues via a physical gate that connects the cytosolic areas of two neighbouring cells; these gates are called *Gap Junctions*. Fig. 2.2 shows how gap junctions connect two cytosols. The gap junctions are composed of two *connexons*, one in each connecting cell, which is formed by six proteins called *connexins*—as shown in Fig. 2.3.

Gap junctions are found in many animal cellular tissues with varying configurations and connectivity. The distribution of the connexins per cell has a fundamental impact

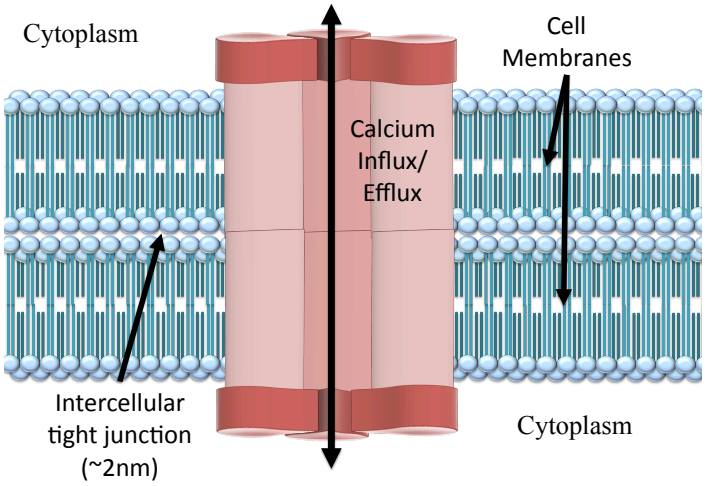

Fig. 2.2 Side view of a gap junction gate. The intercellular tight junction (2*nm*) separates the two neighbouring cells, which are connected via gap junctions. This enables the Ca^{2+} influx and efflux through the cellular membranes.

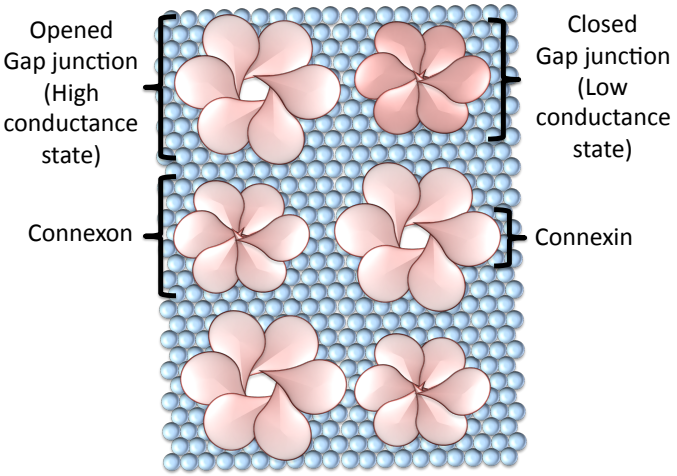

Fig. 2.3 Top view of the gap junctions. A single gap junction gate is referred to as the *connexon*, which is formed by six proteins called *connexin*. These gates have two states: *high conductance* state and a *low conductance* state—equivalently to the opened or closed status of the junction.

on the diffusion behaviour. Changes in those characteristics may lead to different types of diseases, including cancer, cardiac ischemia and cardiac hypertrophy [93]. Given this, control of gap junction behaviour is a possible tool for drug delivery systems and disease treatment. Cellular growth is directly involved with gap junction control: regulatory growth signals are transmitted through gap junctions, and decreased communication capacity may

lead to uncontrolled growth in extreme cases, as in cancer [94]. Studies have shown how communication capacity can control growth, in which connexin genes were transfected into tumorigenic cell lines [95]. Ca^{2+} intercellular signalling plays two fundamental roles in influencing the gap junctions channels. It not only activates the gap junction channel, with intercellular oscillations, but Ca^{2+} ions can also be transferred to a neighbour cell by diffusion. Here the focus is only on the diffusion process of the Ca^{2+} ions through the junction.

Intercellular diffusion only occurs when both connexons are opened at the same time. Ca^{2+} ions can thus flow from a cellular cytosol to another one. The thesis will present how the gap junction behaviour between the cells will affect the capacity of the communication channel within the tissue.

2.4 Characterization of Ca^{2+} Signalling for different types of cells

Three categories for cells that communicate through Ca^{2+} signalling were identified. These includes excitable cells which can be stimulated through electrical current only, non-excitable cells which are stimulated through chemical reactions, and hybrid excitable and non-excitable cells hold properties of both. Examples of cells under each of these classifications include: smooth muscle cells (excitable), epithelial cells (non-excitable) and astrocytes (hybrid). These cell types typically present different characteristics regarding structure, internal reactions, size, and location within the human body.

The state-of-the-art modelling that is discussed in this chapter is limited and is not a good realistic representation of Ca^{2+} signalling-based molecular communication system. Intense modelling and analysis is required to fully understand the behaviour of the molecular communication system, and this can only be achieved by incorporating different properties

of the cells (e.g., gap junctions, different chemical reactions, multiple stages of the intra and intercellular signalling, different cell types and their connectivity). This is one of the motivations for the development of the work presented in this thesis.

2.4.1 Non-excitable cells

Ca^{2+}-signalling-based molecular communication system was first introduced by Nakano et al. in [96] and [97]. In those works, information is encoded through spikes or oscillations of the Ca^{2+} concentration in the cell caused by an external stimulation. The propagation process can possibly lead to switching of paths through diffusion of the ions in selected gap junctions, as well as amplification, which can possibly support signal modulation. An experimental validation was also presented, where Ca^{2+} waves propagated over *HeLa Cx43* cell wires and fluorescent emission was made possible for visualizing the signal transmission [97].

The first end-to-end model of the Ca^{2+} signalling communication system as a relay channel was proposed by Nakano and Liu [60]. A stochastic solver was used to for the Goldbeter's model [61], which was based on the Gillespie algorithm. Goldbeter model is based on two sets of ordinary differential equations that count the oscillatory behaviour of intracellular Ca^{2+} signalling for non-excitable cells. The authors investigated the Ca^{2+}-signalling-based molecular communication from the perspective of information theory with both the transmitter nanomachine and receiver nanomachine embedded inside an array of one dimensional cells. Mutual information impact was studied based on a set of system variables (e.g., concentration, distance, time slot for releasing bits from the transmitter).

2.4.1.1 Epithelial cells

Epithelial cells are one of the most basic type of cells found in animal tissue; they are responsible for a wide set of tasks, including secretion, selective absorption, protection,

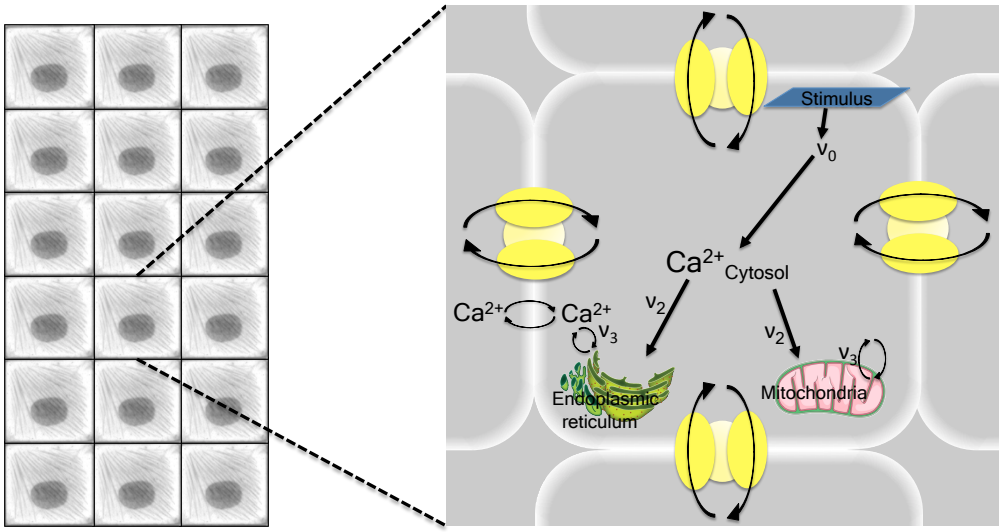

Fig. 2.4 The stages of the Ca^{2+} signalling process in the epithelial cells. The process starts from the stimulation and extracellular leakage of Ca^{2+} ions into the cytosol. This is followed by the transport of the Ca^{2+} ions from the cellular store (or cytosolic space) to the endoplasmic reticulum. After the transport, the endoplasmic reticulum releases the Ca^{2+} ions into the cytosol, where the release will also include the leakage of Ca^{2+} ions. Lastly, the Ca^{2+} ions are transported from the cytosol to the extracellular space.

transcellular transport and detection of sensation. The cells can be found throughout the body, covering both external surfaces (endothelium [81]) and internal organs (kidney cells [87], hepatocytes [84] and pancreatic cells [90]). One interesting characteristic is their tightly packed structure, with almost no intercellular space. Epithelial cells come in a variety of geometrical shapes, including square-shape—referred to as simple cuboidal epithelial cells—which is the structure considered in this thesis. In vitro and in vivo experiments, like those reported in [79][80], have investigated the spatial-temporal dynamics of intercellular Ca^{2+} signalling in this type of cell.

2.4.2 Excitable cells

An electro-chemical relationship between the concentration of Ca^{2+} molecules and cellular membrane voltage is found in excitable cells that enable the propagation of action-potentials.

This mechanism lies the foundations of neuron-neuron signalling to perform communication between nanomachines. Long-range communication is thus possible within the human body, where the nervous system can be used as a backbone network to interconnect numerous nanomachines embedded within the human body. Researchers are focused on modelling such communication system but also looking at particular problems for efficient neuronal transmission.

A neuronal backbone network was proposed as a new communication paradigm by Walsh et al. [98]. This work was extended by Balasubramaniam et al. [99], in which a multi-access protocol was presented. The proposed approach uses a genetic algorithm optimization technique to schedule the transmission window for each transmitter nanomachine, therefore providing multiple access to the neuronal network channel. They also provided test-bed experiments using a living neuronal network to demonstrate how a single bit of information can be transmitted through the stimulation of the neurons.

Recent works have concentrated on modelling the communication performance of the neuronal nanonetworks. Modelling of synaptic transmission based on presynaptic terminals and transmitter array was proposed in [100]. Caccipuoti et al. showed that neuronal information is encoded in the release patterns of the presynaptic terminals. Ramezani et al. [101], on the other hand, were more interested in how the shape of action potential during axonal propagation can affect a neuronal-based molecular communication system. They considered the existence of multiple terminals with univesicular release between two neurons, which is realistic for neurons in the *Hippocampal CA* region. Different neuron terminals have different release probabilities and different shape patterns. An inverse relationship was found between the spike width and the probability of error detection, because theoretically detection techniques are more efficient with detecting wider shape pulses [101].

Even though solid work has been presented for neuron-neuron molecular communication, other tissue types also present the same electro-chemical relationship e.g. smooth muscle

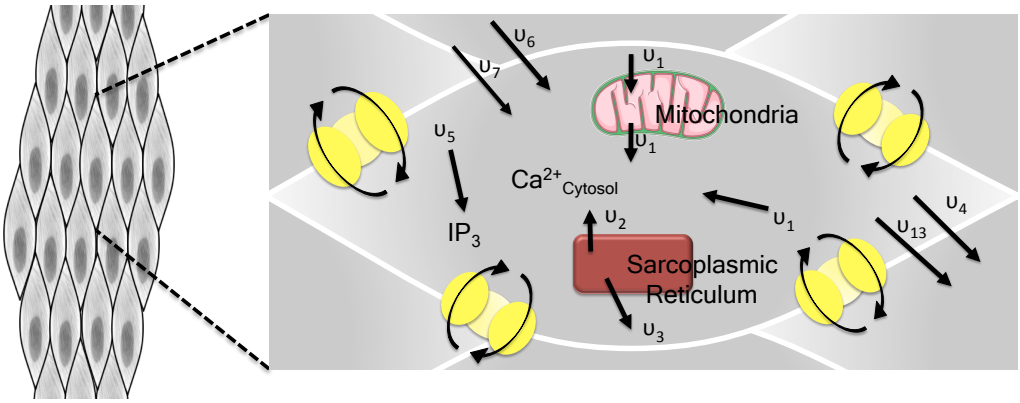

Fig. 2.5 C
a^{2+} signalling process in the arterial smooth muscle cells.The stages of the Ca^{2+} signalling process in arterial smooth muscle cells: The process starts with stimulation and production of Ca^{2+} from the CICR and IP_3 processes. Ca^{2+} is then amplified using mitochondria and sarcoplasmic reticulum. Leakage of Ca^{2+} outwards into the cytosol is performed by the Ca^{2+}-ATPase and Potassium efflux. Leakage of Ca^{2+} inwards within the cell is performed by VOCCS channels and by Na^{+}/Ca^{2+} exchange. Finally, the cytosolic Ca^{2+} ions are propagated throughout the cellular tissue via diffusion.

cells, and yet no molecular communication system has been proposed based on those. In these Ca^{2+} signalling plays a bigger role compared to the neurons and are further explored in the following.

2.4.2.1 Smooth muscle cells

Smooth muscle is an involuntary tissue comprised of thin, elongated muscle cells found along the walls of hollow organs such as the digestive tract (lower part of the esophagus, stomach and intestines), the bladder, the uterus, and various ducts of glands and walls of blood vessels. A number of studies have found that smooth muscle tissues are capable of propagating Ca^{2+} throughout the tissue [82]—intercellular Ca^{2+} signalling in smooth muscle cells helps in the arteries' contractile state.

2.4.3 Hybrid cells

Hybrid cells not only present both excitable and non excitable characteristics but they are able to perform communication within the two domains. The cell type identified for this role is astrocytes.

In [102], the authors looked at the communication of neurons and astrocytes. Astrocytes provide nutrients that support the normal functioning environment of the neurons. The network was translated into a equivalent cascade circuit, where the frequency response of the system was deducted. A new tool to understand this heterogeneous communication and the stimulus-response of the astrocytes-neuron system was proposed. This enabled the analysis of the tripartite synapses under the power spectral density and the impulse response, characterizing the communication channel.

Since astrocytes seem to play an important role in neuron-neuron communication and providing its maintenance and upkeep, investigation into the role of astrocytes communication and its support for neuronal-based molecular communication systems is an important topic. In particular, the failure between the astrocytes and neuron communication can lead to a number of diseases. In this thesis, we investigate how astrocytes can also be utilised for molecular communication, and how the control of communication between the astrocytes and neurons can be achieved.

2.4.3.1 Astrocytes

Astrocytes are a star-shaped form of *Glia* cells, responsible for a wide range of complex and important functions relating to maintenance of the central nervous system. These functions include primary roles in synaptic transmission and information processing by neural circuits. Specifically, these non-neural cells in the brain are responsible for spatial neuron support, neuron nutrients and oxygen supply, neuronal isolation, pathogen destruction, as well as removal of dead neurons. Astrocytes are the most abundant cells within the central nervous

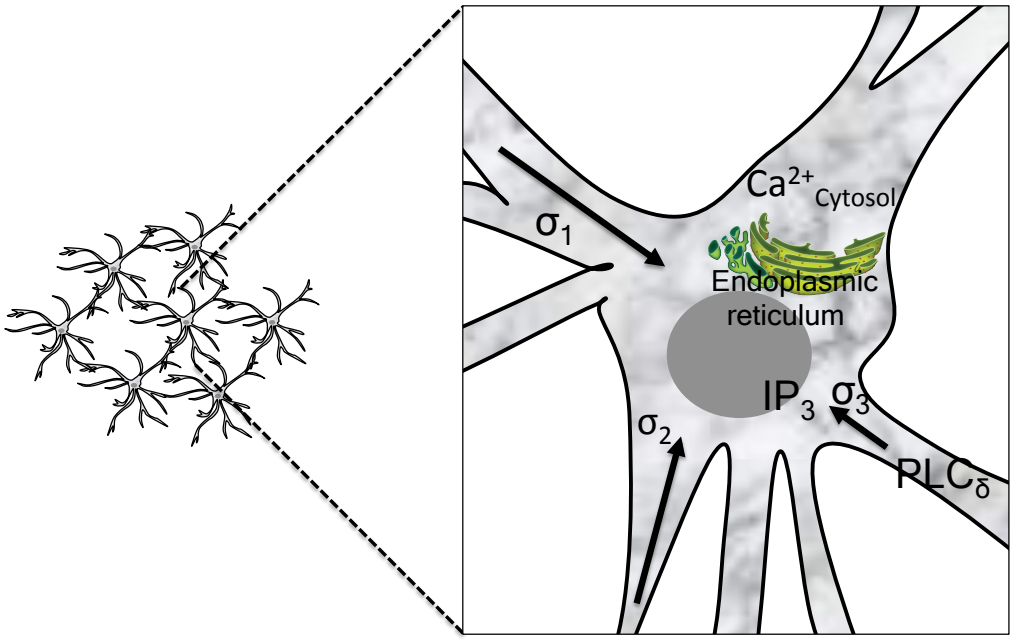

Fig. 2.6 The stages of the Ca^{2+} signalling process in astrocytes. After stimulation, IP_3 is produced by the PLC protein (*Phosphoinositide phospholipase C*), which leads to the increase of the internal Ca^{2+} concentration. This is because we use the isoform PLC, which is correlated with the internal cytosolic Ca^{2+} level. This internal concentration is then amplified using the endoplasmic reticulum. Diffusion of Ca^{2+} ions through the cellular tissue then occurs.

system [103]. They can be found in the spinal cord as well as the brain, where they are responsible for communication with both excitable and non-excitable cells. Studies have shown that astrocytes propagate intercellular Ca^{2+} signals over relatively long distances in response to stimulation [76][77].

2.5 Discussion

The early stage of the molecular communication area is defined by its poor development in the following three pillars, modelling, analysis and applications. One of the reasons of such slow progress is the plurality of molecular communication channels and the lack of research efforts to handle those. They are intrinsic different from each other and many models were

proposed and discussed in the Introduction and in this chapter. In alignment to that, there is also the need of more realistic models and pave the basis for the development of new application using molecular communication. Looking at contributing to all those issues and pillars, this thesis is concentrated in developing models, analysing them and developing applications for Ca^{2+} Signalling-based molecular communication systems. This biological platform is used to perform communication inside cellular tissues in the IoBNT context, and, therefore, guaranteeing access to molecular/nano levels in the body. Then molecular communication and nanomedicine are finally combined as a novel proposed technology, creating the required impact on the scientific community with trying to trigger a large-scale research effort for developing this new technology.

The first research effort for the thesis work is in regard to modelling. Information and communication technology is going to be mixed with biological models for Ca^{2+} signalling to develop molecular communication systems inside cellular tissues. Particularly, Nakano's model for transmitting bits over a line of cells is a great example of that [60]. His communication channel model was developed mixing an intracellular signalling model and a stochastic solver. Even tough Nakano's model is important because of the innovative solution, the following limitations to the model are found: 1) the domain of the model is only 1D and, therefore, unable to be considered as a cellular tissue, 2) the simple model used for intercellular communication does not consider gap junctions, 3) only one cellular tissue type is modelled. An extension of Nakano's model is needed to provide a proper mathematical framework that can be used for developing molecular communication systems for cellular tissues. Models for 3D domain tissues, gap junction stochastic behaviour and different tissue types are then proposed. Secondly is in regard to the analysis, communication and information technology analysis is used to investigate how some of the biological properties of the system affects the communication performance. Inspired by Pierobon [9][18][19], adaptations of telecommunication metrics were used to proper analyse the communication performance

of the molecular communication system whist taking into account the biological properties of cellular tissues. The following metrics were used: molecular gain, molecular delay, capacity, intracellular interference, noise and data rate. And lastly in regard to applications, new applications were designed using a Ca^{2+}-signalling-based molecular communication system, including a cellular tissue deformation detection/inference technique and a regulation technique for intracellular Ca^{2+} signalling for astrocytes in the tripartite synapses. All these contributions are better explained in Chapter 3.

Chapter 3

Thesis Research Summary

This chapter presents the complete list of research articles related to this thesis. The chapter will begin with a short summary for each of the articles, and this will be followed by the mappings of each of the publications to the research questions.

3.1 Dissemination Work

Published Articles:

P1. (*Chapter 4*) M. T. Barros, S. Balasubramaniam, B. Jennings. *Comparative End-to-end Analysis of Ca^{2+} Signaling-based Molecular Communication in Biological Tissues.* IEEE Transactions on Communication, vol. 63, pp. 5128-5142. December 2015.

Summary: A single-link communication system based on Ca^{2+} signalling in 3D tissue was modelled in this article. The 3D model of the tissue includes the intra and inter-cellular Ca^{2+} signalling combined with the stochastic property of the gap junctions closing/opening process. Three main types of cellular tissues within the human body that communicate using Ca^{2+} signalling were modelled as part of the comparative end-to-end analysis, and these cells include epithelial cells (non-excitable cells), smooth

muscle cells (excitable cells) and astrocytes (hybrid cells). The modelling framework is not only important for molecular communication researchers to analyse the communication performance of each tissue with respect to their signalling behaviour and physiological properties, but also for biologists and biotechnologists who are interested in understanding the intercellular Ca^{2+} signalling process that can lead to diseases. The performance metrics used to analyse the communication system includes the end-to-end channel capacity, delay, as well as gain. The analysis found that the propagation characteristics are highly dependent on the stimulation process of the Ca^{2+} ions, its concentration, as well as the physiological shapes of the cells and their connectivity in the tissue.

P2. (*Chapter 5*) M. T. Barros, S. Balasubramaniam, B. Jennings, Y. Koucheryavy.*Transmission Protocols for Calcium Signaling based Molecular Communications in Deformable Cellular Tissues.* IEEE Transactions on Nanotechnology, vol. 13, no.4, pp.779-788, July 2014.

Summary: This article investigated the low performance of OOK modulation for a single-link Ca^{2+}-based molecular communication system, and how this performance can be affected by the flexible structure of the tissue. For the flexible structure analysis, a deformation model for cellular tissues was incorporated. The communication performance analysed the capacity as well as noise between the compressed and uncompressed tissue structure. The analysis showed that the noise found Ca^{2+} signalling is very unique and time-varying compared to conventional wireless networks. There are different types of noise that depends on the location along the path between the transmitter and receiver. The noise is highly affected by the variations in the concentration as well as distance between the transmitter and receiver. In order to improve the performance, the article proposed the communication-by-silence protocols with block coding.

P3. (*Chapter 6*) M. T. Barros, S. Balasubramaniam, B. Jennings, *Using Information Metrics and Molecular Communications to Detect Cellular Tissue Deformation*, IEEE Transaction on Nanobioscience, vol. 13, pp. 278-288, September 2014.

Summary: While molecular communication to date has largely concentrated on characterizing the communication behaviour, very little attention has been put on defining novel applications. In this article the use of Ca^{2+} signalling with synchronized transmission between the nanomachines is used to infer information with regards to the tissue as well as the shape of deformation. The information includes estimating the locations of the transmitters as well as the concentration of the emitted Ca^{2+} ions, and the type of deformation includes single, double, and S-shaped compression. This is achieved by monitoring the concentration of Ca^{2+} signalling within the tissue, and feeding this data into a simple machine learning algorithm that utilises information metrics as well as threshold classifiers. The topology considered in the tissue is a star topology where the transmitter nanomachines will transmit information to the receiver, which in turn collects and performs the classification.

P4. (*Chapter 7*) M. T. Barros, S. Balasubramaniam, B. Jennings, Y. Koucheryavy, *Adaptive Transmission Protocol for Molecular Communications in Cellular Tissues.* In: The IEEE Conference on Communication (ICC 2014), 2014, Sydney, Australia.

Summary: This article integrated the inference technique for the tissue deformation to adaptively change the time-slots for bit transmission between the nanomachines using Ca^{2+} signalling. The results showed that the adaptive transmission protocol was able to accurately infer the type of compression and when the time-slots for bit transmission is changed, this improved the end-to-end data rate for a single-link communication network compared to static time-slots.

Submitted Articles:

Table 3.1 Association between the research questions and publications.

Questions	Publications
RQ1	P1
RQ2	P1 and P2
RQ3	P2 and P4
RQ4	P3
RQ5	P5

P5. (*Chapter 8*) M. T. Barros, S. Balasubramaniam, S. Dey. *Set Point Regulation of Astrocytes' Intracellular Ca^{2+} Signalling in Tripartite Synapses*. Submitted to IEEE Transactions on Nanobioscience, January 2016.

Summary: *Gliotransmitters* found in the tripartite synapses are controlled by the intracellular Ca^{2+} signalling of astrocytes (tripartite synapses is the three-way communication between two neurons and the astrocytes). The gliotransmitters have a huge impact in the quality of synaptic transmission, and therefore, is linked to numerous neurodegenerative diseases, including: Alzheimer's, Parkinson's, and Depression. This usually result from the varying concentration of Ca^{2+} signalling between the neurons and the astrocytes. The use of Ca^{2+} signalling in molecular communication between neurons can also lead to neurodegenerative diseases due to the high concentration required to maintain decent channel capacity. In order regulate the intracellular Ca^{2+} signalling between the cells to a desired level, a feed-forward feedback control mechanism was proposed in this article.

3.2 Thesis Contribution

In the following, a summary contribution for each publication is discussed with respect to the research questions presented in Chapter 1. Table 3.1 presents a summary of publications that correspond to each of the research questions.

1. **Contribution 1:** *Ca^{2+} signalling mathematical framework for molecular communication systems.*

    - **P1 :** A complete mathematical framework for Ca^{2+}-signalling-based molecular communication system was introduced in this paper. Three main extensions was made to the Nakano model.

        (a) *3D modelling :* Nakano's model was limited to a simple array of cells. An extension was added to model 3D structure, and capturing realistic cellular tissue dynamics. This allowed to infer more accurate information on the performance of the Ca^{2+} signalling propagation both temporally and spatially within the tissue.

        (b) *Gap junction stochastic model :* Nakano's model lacked the gap junctions model between the cells. In the proposed framework, the stochastic gap junction model based on the work of Kilinc and Akan [104] was incorporated.

        (c) *Different tissue types :* The framework incorporated three different tissue types, and this includes smooth muscle cells (excitable), epithelium (non-excitable) and astrocytes (hybrid). Excitable tissues are able to conduct electrical current, while non-excitable tissue only rely on chemical reactions as part of their communication. Hybrid tissues, on the other hand, are capable of exhibiting both excitable and non-excitable properties. For each of the tissue types their intracellular and intercellular Ca^{2+} signalling as well as their different shapes and sizes were modelled.

    By incorporating these extensions into the 3D model, allowed accurate characterisation of the communication behaviour relating to the physical properties and structures of the cells, and how this is controlled by the internal chemical reactions. An interesting finding was observed using the information capacity metric. *System performance changes dramatically when the distance between the*

transmitter and receiver nanomachine is increased. As an example, smooth muscle cells present the highest capacity values for short distance transmission while it presents the lowest values for other distances. Diffusion properties once again are the major factor of this behaviour, where the cell's size is able to push large quantity of ions into the immediate neigbouring cells but this dies dramatically as the distance is increased.

The framework analyses the cell-cell diffusion that is affected by the size of the cells, where the larger cells tend to diffuse less ions through the gap junctions due to the amount of space. This in turn also affects the velocity of the ion propagation through the gap junctions. The communication behaviour in 3D is also related to the internal Ca^{2+} concentration that is regulated by the chemical reactions inside the cell. By having different cell types incorporated into the framework, the impact of different sequence in the chemical reactions allows an accurate view of how the state of Ca^{2+} concentration within the cell affects the diffusion to the neighbouring cells. The article also contributes in defining the molecular delay and gain for the communication channel. Unlike electromagnetic-based communication, the molecular delay is measured as the time taken for a determined quantity of molecules to arrive at the receiver.

The analysis from the framework found that *epithelial cells have the lowest delay performance, and this is mainly due to their size compared to smooth muscle and astrocyte cells.* The comparative analysis from the framework also found that the gain is influenced by longer distances in the cell's connectivity within the tissue. For this reason, the astrocyte cells that have long connectivity resulted in the lowest channel gain.

This contribution addresses the research question RQ1.

2. **Contribution 2:** *Characterizing the impact of cell shapes and gap junctions on the Ca^{2+}-signalling-based molecular communication system*

    - **P1 :** As previously discussed, gap junctions have a combined impact on the Ca^{2+} signalling communication performance with other physiological properties such as: size of the cells, number of reactions and diffusion velocity. This article answers this research question by modelling the different gap junction closing/opening behaviour for each type of cell, and analysing the concentration of ions that get diffused to the neighbouring cells. In the case of smooth muscle cells, the gap junctions are constantly opened with respect to time. However, the probability of the opening of gap junction in astrocytes is quite low leading them to be kept closed more often. In the case of epithelial cells, a more dynamic behaviour is observed where the gap junction performance is initially closed for the first few seconds after the Ca^{2+} is stimulated, and appear to stay opened for a very long period afterwards. Finally, different properties such as, permeability and functional voltage are found to determine the gap junction behaviour.
    - **P2 :** As mentioned previously, cellular tissue deformation has an effect on the performance of the proposed Ca^{2+}-signalling-based molecular communication system. This article addresses this research question based on the following findings: 1) *Tissue compression increases Ca^{2+} ion flows.* Under tissue compression, the size of the cells are changed. For larger sizes, the Ca^{2+} ion flows are reduced due to the inverse dependency between the diffusion velocity and the size of the cells. 2) *Tissue deformation increases the information capacity of the channel.* An analogy can be used to explain this result, which is based on the *pipe-effect*. Under deformation, Ca^{2+} ions are directed to a perpendicular direction of the compressed force. In our scenario, the receiver nanomachine is placed in the perpendicular direction of the compression force. This effect leads to an increase

of the incoming Ca^{2+} ions, which in turn increases the information capacity. 3) *Time-slot length for bit transmission patterns are changed due to tissue deformation.* The comparison between the performance of the time-slot length between regular and deformed tissue showed different performance patterns. Lower time-slot lengths led to higher information capacity when the cellular tissue was compressed. This is also due to the pipe-effect described previously, where the diffusion of Ca^{2+} ions will be forced to flow towards the receiver, and minimising diffusions to other directions. This leads to less quantity of noise within the channel, enabling the next bit to be transmitted with shorter waiting periods. This will not be the case when the tissue is not compressed, since larger quantity of noise will remain within the channel and affect the subsequent bit transmissions.

This contribution addresses the research question RQ2.

3. **Contribution 3:** *Modulation and transmission protocols for Ca^{2+}-signalling-based molecular communication system.*

   Biological systems suffer from molecular noise due to their inherent stochastic properties. Intercellular Ca^{2+} signalling is a chaotic process where constant random signalling appears in the channel as part of the cell's self-regulation process. This random signalling as well as the bit transmission contributes to a complex noise pattern within the channel. In the following works presented in papers **P2** and **P4**, development of protocols to minimize noise as well as adaptation methods to the varying cellular tissue structure is presented and discussed.

   - **P2 :** Four different types of noise were found to exist in Ca^{2+}-signalling-based molecular communication system and this includes: source, system, destination and reflection noise. Although the source noise presented the highest accumula-

tive Ca^{2+} concentration when the waves (which represent the bits) are transmitted in response to stimulation, the reflective noise affects the channel the most. This is because of the direct connection between the cells that diffuses the Ca^{2+} ions, leading to a reflective response of the waves that propagate back to the line-of-sight path (the line-of-sight path is the shortest path of cells between the transmitter and receiver nanomachines). This reflection interferes with the transmission of the subsequent bits, reducing the overall data rate performance. Based on this, communication-by-silence protocol was used to overcome the excessive noise effects. Two protocols were proposed: *Dynamic Time-Slot Configuration with Silent Communication* and *Improved Dynamic Time-Slot Configuration with Silent Communication* (*IDTC-SC*). Both protocols uses a counting process between the start and stop bits for conveying information, where the transmitter and receiver nanomachines are required to have synchronised clocks that counts the value to be transmitted. Based on the analysis, the *the IDTC-SC protocol resulted in the highest data rate performance*, and this was due to the incorporation of the block code strategy. The block code strategy divides the streams of bits into blocks that are separated by *Block Transition Bit*. By subdividing into smaller bit trains during the transmission, led to a decrease in the average counting periods of the clock for every transmission.

- **P4 :** Besides the excessive noise, another factor is the deformable shape of the tissue that can affect the flow of ions. Based on the research results published in (**P2**), it was observed that certain types of deformation can provide a positive impact on the information capacity performance. To exploit this behaviour in order to improve the overall performance of the system, an adaptive transmission protocol was proposed where the time-slot length for each bit transmission would adjust depending on the type of compression as well as the duration. In order to

enable this adaptation, two steps are required. In the first step, the cellular tissue deformation detection from **P3** was used to infer the type of deformation. Once this is known, the transmitter nanomachine will adjust the time-slot adaptively. *The results obtained showed that the proposed adaptive transmission protocol was able to improve the information capacity performance when compared to static time-slot configuration.*

This contribution addresses the research question RQ3.

4. **Contribution 4:** *Inference Process to detect cellular tissue deformation.*

   - **P3 :** This article answers this research question by proposing the *Molecular Nanonetwork Inference Process*, which is a technique that utilizies Ca^{2+}-signalling-based molecular communication and a simple machine learning technique to infer the state of compression of the tissue. The machine learning algorithm employs a threshold-based classifier that identifies the threshold boundaries based on a training process. The inference/detection mechanism allows the receiver nanomachine to determine: i) the type of tissue deformation; ii) the amount of tissue deformation; iii) the amount of Ca^{2+} concentration emitted from the transmitter nanomachine; and iv) the distance between transmitter and receiver nanomachines. *The Molecular Nanonetwork Inference Process reached an average level of 80% percent accuracy.* The application of this inference process is for detection of diseases and other abnormality within the tissue (e.g., impairments in the calcium signalling process). For example, current mammography techniques to examine breast cancer requires the patients to be exposed to radiations in order to obtain images of the tumour cells [105]. However, exposing the patients to frequent radiations is also dangerous and can lead to other forms of cancer. Therefore, the proposed inference method can provide data from

embedded nanomachines within the breast tissue that performs periodic sensing. Based on the accuracy of the Molecular Nanonetwork Inference Process, the detection of diseases can also obtain similar accuracy.

This contribution addresses the research question RQ4.

5. **Contribution 5:** *Application of control theory to Ca^{2+}-signalling-based molecular communication system*

   - **P5 :** This article addresses this research question by proposing a feed-forward feedback control model that is incorporated into the astrocytes to control the Ca^{2+} signalling concentration in the tripartite synapse. In particular, the aim is to maintain the concentration within the limits so that this doesn't lead to neurodegenerative diseases.

     For the case of neurodegenerative diseases prevention, three regions for intracellular Ca^{2+} concentration were defined: *extreme high region*, *extreme low region*, and *stable region*. The extreme high region is any value higher than the maximum Ca^{2+} concentration levels, while the extreme low region is any value lower than the minimum Ca^{2+} concentration levels. The objective of using the control model is to regulate the Ca^{2+} concentration in order to maintain stability within the safe region. *The feed-forward feedback control eliminated intracellular Ca^{2+} oscillation as well as maintained stable regulated Ca^{2+} concentration in the stable region.*

     The applications of this feed-forward feedback control model is to possibly lower the probability of neurodegenerative disease spreading when the Ca^{2+} signalling is impaired. This takes a preventive measure and can slow the progression of the disease, where engineered astrocytes with the control model will regulate the quantity of Ca^{2+} concentration, which in turn will control the gliotransmitters

between the cells. The implementation of the feed-forward feedback control technique can be performed using IP3 insertion and extraction. While IP3 insertion can be straightforward, IP3 extraction can be realised using inhibitory chemicals disabling the intercellular Ca^{2+} signalling.This article also showed how the control model can enable molecular nanonetworks to be deployed into the brain without leading to neurodegenerative diseases. This has not been previously investigated, where integrating molecular communication nanonetworks into the brain for sensing and monitoring may result in excessive Ca^{2+} emission. However, the control model will ensure that the concentration are within the safe limits while ensuring that the data rate is not compromised.

This contribution addresses the research question RQ5.

Chapter 4

Comparative End-to-end Analysis of Ca^{2+} Signaling-based Molecular Communication in Biological Tissues

Journal Title:	IEEE Transactions on Communications
Article Type	Regular Paper
Complete Author List	Michael Taynnan Barros, Sasitharan Balasubramaniam and Brendan Jennings
Keywords	Molecular Communication; nanonetworks; Ca^{2+} signaling, information theory, tissue deformation
Status	Published: v. 63, p 5128-5142. December 2015. doi: 10.1109/TCOMM.2015.2487349

5128 IEEE TRANSACTIONS ON COMMUNICATIONS, VOL. 63, NO. 12, DECEMBER 2015

Comparative End-to-End Analysis of Ca^{2+}-Signaling-Based Molecular Communication in Biological Tissues

Michael Taynnan Barros, *Student Member, IEEE*, Sasitharan Balasubramaniam, *Senior Member, IEEE*, and Brendan Jennings, *Member, IEEE*

***Abstract*—Calcium (Ca^{2+})-signaling-based molecular communication is a short-range communication process that diffuses and propagates ions between the cells of a tissue. The communication process is initiated via stimulation and amplification of the production of Ca^{2+} ions within a cell; these ions then diffuse through a physical connection between cells called a gap junction. Ca^{2+} signaling can be found in different classes of cell. In *excitable* cells, initiation of the Ca^{2+}-signaling process is accompanied by an electrical component; for *nonexcitable* cell types, the electrical component is absent; while *hybrid* cells exhibit both behaviors. This paper provides a comparison and analysis of the communication behavior in tissues comprised three specific cell types that utilize Ca^{2+} signaling: *epithelium cells* (nonexcitable), *smooth muscle cells* (excitable), and *astrocytes* (hybrid). The analysis focuses on spatiotemporal Ca^{2+} concentration dynamics and how they are influenced by the intracellular signaling process, the molecular diffusion delay, the gain and capacity of the communication channel, as well as intracellular signaling interference. This analysis of the communication behavior in the context of tissues provides insights useful for, *inter alia*, the design of nanomachines that are situated within tissues and that use analysis of the communication channel to infer tissue health.**

***Index Terms*—Molecular communication, nanonetworks, Ca^{2+} signaling, information theory, cellular tissues.**

I. Introduction

IN RECENT years, a growing research community has formed around modelling biological communications at the nanoscale, a research field referred to as *Molecular Communication* [1], [2], [3], [4], [5]. Modelling biological cells and their interactions as a communication system can provide opportunities in emerging applications of nanotechnology and nanomedicine [6], [7]. Since the birth of this research field, numerous biological components and processes have been analyzed for their suitability for realizing molecular communication systems, including: diffusion-based systems [8], [9], [10], bacterial communication [11], FRET [12], [13] and neuronal communication [14], [15].

A particular biological signaling process proposed as a basis for molecular communication, one which is found in most multi-cellular systems, is *Calcium (Ca^{2+}) signaling* [16]. Ca^{2+} signaling is a short-range communication process commonly used by cells within a tissue. The propagation of Ca^{2+} comprises two stages: *intracellular* and *intercellular* signaling. Intracellular signaling results from internal stimulation that leads to generation and/or amplification of cytosolic Ca^{2+} concentrations. Intercellular signaling involves propagation of cytosolic Ca^{2+} throughout the cellular tissue. Diffusion of Ca^{2+} ions is mediated through gates that connect two cytosolic areas of the cells; these gates are termed *Gap Junctions*. Ca^{2+} signaling is exhibited by a number of different classes of biological cells, but the properties and characteristics of these cells (e.g., size, spatio-temporal signaling behavior, intracellular signaling components) can vary significantly, resulting in a significant impact on the behavior of Ca^{2+} propagation. In this paper, we investigate three different types of cells in order to study the communication characteristics within a three dimensional cellular tissue; these are: *excitable cells* (specifically smooth muscle cells), *non-excitable cells* (specifically epithelial cells) and *hybrid excitable and non-excitable cells* (specifically astrocytes).

The main contributions of the paper are:

- *Communication Theoretic Analysis of Ca^{2+} signaling*—a comparative analysis of the end-to-end communication system for the three different types of tissue. For each tissue, we consider the differences in intra- and inter-signaling process for Ca^{2+} stimulation and generation, as well as the physiological differences in the cells, to analyze the spatio-temporal Ca^{2+} concentration dynamics, molecular delay, channel gain, capacity and intracellular signaling interference. This analysis provides the first comparative analysis of the impact of the cellular properties of different tissue types on the transmission of digital bits using Ca^{2+} signaling through the tissue.

Manuscript received March 20, 2015; revised July 22, 2015 and September 23, 2015; accepted September 29, 2015. Date of publication October 5, 2015; date of current version December 15, 2015. This work was supported in part by the Irish Higher Education Authority under the Program for Research in Third Level Institutions (PRTLI) cycle 5, which is cofunded by the European Regional Development Fund (ERDF), via the Telecommunications Graduate Initiative (http://www.tgi.ie); in part by the Science Foundation Ireland via the CONNECT Research Centre under Grant 13/RC/2077; and in part by the FiDiPro Program of Academy of Finland (Nano Communication Networks), 2012–2016, as well as the Academy Research Fellow Grant (no. 284531). The associate editor coordinating the review of this paper and approving it for publication was M. Pierobon.

M. Taynnan Barros and B. Jennings are with the Telecommunication Software and Systems Group (TSSG), Waterford Institute of Technology (WIT), Waterford, Ireland (e-mail: mbarros@tssg.org; bjennings@tssg.org).

S. Balasubramaniam is with the Nano Communications Center (NCC), Department of Electronics and Communication Engineering, Tampere University of Technology (TUT), Tampere 33720, Finland (e-mail: sasi.bala@tut.fi).

Color versions of one or more of the figures in this paper are available online at http://ieeexplore.ieee.org.

Digital Object Identifier 10.1109/TCOMM.2015.2487349

- *Integrated Ca^{2+} Signaling 3D Tissue Model*—we use stochastic modelling to model the spatio-temporal dynamics of Ca^{2+} signaling [17], presenting a single stochastic mathematical framework by which three dimensional cellular tissues communication of Ca^{2+} signaling for the three cell types can be analyzed. Internal cellular reactions are modeled as being triggered by an stochastic algorithm, and this is coupled with intercellular diffusion process that is also stochastically scheduled. The framework also integrates the opening/closing gap junctions model of Kilinc and Akan [18]—it is this opening/closing behavior that enables cell-cell communication (intercellular communication).

A thorough understanding of the behavior of Ca^{2+} signaling as an end-to-end communication system, to which the analysis here contributes, will be an essential step towards enabling a range of applications, including:

1) *Communicating nanomachines*: Understanding the communication characteristics of Ca^{2+} signaling for each type of cell can provide guidelines in designing nanomachines that are able to control and stimulate the intracellular signaling process for communication. Moreover, this understanding will provide the basis for design of nanonetworks with optimum communication behavior embedded within a tissue;
2) *Modeling diseases*: Impairments in spatio-temporal dynamic Ca^{2+} signaling may be indicative of numerous diseases. These include cancer, Alzheimer's, as well as muscle diseases known as soft tissue diseases [19], [20], [21]. Therefore, understanding communication characteristics in different tissue conditions can lead to new methodologies for early disease detection;
3) *Development of intelligent drug delivery systems*: New drug delivery approaches can be optimized through understanding the performance of Ca^{2+} signaling and gap junction properties, so that optimal quantities of drug molecules to diffuse to target sites can be determined for therapy [7].

The paper is organized as follows. §II presents essential background information about Ca^{2+} signaling as well as the basic Ca^{2+} signaling-based molecular communication model. §III, §IV and §V respectively present specializations of the basic Ca^{2+} signaling-based molecular communication model for excitable, non-excitable and hybrid cell types. §VI introduces the gap junction model, whilst §VII presents the overall mathematical framework. §VIII presents the end-to-end analysis; finally, §IX concludes the paper.

II. Background on Ca^{2+} Signaling

Intracellular Ca^{2+} signaling occurs in the following way: by stimulating the IP_3 [1], bits are encoded through stimulation of Ca^{2+} signals and released (*Stimulation*). At the same time, the released IP_3 also indirectly controls the influx of Ca^{2+} ions to the endoplasmic reticulum and its storage in the cytosolic area (*Storage*). Besides the stimulation process, certain cellular components are also capable of self-generating Ca^{2+} ions (*Amplification*). Finally, exchange of Ca^{2+} ions is conducted in two ways: cell-cell communication (*Diffusion*) and aleatory exchange of Ca^{2+} to the extracellular space (*Release*) [22].

Intercellular Ca^{2+} signaling is central to various physiological and regulatory purposes (e.g., cell growth and proliferation, fertilization, muscle contraction, neuronal transmission, cellular motility and differentiation), and is initiated by IP_3 stimulation, or through hormonal or neurotransmitter signaling. This biological communication platform is found in a variety of cell types, including: *glial or astrocytes* [23], [24], *neurons* [25], *ephitelium* [26], [27], *endothelium* [28], *smooth muscle* [29], *cardiomyocytes* [30], *hepatocytes* [31], *osteocytes* [32], *chondrocytes* [33], *kidney* [34], *mammary gland* [35], *mast* [36], *pancreatic* [37], and *keratinocytes* [38].

Goldbeter et al. [22] modelled the internal cellular regulatory system of Ca^{2+}. Their model accurately describes internal cellular reactions responsible for the production, storage and release of Ca^{2+}. This work originated a variety of models for different types of tissues [39], [26], [27], [23], [24], [29], also with different methodologies [40], [41], [42]. Ca^{2+} signaling has also been analyzed from the perspective of communications, see for example [43], [44], [45]. Even though most of these models are validated, they fail to present one or more of the following characteristics: 1) gap junction cellular coupling; 2) analysis of communication characteristics in three-dimensional tissues; 3) both inter and intracellular analysis; or 4) comparison between tissue types. Moreover, another problem is getting a closed form expression over distance and time for the molecular propagation. This is due to the sum-over-trips problem: the infinite number of trips taken from cell-cell communication, as explored by Harris and Timofeeva [46]. The model presented here addresses these deficiencies, providing a comprehensive treatment of the behavior of intracellular and intercellular Ca^{2+} signaling.

As described in the introduction, we have identified three categories for cells that communicate through Ca^{2+} signaling. We define excitable cells as those that can be stimulated through electrical current only, while non-excitable cells are stimulated through chemical reactions only, and hybrid excitable and non-excitable cells hold properties of both. Examples of cells under each of these classifications include: smooth muscle cells (excitable), epithelial cells (non-excitable) and astrocytes (hybrid). These cell types typically present different characteristics regarding structure, internal reactions, size, and location within the human body. They are distributed throughout the entire human body, but specific to different localities, as illustrated in Fig. 1. Their size varies between 0.5 μm to 50 μm with very different shapes, e.g., smooth muscle cells present a thin elongated elliptical shape, epithelial cells have a square shape and astrocytes have a more complex branching structure. Such cellular characteristics are further described in the following sections, where we will compare and analyze their different Ca^{2+} intracellular signaling properties.

In Fig. 1, the biological process is mapped to a communication system model—the Ca^{2+} ions release mechanism is considered as the transmitter, the propagation of Ca^{2+} across the tissue is considered as the channel, and finally the receiver is represented as regions of cells where the Ca^{2+} concentration

[1] Inositol 1,4,5-trisphosphate (IP_3) is a secondary message molecule that travels through the cytosol and stimulates the release of Ca^{2+} from the endoplasmic reticulum to the cytosol.

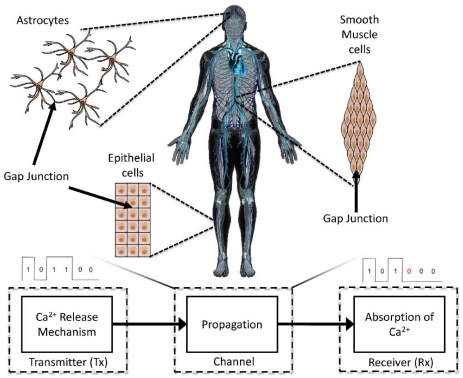

Fig. 1. Block diagram that outlines the Ca^{2+} signaling-based molecular communication model. A Ca^{2+} release mechanism (*transmitter (Tx)*) will lead to propagation of ions inside the tissue (*channel*), where Ca^{2+} will be detected by a group of cells at a certain distance (*receiver (Rx)*).The figure shows the example locations of astrocytes, epithelium and smooth muscle cells, which are explained in Sections III, IV and V. Intercellular communication is enabled through the opening/closing of the gap junctions.

level are measured and analyzed. Cells are connected via gap junctions, which once opened will allow the propagation of Ca^{2+} ions from one cell to another. The different structural properties that characterize the three studied cellular tissues are also depicted in Fig. 1. Fig. 2 shows the block diagram of intracellular Ca^{2+} signaling for the three selected cell types—five common processes were found for all the cells, but the considerable differences regarding the flows between blocks and their intensity are the real focus of our analysis. These differences are important for understanding the Ca^{2+} ion propagation across the cellular tissue.

III. Excitable Cells—Arterial Smooth Muscle Cells

In this section we present the model for the intracellular signaling of smooth muscle cells. Smooth muscle is an involuntary tissue comprised of thin, elongated muscle cells found along the walls of hollow organs such as the digestive tract (lower part of the esophagus, stomach and intestines), the bladder, the uterus, and various ducts of glands and walls of blood vessels. We focus our analysis on arterial smooth muscle cells, found in the arteries of human circulatory system, where their contraction and relaxation is responsible for the regulation of blood pressure and flow. A number of studies have found that smooth muscle tissues are capable of propagating Ca^{2+} throughout the tissue [29]—intercellular Ca^{2+} signaling in smooth muscle cells helps in the arteries' contractile state.

A model of Ca^{2+} oscillation in arterial smooth muscle cells is found in [29], [47]; a visual illustration is provided in Fig. 3. It models five pools of Ca^{2+} storage, including: the cytosolic Ca^{2+} concentration (C_s) (Eq 1); the IP_3 concentration (I_s) (Eq 2); the sarcoplasmic Ca^{2+} concentration (S_s) (Eq 3); the cell membrane potential (V_s) (Eq 4); and the open state probability (Ψ_s) of Ca^{2+} activated potassium channels (Eq 5). The dynamic changes in the pool concentration are represented as:

$$\frac{dC_s}{dt} = \upsilon_1 - \upsilon_2 + \upsilon_3 - \upsilon_4 + \upsilon_5 - \upsilon_6 + \upsilon_7 \quad (1)$$

$$\frac{dI_s}{dt} = \upsilon_8 + \upsilon_9 - \upsilon_{10} \quad (2)$$

$$\frac{dS_s}{dt} = \upsilon_2 - \upsilon_1 - \upsilon_3 \quad (3)$$

$$\frac{dV_s}{dt} = \gamma(-\upsilon_{11} - \upsilon_{12} - 2\upsilon_6 - \upsilon_7 - \upsilon_{13}) + \Psi \quad (4)$$

$$\frac{d\Psi_s}{dt} = \lambda(\Lambda - \Psi_s) \quad (5)$$

In the following, we are going to integrate the equations above to include the internal cellular reactions, which are illustrated in Fig. 3. The intracellular signaling process, upon stimulation, is composed of multiple parallel and sequential reactions. A main process that occurs internally is the Ca^{2+} regeneration υ_1, also known as the Ca^{2+} Induced Ca^{2+} Release (*CICR*), which is modelled as:

$$\upsilon_1 = \Omega \frac{S_s^2}{S_s^2 + s_c^2} \frac{C_s^4}{C_s^4 + c_c^4} \quad (6)$$

in which Ω is the rate constant, s_c is the half-point of the Ω Ca^{2+} efflux sigmoidal and c_c is the half-point of the rate constant Ω activation sigmoidal.

Upon stimulation, the Ca^{2+} uptake from the *sarcoplamic reticulum* υ_2 is represented as:

$$\upsilon_2 = \phi \frac{C_s^2}{C_s^2 + c_b^2} \quad (7)$$

in which ϕ is the sarcoplasmic reticulum uptake rate constant and c_b is the half-point of the sarcoplasmic reticulum *ATPase* activation sigmoidal. The leakage of Ca^{2+} from the sarcoplamic reticulum is modelled by $\upsilon_3 = LS_s$, in which L is the Ca^{2+} leakage from the sarcoplamic reticulum constant.

The υ_4 term models the Ca^{2+} extrusion from the arterial smooth muscle cells by Ca^{2+}-ATPase pumps, which are responsible for the metabolism and energy management in the cell:

$$\upsilon_4 = \phi_c \left(1 + \frac{\Psi_s - v_d}{\varrho_d}\right) \quad (8)$$

in which ϕ_c is the rate constant, v_d is the voltage dependence, ϱ_d is the slope of voltage dependence of extrusion ATPase.

The generation of IP_3, termed υ_5, is modelled as:

$$\upsilon_5 = F \frac{I_s^2}{K_I^2 + I_s^2} \quad (9)$$

in which F is the half-saturation constant for agonist-dependent Ca^{2+} entry and K_I^2 is the rate of IP_3 degradation.

The υ_6 term models the Ca^{2+} influx through Voltage-Operated Ca^{2+} Channel (*VOCCS*) channels:

$$\upsilon_6 = \chi_C \frac{\Psi_s - v_{C1}}{1 + e^{-[(\Psi_s - v_{C2})/\varrho_C]}} \quad (10)$$

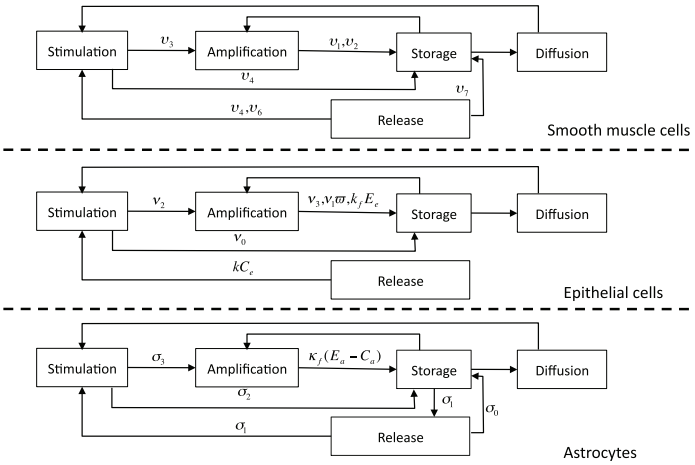

Fig. 2. Block diagram of the intracellular Ca^{2+} signaling for Smooth Muscle cells, Epithelial cells and Astrocytes. The five main common blocks involved in this process are: Stimulation, Amplification, Storage, Release and Diffusion. However, significant differences in terms of the contributing factors and the intensity of the flows mean that the overall process behavior varies considerably. Correctly modelling these factors is essential to accurately characterize signal propagation characteristics.

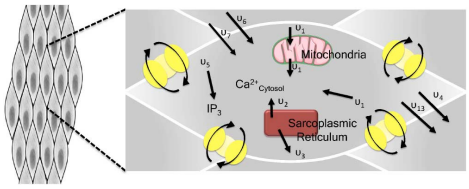

Fig. 3. The stages of the Ca^{2+} signaling process in Arterial Smooth Muscle cells: The process starts with stimulation and production of Ca^{2+} from the CICR and IP_3 processes. Ca^{2+} is then amplified using mitochondria and sarcoplasmic reticulum. Leakage of Ca^{2+} outwards into the cytosol is performed by the Ca^{2+}-ATPase and Potassium efflux. Leakage of Ca^{2+} inwards within the cell is performed by VOCCS channels and by Na^+/Ca^{2+} exchange. Finally, the cytosolic Ca^{2+} ions are propagated throughout the cellular tissue via diffusion.

in which χ_C is the whole cell conductance, v_{C1} is the reversal potential, v_{C2} is the half-point, and ϱ_C is the maximum slope of the VOCC activation sigmoidal.

The Na^+/Ca^{2+} ratio exchange, termed υ_7, is represented as:

$$\upsilon_7 = \Upsilon_7 \frac{C_s}{C_s + c_7}(\Psi_s - v_p) \tag{11}$$

in which Υ_7 is the whole cell conductance, c_7 is the half-point for activation, and v_p is the reversal potential for the Na^+/Ca^{2+} exchange.

The constant υ_8 is the rate of PLC (Phosphoinositide phospholipase C) activated by the receptor-ligand agonists, while the term υ_9, represented as:

$$\upsilon_9 = E \frac{C_s^2}{K_C^2 + C_s^2} \tag{12}$$

models the protein $PLC-\delta$, in which E is the maximum rate of $PLC-\delta$ and K_C^2 is the half-saturation constant for Ca^{2+} activation of $PLC-\delta$.

The term $\upsilon_{10} = K_I I_s$, models IP_3 degradation. The term υ_{11} models the Na^+-K^+-ATPase, which is another internal cellular regulation process. The υ_{12} models the chloride channel and is represented as:

$$\upsilon_{12} = \Upsilon_{12}(\Psi_s - v_h) \tag{13}$$

in which Υ_h is the whole cell conductance for Cl^- current and v_h is the reversal potential for K^+.

Potassium K^+ efflux in the cytosol is modelled by:

$$\upsilon_{13} = \Upsilon_{13} W_s(\Psi_s - v_K) \tag{14}$$

in which Υ_{13} is the whole cell conductance for K^+ efflux and v_K is the reversal potential for K^+.

One property of the smooth muscle cells is the ability to conduct electrical current. This is added to the model with the electrical coupling among cells as is expressed as:

$$\Psi = -g \sum_j (\Psi_s - \Psi_j) \tag{15}$$

in which g is the homo-cellular electrical coupling coefficient and j is the index for the number of neighbouring cells. The K^+ channel activation is performed through both Ca^{2+} propagation and electrical voltage, and is represented as:

$$\Lambda = \frac{(C_s + c_w)^2}{(C_s + c_w)^2 + \eta e^{-[(\Psi_s - v_{c3})/\varrho_K]}} \tag{16}$$

in which c_w is the translation factor for Ca^{2+} dependence of K_{Ca} channel activation sigmoidal, η is the translation factor for

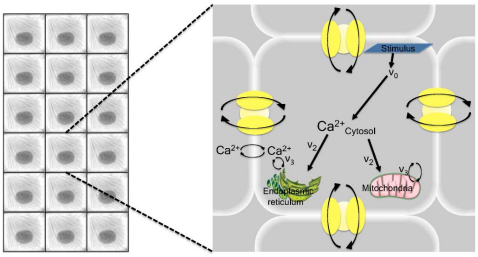

Fig. 4. The stages of the Ca^{2+} signaling process in the epithelial cells. The process starts from the stimulation and extracellular leakage of Ca^{2+} ions into the cytosol. This is followed by the transport of the Ca^{2+} ions from the cellular store (or cytosolic space) to the endoplasmic reticulum. After the transport, the endoplasmic reticulum releases the Ca^{2+} ions into the cytosol, where the release will also include the leakage of Ca^{2+} ions. Lastly, the Ca^{2+} ions are transported from the cytosol to the extracellular space.

membrane potential dependence of K_{Ca} channel activation sigmoidal, V_{C3} is the half-point for the K_{Ca} channel activation sigmoidal and ϱ_K is the maximum slope of the K_{Ca} activation sigmoidal.

IV. Non-Excitable Cells—Epithelial Cells

Epithelial cells are one of the most basic type of cells found in animal tissue; they are responsible for a wide set of tasks, including secretion, selective absorption, protection, transcellular transport and detection of sensation. Epithelial cells can be found throughout the body, covering both external surfaces (endothelium [28]) and internal organs (kidney cells [34], hepatocytes [31] and pancreatic cells [37]). One interesting characteristic is their tightly packed structure, with almost no intercellular space. Epithelial cells come in a variety of geometrical shapes, including square-shape—referred to as simple cuboidal epithelial cells—which is the structure we consider in our analysis. In vitro and in vivo experiments, like those reported in [26], [27], have investigated the spatial-temporal dynamics of intercellular Ca^{2+} signaling in this type of cell.

The model proposed by Goldbeter et al. [22] is used for modeling Ca^{2+} signaling [48] in epithelial cells; Fig. 4 provides a visual presentation of the model. Equations (17) and (18) describe the behavior of the cytosolic Ca^{2+} concentration (C_e), as well as the secondary Ca^{2+} pool concentration (E_e) [22]. These equation show how the Ca^{2+} oscillations result from a simple regenerative process that requires a secondary pool for system equilibrium. The secondary pool generally is used for Ca^{2+} regeneration, however, it has also other functions including protein transport. In epithelial cells, the secondary pool is usually the endoplasmic reticulum. The primary pool has an influx magnitude $v_1\varpi$, where ϖ represents the saturation function of the receptors and v_1 represents the rate of Ca^{2+} release. The components of the equations as well as their roles, illustrated in Fig. 4, include: 1) v_0: Ca^{2+} leakage from the extracellular space into the cellular cytosol; 2) v_2: transport of Ca^{2+} ions from the cellular cytosol to the endoplasmic reticulum, defined by (19); 3) v_3: release of Ca^{2+} from the cellular endoplasmic reticulum into the cytosol, defined by (20); 4) $k_f E_e$: Ca^{2+} leakage from the endoplasmic reticulum to the cytosol; 5) kC_e: transport of Ca^{2+} ions from the cytosol to the extracellular space. The cytosolic Ca^{2+} concentration (C_e), as well as the secondary Ca^{2+} pool concentration (E_e) is represented as:

$$\frac{dC_e}{dt} = v_0 + v_1\varpi - v_2 + v_3 + k_f E_e - kC_e \tag{17}$$

$$\frac{dE_e}{dt} = v_2 - v_3 - k_f E_e \tag{18}$$

However, before the Ca^{2+} ions are diffused to the neighbouring cells, the ions will first need to be activated through the IP_3 receptors, which is an internal cellular secondary channel that leads to self-amplification. This process will increase the cytosolic Ca^{2+} concentration to be ready for diffusion. The following equations represent the Ca^{2+} self-amplification mechanism from the Ca^{2+} pool due to the activation of the IP_3 receptors:

$$v_2 = V_{M2}\frac{C_e^n}{k_2^n + C_e^n} \tag{19}$$

$$v_3 = V_{M3}\frac{E_e^m}{k_R^m + E_e^m}\cdot\frac{C_e^p}{k_A^p + C_e^p} \tag{20}$$

where: V_{M2} and V_{M3} are the rate constants; k_2, k_R and k_A are the threshold constants; and n, m and p are the Hill coefficients [22], which are used to quantify cooperative binding—meaning the interaction of one or more molecules into a binding structure.

V. Hybrid Cells—Astrocytes

Astrocytes are a star-shaped form of *Glia* cells, responsible for a wide range of complex and important functions relating to maintenance of the health of the central nervous system. These functions include primary roles in synaptic transmission and information processing by neural circuits. Specifically, these non-neural cells in the brain are responsible for spatial neuron support, neuron nutrients and oxygen supply, neuronal isolation, pathogen destruction, as well as removal of dead neurons. Astrocytes are the most abundant cells within the central nervous system [49]. They can be found in the spinal cord as well as the brain, where they are responsible for communication with both excitable and non-excitable cells. Studies have shown that astrocytes propagate intercellular Ca^{2+} signals over relatively long distances in response to stimulation [23], [24].

In this section we introduce a model describing Ca^{2+} oscillations in astrocytes that was proposed by Lavrentovich and Hemkin [50]; this model is visualized in Fig. 5. The model is in accordance with experimental observation [50]. Similar to the smooth muscle excitable cells, there are Ca^{2+} pool storage models, which includes: Ca^{2+} concentration in the cytosol

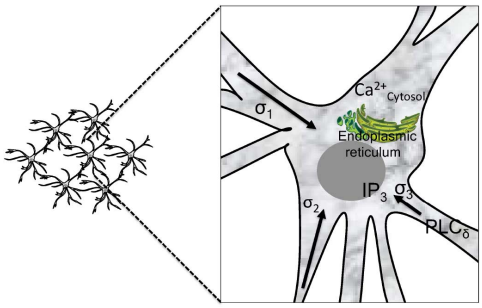

Fig. 5. The stages of the Ca^{2+} signaling process in astrocytes. After stimulation, IP_3 is produced by the PLC protein (*Phosphoinositide phospholipase C*), which leads to the increase of the internal Ca^{2+} concentration. This is because we use the isoform PLC, which is correlated with the internal cytosolic Ca^{2+} level. This internal concentration is then amplified using the endoplasmic reticulum. Diffusion of Ca^{2+} ions through the cellular tissue then occurs.

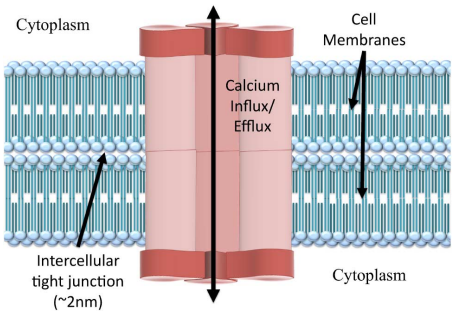

Fig. 6. Side view from a gap junction gate. The intercellular tight junction ($2nm$) separates the two neighbouring cells, which are connected via gap junctions. This enables the Ca^{2+} influx and efflux through the cellular membranes.

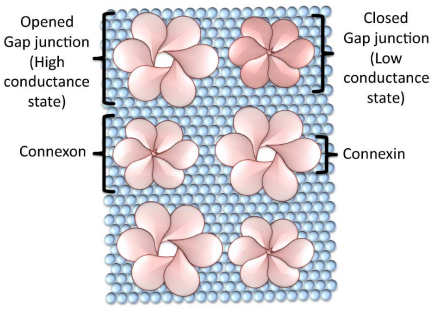

Fig. 7. Top view of the gap junctions. A single gap junction gate is referred to as the *connexon*, which is formed by six proteins called *connexin*. These gates have two states: *high conductance* state and a *low conductance* state—equivalently to the opened or closed status of the junction.

(C_a) (Eq. 21); Ca^{2+} concentration in the endoplasmic reticulum (E_a) (Eq. 22); and IP_3 concentration (I_a) (Eq. 23). They are represented by the following equations:

$$\frac{dC_a}{dt} = \sigma_0 - \kappa_o C_a + \sigma_1 - \sigma_2 + \kappa_f (E_a - C_a) \tag{21}$$

$$\frac{dE_a}{dt} = \sigma_2 - \sigma_1 - \kappa_f (E_a - C_a) \tag{22}$$

$$\frac{dI_a}{dt} = \sigma_3 - \kappa_d I_a \tag{23}$$

where σ_0 is the flow of Ca^{2+} from the extracellular space into the cytosol[2], $\kappa_o C_a$ is the rate of Ca^{2+} efflux from the cytosol to the extracellular space, $\kappa_f (E_a - C_a)$ is the leak flux from the endoplasmic reticulum into the cytosol and $\kappa_d I_a$ is the degradation of IP_3.

The σ_1 term (Eq. 24), models the Ca^{2+} flux from the endoplasmic reticulum to the cytosol via IP_3 stimulation. In common with excitable and non-excitable cells, this mechanism directly affects the cytosolic concentration of Ca^{2+}. It is represented as:

$$\sigma_1 = 4\Sigma_{M3} \frac{\kappa_{C1}^n C_a^n}{(C_a^n + \kappa_{C1}^n)(C_a^n + \kappa_{C2}^n)} \cdot \frac{I_a^m}{\kappa_I^m + I_a^m} (E_a - C_a) \tag{24}$$

where Σ_{m3} is the maximum flux value of Ca^{2+} into the cytosol, κ_{C1}^n and κ_{C2}^n are the activating and inhibiting variables for the IP_3 and the m and n are the Hill coefficients.

The efflux of Ca^{2+} from the sarco(endo)plasmic reticulum to the endoplasmic reticulum is modelled as σ_2:

$$\sigma_2 = \Sigma_{M2} \frac{C_a^2}{\kappa_2^2 + C_a^2} \tag{25}$$

[2]This term can be extended into a voltage dependent term, called voltage-gated Ca^{2+} channels, which was further studied in [51].

where Σ_{M2} is the maximum flux of Ca^{2+} in this process. Finally, σ_3 describes IP_3 generation by the Phosphoinositide phospholipase C (PLC) protein:

$$\sigma_3 = \Sigma_p \frac{C_a^2}{\kappa_p^2 + C_a^2} \tag{26}$$

where Σ_p is the maximum flux of Ca^{2+} in this process, and p is the Hill coefficient.

VI. Modeling Gap Junction Behavior

In intercellular communication Ca^{2+} ions are propagated through cellular tissues via a physical gate that connects the cytosolic areas of two neighbourings cells; these gates are called *Gap Junctions*. Fig. 6 shows how gap junctions connect two cytosols. The gap junctions are composed of two *connexons*, one in each connecting cell, which is formed by six proteins called *connexins*—as shown in Fig. 7.

Gap junctions are found in many animal cellular tissues with varying configurations. The distribution of the connexins

per cell has a fundamental impact on the diffusion behavior. Changes in those characteristics may lead to different types of diseases, including cancer, cardiac ischemia and cardiac hypertrophy [52]. Given this, control of gap junction behavior is a possible tool for drug delivery systems and disease treatment. Cellular growth is directly involved with gap junction control: regulatory growth signals are transmitted through gap junctions, and decreased communication capacity may lead to uncontrolled growth in extreme cases, as in cancer [53]. Studies have shown how communication capacity can control growth, in which connexin genes were transfected into tumorigenic cell lines [54]. Ca^{2+} intercellular signaling plays two fundamental roles in influencing the gap junctions channels. It not only activates the gap junction channel, with intercellular oscillations, but Ca^{2+} can also be transferred to a neighbour cell by diffusion. Here we focus only on the diffusion process of the Ca^{2+} ions through the junction.

Intercellular diffusion only occurs when both connexons are opened at the same time. We present in this section a stochastic model that models when both gates are opened in each cell. According to the selected cell types studied in this paper, we identified two different types of connexins: *Cx43* for astrocytes and smooth muscle cells and *Cx45* for epithelial cells.

A stochastic model of gap junction behavior was introduced by Baigent et al. [55] and first studied for molecular communication by Kilinc and Akan [18]. The model considers voltage-sensitive gap junctions which are assumed to have two states of conductance for each connexin: an open state with high conductance and a closed state with low conductance as illustrated in Fig. 7. Based on this, we consider four basic combination of states from each connexin of the connexon:

- *State HH*: Both gates are in a high conductance state. This probability is denoted by p_{HH};
- *State HL*: One gate is in a high conductance state and the other is in a low conductance state. This probability is denoted by p_{HL};
- *State LH*: One gate is in a low conductance state and the other is in a high conductance state. This probability is denoted by p_{LH};
- *State LL*: Both gates are in a low conductance state. This probability is denoted by p_{LL}.

Experimental validation of the model indicated that the LL state appears to present very low occurrence rates [56], thus we neglect that state here. Thus, the probabilities should follow:

$$p_{HH} + p_{HL} + p_{LH} = 1 \tag{27}$$

Moreover, p_{HH}, p_{HL} and p_{LH} are interrelated as follows:

$$\frac{dp_{HL}}{dt} = \beta_1(\vartheta_j) \times p_{HH} - \alpha_1(\vartheta_j) \times p_{LH} \tag{28}$$

$$\frac{dp_{LH}}{dt} = \beta_2(\vartheta_j) \times p_{HH} - \alpha_2(\vartheta_j) \times p_{HL} \tag{29}$$

where the control of the gap junctions permeability is mediated through the potential difference of the membrane of two adjacent cells (ϑ_j), the gate opening rate is α and gate closing rate is β. The terms $\alpha_1(\vartheta_j)$, $\alpha_2(\vartheta_j)$, $\beta_1(\vartheta_j)$ and $\beta_2(\vartheta_j)$ are defined as:

$$\alpha_1(\vartheta_j) = \lambda e^{-A_\alpha(\vartheta_j - \vartheta_0)} \tag{30}$$

$$\alpha_2(\vartheta_j) = \lambda e^{A_\alpha(\vartheta_j + \vartheta_0)} \tag{31}$$

$$\beta_1(\vartheta_j) = \lambda e^{A_\beta(\vartheta_j - \vartheta_0)} \tag{32}$$

$$\beta_2(\vartheta_j) = \lambda e^{-A_\beta(\vartheta_j + \vartheta_0)} \tag{33}$$

where ϑ_0 is the junctional voltage at which the opening and closing rates of the gap junctions have the same common value λ, and A_α and A_β are constants that indicate the sensitivity of a gap junction to the junctional voltage.

For our analysis we used experimental data from the literature [55], [57], [58], [59] for both types of connexin (*Cx43* and *Cx45*) to solve the equations presented in this section; the parameter values used are listed in Table I. We can observe the stochastic behavior of the gap junctions opening and closing for the three cell types in Fig. 8. We assume that the initial probability values are the same for all variables. All the results present different probability distribution for the two types of gap junctions. Since the opening and closing probabilities of the gap junctions are different for the different cellular tissue types, we expect different patterns of Ca^{2+} propagation (due also to the impact of different internal cellular properties).

TABLE I
EXPERIMENTAL VARIABLE VALUES FOR CX43 AND CX45 WITH THREE DIFFERENT TYPES OF CELLS: SMOOTH MUSCLE CELLS, EPITHELIUM AND ASTROCYTES [55] [57] [58] [59]

Variable	Value		
	Smooth Muscle Cells	Ephitelium	Astrocytes
λ	0.69	0.06	0.37
ϑ_j mV	28	0	90
ϑ_0 mV	62	11.1	60
A_α $(\text{mV})^{-1}$	0.004	0.045	0.008
A_β $(\text{mV})^{-1}$	0.07	0.057	0.67

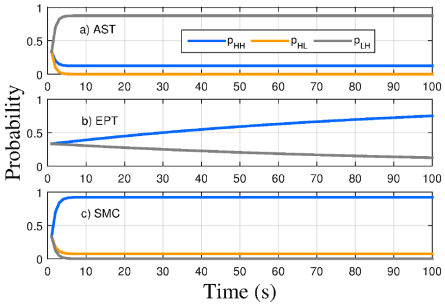

Fig. 8. Probability values of states p_{HH}, p_{HL} and p_{LH} for (a) astrocyte tissues, (b) epithelium tissues, and (c) smooth muscle cells. Two different gap junctions are analyzed: *Cx43* for (a) and (c); and *Cx45* for (b). All parameter values used for these calculations are listed in Table I.

TABLE II
SIMULATION PARAMETERS FOR ASTROCYTES [50]

Variable	Value
C_a	$0.1\mu M$
E_a	$1.5\mu M$
I_a	$0.1\mu M$
σ_0	$0.05\ \mu M$
κ_o	$0.5\ s^{-1}$
κ_f	$0.5\ s^{-1}$
κ_d	$0.08\ s^{-1}$
Σ_{M2}	$15\mu M/s$
κ_2	$0.1\mu M$
Σ_p	$0.05\mu M/s$
κ_p	$0.3\mu M$
n	2.02
κ_{C1}	$0.15\mu M$
κ_{C2}	$0.15\mu M$
κ_I	$0.1\mu M$
Σ_{M3}	$40.0s^{-1}$
m	2.2
D	$350\mu m^2/s$

TABLE III
SIMULATION PARAMETERS FOR EPITHELIAL CELLS [22]

Variable	Value
C_E	$0.01\mu M$
E_e	$0.1\mu M$
v_0	$1\mu M$
v_1	$1001/s$
ϖ	1
k_f	$11/s$
k	$4.21/s$
V_{M2}	$50\ \mu M/s$
k_2	$1\mu M$
k_R	$2\mu M$
k_A	$0.9\mu M$
p	4
m	2
n	2
D	$10\mu m^2/s$

TABLE IV
SIMULATION PARAMETERS FOR SMOOTH MUSCLE CELLS [47]

Variable	Value
γ	$1970\ mV/\mu M$
λ	45.0
C_s	$0.1\mu M$
I_s	$0.82\mu M$
V_s	$-44mV$
W_s	0.06
S_s	$0.9\mu M$
Ω	$55\mu M/s$
s_c	$2.0\mu M$
c_c	$0.9\mu M$
ϕ	$2.025\mu M/s$
c_b	$1.0\mu M$
ϕ_c	$0.08s^{-12}$
v_d	$-100.0mV$
ϱ_d	$250.0mV$
F	$0.23\mu M/s$
K_I	$1\mu M$
χ_C	$0.00129\mu M mV^{-1}s^{-1}$
v_{C1}	$100mV$
v_{C2}	$-24.0mV$
ϱ_C	8.5mV
Υ_7	$0.007\mu M mV^{-1}s^{-12}$
c_7	$0.5\mu M$
v_p	$-30mV^2$
E	$0\mu M/s^2$
K_C	$0.3\mu M$
Υ_{12}	$0.00134\mu M mV^{-1}s^{-1}$
v_h	$-25.0mV$
Υ_{13}	$0.002\mu M mV^{-1}s^{-12}$
v_K	$-94.0mV$
g	$1000s^{-1}$
c_w	$0\ \mu M$
η	$0.13\mu M^2$
v_{C3}	$-27.0mV$
ϱ_K	$12.0mV$
D	$250\mu m^2/s$

VII. INTEGRATED Ca^{2+} SIGNALING 3D TISSUE MODEL

Intracellular Ca^{2+} signaling models were presented in §III, §IV and §V for the smooth muscle cells, epithelial cells and astrocytes, respectively. §VI discussed the closing and opening behavior of the gap junctions that will influence intercellular Ca^{2+} diffusion. In this section, a single mathematical framework groups the aforementioned models alongside diffusion and 3D cellular tissue modelling. Both intracellular and intercellular signaling are modelled together in this framework. Spatio-temporal dynamics can be studied across a 3D cellular tissue with an in-depth analysis, correlating phenomenona and variables at different scales. We divide the description in two parts: first we discuss 3D modelling of the cellular tissues, then we discuss the stochastic model for the scheduling of reactions within individual cells. This framework is an extension of the models presented by Nakano and Liu [60] and our own previous work [61], [62], [63].

A. 3D Modelling of Cellular Tissue Structure

We consider a cellular tissue space (S) composed of $I \times J \times K$ cells (c), where $c_{i,j,k}$ ($i = 1 \ldots I$; $j = 1, \ldots J$ and $k = 1, \ldots K$) denotes an arbitrary cell in the tissue. The cells are connected with a maximum of six neighboring cells. In the case of the excitable and non-excitable cells, the organization of the cells is assumed to be a layered lattice. However, for astrocytes, the organization is going to depend on the type of topology connection. We use simple regular connection to perfectly match our lattice model, that is based on the study of astrocytes topologies [64].

Consider that each cell contains a set of internal reactions of P1 and P2 pools as depicted in Fig. 9. Each reaction and pool for a specific cell type were defined in §III, §IV and §V for the three cell classes. The stochastic solver computes the values of each pool over time, selecting and executing scheduled reactions. The pool will be negatively or positively affected by a constant α when a certain reaction is executed.

Modelling diffusion in a cellular tissue area captures the temporal-spatial dynamics of intercellular Ca^{2+} signaling. We use Ca^{2+} concentration difference to model this temporal-spatial characteristic, as follows [60]:

$$Z_\Delta(i, j, k, n, m, l) = \frac{D}{v}(|Z_{n,m,l} - Z_{i,j,k}|) \times p_{(.)} \qquad (34)$$

where $n \in (i-1, i+1)$, $m \in (j-1, j+1)$, $l \in (k-1, k+1)$, D is the diffusion coefficient, v is the volume of the cell, and Z_Δ is the difference in Ca^{2+} concentration between the cells.

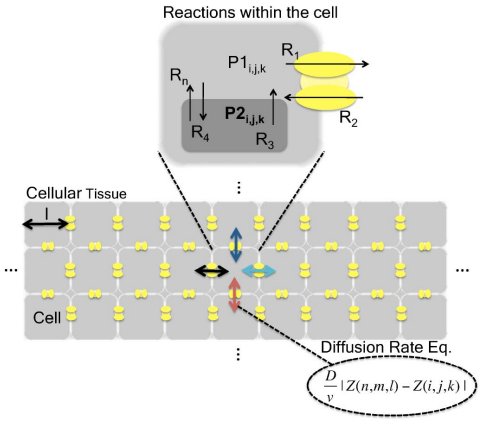

Fig. 9. Depiction of a three-layered cellular tissue, where each layer contains an array of cells. Both the reactions within cells and the diffusion process to neighbouring cells are shown.

$p_{(.)}$ is the probability of the gap junction opening and closing. Based on §VI, we define three different diffusion reactions for each cellular connection. Such reactions are the multiplication of the probabilities (p_{HH}, p_{HL} and p_{LH}) with the regular cell-to-cell diffusion probability.

B. Stochastic Solver

We present in this section a stochastic solver, which determines the quantity of each pool over time. At each time step, the Gillespie algorithm [65] is executed to select a random cell and a random internal reaction of that cell based on probability $P(r_j, \tau_t)$ (Eq. 38), also scheduling a time step (t) to each one of them.

The process of executing one of the distinct reactions in R requires a scheduling process divided in two phases—selecting a reaction and selecting a time step. Each reaction is allocated a reaction constant (a_r). Considering that α_0 is the summation of all a_r in R, the next reaction chosen r_u will be:

$$r_u = \text{MAX}\left\{\frac{a_{r_j}}{\alpha_0} = \frac{a_{r_j}}{\sum_{j=1}^{|R|} a_{r_j}}\right\}, u \in \mathbb{N}, u \in R \quad (35)$$

which follows the *roulette wheel selection* process, which selects the events based on their probability values. However, u must satisfy the following restriction:

$$\sum_{j=1}^{u-1} \frac{\alpha_{r_j}}{\alpha_0} < \rho_2 \leq \sum_{j=1}^{u} \frac{\alpha_{r_j}}{\alpha_0} \quad (36)$$

in which ρ_2 is a uniform random variable with values in the range (0,1).

At each time step (t), a time lapse (τ_t) is derived based on α_0, and is represented as:

$$\alpha_0 \cdot \tau_t = \ln\frac{1}{\rho_1} \quad (37)$$

in which ρ_1 is a uniform random variable with values in the range (0,1). This process ends when $\sum_{i=0}^{|T|} \tau_i < t_\theta$, where T is the set of t and t_θ is the maximum simulation time.

The effect of executing a reaction is basically changing the values of the pools. According to the differential equation in hand, a constant will change the value of the pool according to the positive or negative effect of the executed reaction. The probability of selecting a reaction ($P(r_j, \tau_t)$) is defined as follows:

$$P(r_j, \tau_t)dt = \alpha_{r_j} e^{-\alpha_0 \tau_t} dt \quad (38)$$

The $P(r_j, \tau_t)$ favours a cell $c_{i,j,k}$ with a high value in its pool. Consequently, a high quantity of Ca^{2+} will lead to diffusion, which will model the propagation of the molecules across the cellular space.

VIII. End-to-End Communication Analysis

We now present an end-to-end analysis of the biological Ca^{2+} signaling process. As discussed in §II, the biological process was mapped into a communication system with the intention to provide a greater understanding of those tissue types using communication and information theory tools. We divide our analysis into five different parts: spatio-temporal Ca^{2+} concentration dynamics, end-to-end molecular delay, channel gain, information capacity, and intracellular signaling interference.

For all the results presented here we assume the transmitter (Tx) is positioned at the center of the cellular tissue, and the receiver (Rx) is positioned in the same layer but at a certain distance away (Dx) from the Tx, where Dx is the number of cells between the Tx and the Rx. A comparison of the actual size of the three different cell types we consider is shown in Fig. 11. Also, all used parameters values are found in Tables II, III and IV.

A. Spatio-Temporal Ca^{2+} Concentration Dynamics

The Ca^{2+} concentration levels can be analyzed through heat maps, giving insights into spatio-temporal molecular propagation patterns. Fig. 10 presents a heat map graph of a *3 x (10 x l) x (20 x l) (μm)* cellular space, where l is the length of each cell, as shown in Fig. 11. The stimulation produces an oscillation of the Ca^{2+} concentration levels, which are depicted on the right hand side in Fig. 10.

Regarding the oscillation of Ca^{2+} concentration levels, the three tissues present different oscillation frequency values. Based on experimental data [29], [22], [50], the astrocytes have the lowest frequency ($f = 0.1$ Hz), while the smooth muscle cells ($f = 0.5$ Hz) and epithelial cells ($f = 1$ Hz) have the higher frequencies. An interesting observation is the highest values for Ca^{2+} concentration levels reached in each tissue.

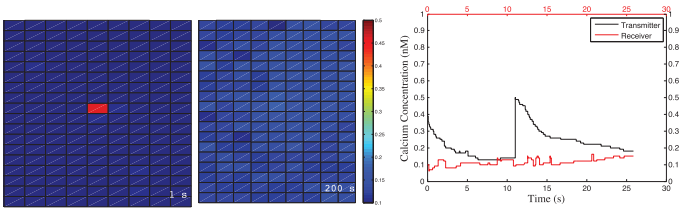

(a) Astrocytes.

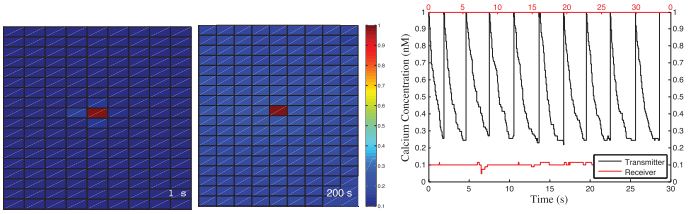

(b) Ephitelium Cells.

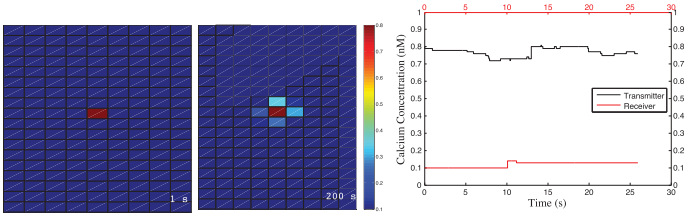

(c) Smooth Muscle Cells.

Fig. 10. The Ca^{2+} concentration heat maps (left) and Ca^{2+} oscillation for a single cell (right). The Rx concentration is $500nM$, Dx is 8 cells, and the oscillation values are: Astrocytes ($f = 0.1\ Hz$), smooth muscle cells ($f = 0.5\ Hz$) and epithelial ($f = 1\ Hz$).

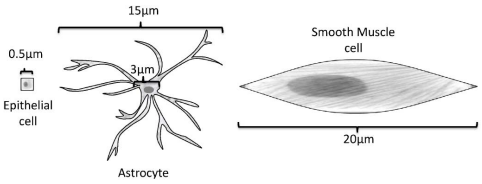

Fig. 11. Comparison between the size of an epithelial, smooth muscle, and astrocyte cell.

The epithelium has the highest value ($Z = 1$ μM), followed by smooth muscle cells ($Z = 0.8$ μM) and astrocytes ($Z = 0.6$ μM). These tissues present naturally different diffusion properties, which are expressed into the diffusion coefficient (D). Intuitively, higher values of the diffusion coefficients lead to higher diffusion rates.

Observing the Ca^{2+} concentration levels alone in Fig. 10, a difference in patterns and values can be seen. In smooth muscle cells, the propagation of Ca^{2+} is limited to short μm distance. For the epithelium tissue, Ca^{2+} travels much faster. This difference in behavior can be explained from Eq. 34, in which the tissue diffusion coefficients alongside with the cell volume and the gap junctions' opening probability will dictate the diffusion probability. Even though the coefficient of diffusion is higher for smooth muscle cell ($D = 250$ (μm^2/s)), their volume ($v = 8000\ \mu m^3$) will decrease the probability of this reaction to occur. Epithelial cells ($D = 10$ (μm^2/s)), on the other hand, are more likely to diffuse Ca^{2+} due to a lower volume ($v = 0.0125\ \mu m^3$). And finally for astrocytes, it stands somewhere between epithelial cells and smooth muscle cells, in which coefficient of diffusion ($D = 350$ (μm^2/s)) and their volume ($v = 141.13\ \mu m^3$) present a fast propagation of Ca^{2+} even though the cell size (Fig. 11) is relatively large compared to epithelial cells.

B. End-to-End Molecular Delay

One of the main characteristics of molecular communication compared to electromagnetic communication is that molecules are spatially transmitted at far slower rates. Thus, it is understandable that end-to-end delay will be a critical consideration. To fairly measure the amount of molecules that are transmitted as well as the time it travels over a certain distance of a cellular tissue, we propose measuring the amount of Ca^{2+} transmitted

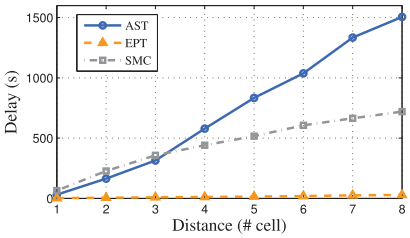

Fig. 12. End-to-end delay as a function of the distance (number of cells) for a 3 x (3 x l) x (20 x l) (μm) cellular tissue for arterial smooth muscle cells (SMC), epithelium cells (EPT) and astrocyte cells (AST). The oscillation frequency is $1kHz$, for astrocytes with the Tx concentration of $2000nM$ and the Rx concentration of $100000nM$. For epithelial cells the Tx concentration is $2000nM$ and the Rx concentration is $10000nM$, and for the smooth muscle cells, the Tx concentration is $2000nM$ and the Rx concentration is $1000nM$.

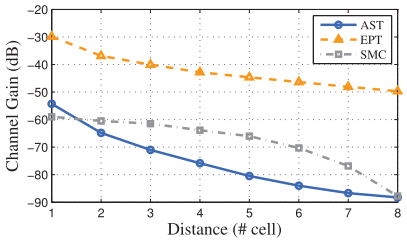

Fig. 13. End-to-end gain as a function of the distance (number of cells) for a 3 x (3 x l) x (20 x l) (µm) cellular tissue for arterial smooth muscle cells, epithelium cells and astrocyte cells. The oscillation frequency is $1kHz$, for astrocytes with the Tx concentration of $2000nM$ and the Rx concentration of $100000nM$. For epithelial cells the Tx concentration is $2000nM$ and the Rx concentration is $10000nM$, and for the smooth muscle cells, the Tx concentration is $2000nM$ and the Rx concentration is $1000nM$.

compared to the Ca^{2+} received over time. In this way, delay is appropriately measured for each bit, since the information is encoded into molecular concentration of Ca^{2+} signals. The proposed method is modelled by the following formula:

$$\int_0^{T_R} C_R(x,t)\,\mathrm{d}t = \int_0^{T_T} C_T(t)\,\mathrm{d}t, \tag{39}$$

in which, C_R is a function that returns the Ca^{2+} concentration of a Rx at time t, C_T returns the Tx Ca^{2+} concentration at time t, T_T is the time slot length of the Tx and T_R is the time slot length of the Rx. Here, the end-to-end delay will be T_R.

Fig. 12 presents the end-to-end delay results for the three cellular tissues. All three present a natural increase of the delay over the distance. Epithelial cells present the lowest delay values, and this is due to the actual size of the cells as shown in Fig. 11. Astrocytes have the medium delay performance while the smooth muscle cells have the highest delay values. In the case of the astrocytes, when the distance of the cells is higher than three, the IP_3 regeneration process from the astrocytes start producing and releasing Ca^{2+} ions and delays the signal (Eqs 23 and 24). In the case of smooth muscle cells, which also have have IP_3 (Eq 9), its most frequent reaction are involved with the electrical signal flow (Eqs 13, 14 and 15), which contributes to the delayed performance.

C. End-to-End Channel Gain

Due to the equal diffusion direction probability (Eq. 34), Ca^{2+} may not reach the Rx. Naturally, the amplitude of the received signal is negatively affected by longer distances between the Tx and Rx. We analyze this phenomenon using gain, which is calculated using the following formula [66]:

$$\Gamma(f) = 10log\left(\frac{\Gamma_T(f)}{\Gamma_{T0}(f)}\right), \tag{40}$$

where $\Gamma_T(f)$ is the average peak concentration and $\Gamma_{T0}(f)$ is the initial peak concentration.

Fig. 13 presents the results for the end-to-end channel gain with respect to the distance (number of cells). The results confirm the intuition that longer distances affect negatively in the performance of the system. Astrocytes present the lowest channel gain, which can be explained by their diffusion mechanism (Eq 34)—their gap junctions are often opened, allowing a more free diffusion, which in turn negatively affects the signal propagation. Epithelial cells present the highest channel gain, and this because of the higher number of cells that the signal propagates through. Once again, based on Eq 34 the cell volume will dictate the diffusion performance, and since epithelial have the smallest size, the quantity of Ca^{2+} ion flow is the highest. Finally for smooth muscle cells, the slow decrease of Ca^{2+} after the stimulation (Eq 1) allows an intense propagation of Ca^{2+} across the tissue, but since its size is not comparable to the epithelium cell, the channel gain is not as high.

D. End-to-End Information Capacity

For the end-to-end information capacity analysis we define a state transition process for the Rx and Tx. For the Tx (x) two states are defined, the stimulation and release of Ca^{2+} ($x = x_1$) and silence ($x = x_0$). This resembles the modulation process used in *On-Off Keying (OOK)*, where $x = x_1$ when a bit 1 and $x = x_0$ for bit 0 is transmitted. For Rx, the amount of received Ca^{2+} will change its state, transitioning from active ($y = y_1$) and inactive ($y = y_0$). Based on a bit sequence B, the Tx will change its state accordingly and Rx infers the bit sequence.

Time steps are discretized into time-slots (of duration T_b) for a single bit transmission, where we assume that both the Rx and the Tx are fully synchronized. The synchronization means that the Rx as well as the Tx will have the same clock timing, and will be aware of each bit transmission in the slot. This assumption is common in the literature [60], [18], [67] and can be justified because of the high values of T_b, which enables a much higher synchronization time compared to conventional communication systems.

Shannon's entropy can be used in biological systems to represent the information content (in bits) in various processes [68]:

$$H(X) = -\sum_{x\in X}^{P}(x)\log_2 P(x) \tag{41}$$

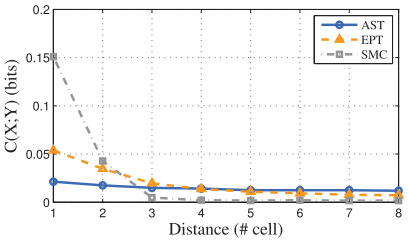

Fig. 14. End-to-end capacity as a function of the distance (number of cells) for a 3 x (3 x l) x (20 x l) (μm) cellular tissue, for the arterial smooth muscle, epithelium and astrocytes cells. For astrocytes the Tx concentration is $2000nM$ and the Rx concentration is $100000nM$. For epithelial cells, the Tx concentration is $2000nM$ and the Rx concentration is $5000nM$, and for smooth muscle cells the Tx concentration is $2000nM$ and the Rx concentration is $10000nM$.

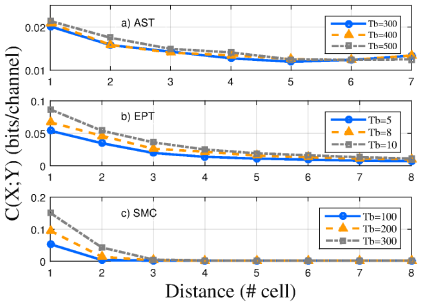

Fig. 15. End-to-end capacity as a function of the distance (number of cells) for a 3 x (3 x l) x (20 x l) (μm) cellular tissue with the time-slot length of 2, 5, 8, and 10 seconds. For astrocytes the Tx concentration is $2000nM$ and the Rx concentration is $100000nM$. For epithelial cells the Tx concentration is $2000nM$ and the Rx concentration is $10000nM$, and for smooth muscle cells the Tx concentration is $2000nM$ and the Rx concentration is $1000nM$.

Also, conditional entropy is defined based on the joint distribution and the conditional distribution of x and y:

$$H(X|Y) = -\sum_{x\in X}\sum_{y\in Y} p(x,y)\log_2 p(x|y), \tag{42}$$

where $Y = \{y_0, y_1\}$.

All the remaining probabilities are defined as follows:

$$p(x) = p(x = x_0) + p(x = x_1) \tag{43}$$
$$p(y) = (p(y = y_0) + p(y = y_1)) * p(y|x) \tag{44}$$
$$p(y = y_0|x = x_0) = 1 - p(y = y_1|x = x_0) \tag{45}$$
$$p(y = y_0|x = x_1) = 1 - p(y = y_1|x = x_1) \tag{46}$$

The *mutual information* $I(X;Y)$ is used to determine the mutual dependence between two variables, and is represented through the following equation:

$$I(X;Y) = H(X) - H(X|Y),$$
$$= \sum_{y\in Y}\sum_{x\in X} p(x)p(y|x)\log_2\frac{p(y|x)}{p(y)} \tag{47}$$

In our analysis, we utilize the mutual information $I(X;Y)$ to analyze the quantity of information that is transmitted from the Tx to Rx. The probabilities $p(x)$ and $p(y)$ represents the probability of each state on the Tx or Rx, respectively. Since T_b is relatively large, the effects of memory in the bit transmission are minimized and we can assume that the channel is memoryless. Capacity is then defined as:

$$C(X;Y) = \max_{p(x)} I(X;Y) \tag{48}$$

1) Capacity Versus D_x: The end-to-end capacity results with respect to distance are presented in Fig. 14. In this analysis, the activation of the receiver is mediated through two variables: the receiver concentration and internal Ca^{2+} concentration. The values for the receiver concentration are 10,000 nM for smooth muscle cells, 5,000 nM for epithelial cells and 100,000 nM for astrocytes. It is clear that for longer (more than four cells) distance all the three tissue types present poor capacity values with astrocytes having the highest values followed by epithelial cells and lastly, the smooth muscle cells. This is the same order to the quantity of receiver concentration values, where more a sensitive receiver can be activated by Ca^{2+} that travelled from longer distances.

The level of Ca^{2+} ions in Fig. 10 is higher for shorter distances in smooth muscle cells compared to both epithelial cells and astrocytes, which maintain a high capacity value until the second cell. This is the outcome of the diffusion (Eq 34) process and the internal Ca^{2+} regeneration processes that impacts the receiver's activation. In smooth muscle cells, diffusion is not as efficient due to the cells volume and typically closed gap junctions (Fig. 8), however its internal IP_3 (Eq 9) allows a maintenance of high concentration of Ca^{2+} for short distances. Astrocytes have a very effective Ca^{2+} regeneration process due to their IP_3 (Eqs 23 and 24). However, their efficient diffusion process maintains a low internal Ca^{2+} concentration, with the fastest coefficient of diffusion ($D = 350$ ($\mu m^2/s$)). This causes a faster propagation of Ca^{2+} throughout the whole tissue (Fig. 10), which also explains a close to flat performance. Finally, for epithelial cells, with no IP_3 regeneration, diffusion plays a bigger role, where small volume with relatively fast propagation speed allows fair performance over short distances.

2) Capacity Versus T_b: Fig. 15 presents the capacity versus T_b analysis with respect to varying distances. Changing the T_b does not significantly impact on the distribution pattern of the capacity over the distance. Therefore, the results are valid with the same explanation used above. However, increasing the T_b does increase the information capacity, especially if the tissue has long delay values, e.g., for astrocytes or smooth muscle cells. This happens because the effects of the transmitted bit on the next one will be minimized, allowing conveying more information for a longer time.

E. Intracellular Signaling Interference

Capacity is indirectly related to the cytosolic Ca^{2+} concentration in Rx. However, Ca^{2+} concentration at the Rx is not only generated due to transmission. Even though the

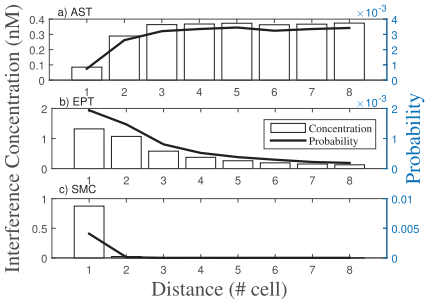

Fig. 16. Total interference of the three different tissues for a 3 x (3 x l) x (20 x l) (μm) cellular space. Transmission of a single pulse with Tb as 10 s. For astocytes (a) the Tx concentration is $2000nM$ and the Rx concentration is $100000nM$. For epithelial cells (b) the Tx concentration is $2000nM$ and the Rx concentration is $10000nM$. And for smooth muscle cells (c) Tx concentration is $2000nM$ and the Rx concentration is $1000nM$.

concentration due to transmission is higher than the concentration in steady state, internal cellular reactions can interfere with the reception of information encoded into the propagated Ca^{2+} concentration—this effect is called intracellular signaling interference. Such interference can occur differently in each tissue type because Ca^{2+} oscillations are regulated differently.

In Fig. 16, we show the interference concentration in the Rx and the probability of interference. The probability is computed as the frequency of interference over the set of reactions inside the tissue. The scenario is the same used in the previous section, where a pulse is transmitted with a certain T_b. For epithelial cells and for smooth muscle cells, intracellular signaling interference is decreased over distance. However, the opposite is found with astrocytes. The reason for this is the lack of Ca^{2+} ions at further distance, which activates the regulatory regeneration of Ca^{2+} due to IP_3 increase (Eqs 23 and 24) and this is followed by a direct response from the secondary pool of the cell (Eq 22).

The IP_3 is necessary for Ca^{2+} regeneration, which unfortunately in this case leads to higher interference. Experiments have shown that certain types of proteins can inhibit the propagation of IP_3, which is ideal for decreasing the intracellular interference. On the other hand, in smooth muscle cells, the IP_3 regulation is not as frequent compared to astrocytes, where the transmission of electrical current plays the major role (Eqs 13, 14 and 15). Finally for epithelial cells, there is no IP_3 mechanism, and therefore Ca^{2+} is only regenerated by the secondary pool at lower levels (Eq 18).

IX. Conclusions

The emergence of molecular communication has attracted communication engineers to hypothesize communication systems utilizing biological components. In particular, a number of proposals for molecular communication are based on utilizing existing natural biological communication processes to encode information for transmission. One such process is Ca^{2+} signaling, which is found in a range of cell types within the human body. Although the natural short range communication of Ca^{2+} signaling makes it ideal for molecular communication, there has been no work to date that has investigated the impact that different types of cells have on the Ca^{2+} signaling performance. In this paper we investigated three different types of cells from a three-dimensional tissue perspective: excitable cells (smooth muscle cells), non-excitable cells (epithelial cells) and hybrid cells (astrocytes). Using the intracellular signaling behavior, intercellular signaling behavior, as well as the gap junction behavior, we outlined an integrated mathematical model for analysis of end-to-end communication behavior in a 3D tissue.

Using our model we investigated spatio-temporal Ca^{2+} concentration dynamics, molecular delay, channel gain, information capacity and intracellular signaling interference within the three tissue types. Our results suggest that the complex intracellular behavior, as well as the varying gap junction behavior, and size and structure of connections between the cells can impact on the communication performance differently. We believe that our findings could benefit molecular communication researchers when designing nanomachines or artificial nanonetworks. At the same time, the breakdown of the intercellular and intracellular signaling may also benefit biotechnologists to understand the breakdown of the Ca^{2+} signaling process in diseased cells. This could be through monitoring the performance of the channel capacity, delay, gain, as well as quantity of interference within the tissue. This would enable new opportunities for targetted drug delivery at the nanoscale.

References

[1] D. Kilinc and O. B. Akan, "A theoretical modeling and analysis of communication via heat flow at nanoscale," *IEEE Trans. Commun.*, vol. 62, no. 10, pp. 3600–3609, Oct. 2014.
[2] I. F. Akyildiz and J. M. Jornet, "The internet of nano-things," *IEEE Wireless Commun.*, vol. 17, no. 6, pp. 58–63, Dec. 2010.
[3] M. Kuran, T. Tugcu, and B. O. Edis, "Calcium signaling: Overview and research directions of a molecular communication paradigm," *IEEE Wireless Commun.*, vol. 19, no. 5, pp. 20–27, Oct. 2012.
[4] I. Akyildiz, F. Fekri, R. S. C. R. Forest, and B. K. Hammer, "Monaco: Fundamentals of molecular nano-communication networks," *IEEE Wireless Commun.*, vol. 19, no. 5, pp. 12–18, Oct. 2012.
[5] B. Atakan, S. Balasubramaniam, and O. B. Akan, "Body area nanonetworks with molecular communications in nanomedicine," *IEEE Commun. Mag.*, vol. 50, no. 1, pp. 28–34, Jan. 2012.
[6] R. Langer and J. P. Vacanti, "Tissue engineering," *Science*, vol. 260, no. 5110, pp. 920–926, 1998.
[7] Y. Chahibi, M. Pierobon, O. S. Sang, and I. F. Akyildiz, "A molecular communication system model for particulate drug delivery systems," *IEEE Trans. Biomed. Eng.*, vol. 60, no. 12, pp. 3468–3483, Dec. 2013.
[8] M. Pierobon and I. F. Akyildiz, "Diffusion-based noise analysis for molecular communication in nanonetworks," *IEEE Trans. Signal Process.*, vol. 59, no. 6, pp. 2532–2547, Jun. 2011.
[9] M. Pierobon and I. F. Akyildiz, "Capacity of a diffusion-based molecular communication system with channel memory and molecular noise," *IEEE Trans. Inf. Theory*, vol. 59, no. 2, pp. 942–954, Feb. 2013.
[10] M. Pierobon and I. F. Akyildiz, "A statistical-physical model of interference in diffusion-based molecular nanonetworks," *IEEE Trans. Commun.*, vol. 62, no. 6, pp. 2085–2095, Jun. 2014.
[11] S. Balasubramaniam and P. Lio, "Multi-hop conjugation based bacteria nanonetworks," *IEEE Trans. NanoBiosci.*, vol. 12, no. 1, pp. 47–59, Mar. 2013.
[12] M. Kuscu and O. B. Akan, "A physical channel model and analysis for nanoscale molecular communications with Forster resonance energy transfer (FRET)," *IEEE Trans. Nanotechnol.*, vol. 11, no. 1, pp. 200–207, Jan. 2012.

[13] M. Kuscu, D. Malak, and O. B. Akan, "An information theoretical analysis of broadcast networks and channel routing for FRET-based nanoscale communications," in *Proc. IEEE Int. Conf. Commun. (ICC)*, 2012, pp. 6167–6171.

[14] D. Malak and O. B. Akan, "A communication theoretical analysis of synaptic multiple-access channel in hippocampal-cortical neurons," *IEEE Trans. Commun.*, vol. 61, no. 6, pp. 2457–2467, Jun. 2013.

[15] S. Balasubramaniam *et al.*, "Development of artificial neuronal networks for molecular communication," *Nano Commun. Netw.*, vol. 2, pp. 150–160, 2011.

[16] T. Nakano, T. Suda, T. Koujin, T. Karaguchi, and Y. Hiraoka, "Molecular communication through gap junction channels: System, design, experiment, and modelling," in *Proc. 2nd Int. Conf. Bio Inspired Models Netw. Inf. Comput. Syst. (BIONETICS'07)*, 2007, pp. 139–146.

[17] L. Leybaert and M. J. Sanderson, "Intercellular Ca2+ waves: Mechanisms and functions," *Physiol. Rev.*, vol. 92, pp. 1359–1392, 2012.

[18] D. Kilinc and O. B. Akan, "An information theoretical analysis of nanoscale molecular gap junction communication channel between cardiomyocytes," *IEEE Trans. Nanotechnol.*, vol. 12, no. 2, pp. 129–136, Mar. 2013.

[19] S. Somlo and B. Ehrlich, "Human disease: Calcium signaling in polycystic kidney disease," *Curr. Biol.*, vol. 11, no. 9, pp. R356–R360, 2001.

[20] I. Bezprozvanny, "Calcium signaling and neurodegenerative medicine," *Trends Mol. Med.*, vol. 15, no. 3, pp. 89–100, 2009.

[21] T. Capiod, Y. Shuba, R. Skyryma, and N. Prevarskaya, "Calcium signalling and cancer cell growth," *Subcellular Biochem.*, vol. 45, no. 1, pp. 405–427, 2007.

[22] A. Goldbeter, G. Dupont, and M. J. Berridge, "Minimal model for signal-induced Ca2+ oscillations and for their frequency encoding through protein phosphorylation," *Proc. Nat. Acad. Sci., USA*, vol. 87, pp. 1461–1465, 1990.

[23] E. Scemes and C. Giaume, "Astrocytes calcium waves: What they are and what they do," *Glia*, vol. 54, pp. 716–725, 2006.

[24] E. Scemes, S. O. Saudicani, G. Dahl, and D. C. Spray, "Connexin and pannexin mediated cell–cell communication," *Neuron Glia Biol.*, vol. 3, pp. 199–208, 2007.

[25] A. C. Charles, S. K. Kodali, and R. F. Tyndale, "Intercellular calcium waves in neurons," *Mol. Cell. Neurosci.*, vol. 7, no. 5, pp. 337–353, 1996.

[26] K. Motoyama, I. E. Karl, M. W. Flye, D. F. Osborne, and R. S. Hotchkiss, "Effect of Ca2+ agonists in the perfused liver: Determination via laser scanning confocal microscopy," *Amer. J. Physiol.*, vol. 276, pp. R575–R585, 1999.

[27] L. D. Robb-Gaspers and A. P. Thomas, "Coordination of Ca2+ signalling by intercellular propagation of Ca2+ waves in the liver," *J. Biol. Chem.*, vol. 270, pp. 8102–8107, 1995.

[28] P. Gomes, S. P. Srinivas, J. Vereecke, and B. Himpens, "Gap junctional intercellular communication in bovine corneal endothelial cells," *Exp. Eye Res.*, vol. 83, no. 5, pp. 1225–1237, 2006.

[29] N. Halidi, F.-X. Boittin, J.-L. Beny, and J.-J. Meister, "Propagation of fast and slow intercellular Ca2+ waves in primary cultured arterial smooth muscle cells," *Cell Regul.*, vol. 50, no. 5, pp. 459–467, 2011.

[30] S. O. Suadicani, M. J. Vink, and D. C. Apray, "Slow intercellular Ca2+ signalling in wild-type and Cx43-null neonatal mouse cardiac myocytes," *Amer. J. Physiol. Heart Circul. Physiol.*, vol. 279, pp. H3076–H3088, 2000.

[31] L. D. Gaspers and A. P. Thomas, "Calcium signaling in liver," *Cell Calcium*, vol. 38, pp. 329–342, 2005.

[32] N. R. Jorgensen, "Short-range intercellular calcium signaling in bone," *Acta Pathol. Microbiol. Immunol. Scand. Suppl.*, vol. 118, pp. 5–36, 2005.

[33] T. Kono, T. Nishikori, H. Kataoka, Y. Uchio, M. Ochi, and K. Enomoto, "Spontaneous oscillation and mechanically induced calcium waves in chondrocytes," *Cell Biochem. Funct.*, vol. 24, pp. 103–111, 2006.

[34] J. P. Peterdi, "Calcium wave of tubuloglomerular feedback," *Amer. J. Physiol. Renal Physiol.*, vol. 291, pp. F473–F480, 2006.

[35] K. Enomoto, K. Furuya, S. Yamagishi, and T. Maeno, "Mechanically induced electrical and intracellular calcium responses in normal and cancerous mammary cells," *Cell Calcium*, vol. 13, pp. 501–511, 1992.

[36] Y. Osipchuk and M. Cahalan, "Cell-to-cell spread of calcium signals by ATP receptors in mast cells," *Nature*, vol. 359, pp. 241–244, 1992.

[37] D. I. Yule, E. Stuenkel, and J. A. Williams, "Intercellular calcium waves in rat pancreatic acini: Mechanisms of coactivation," *Amer. J. Physiol. Cell Physiol.*, vol. 271, pp. C1285–C1294, 1996.

[38] S. Koizumi, K. Fujisjita, K. Inoue, Y. Shigemoto-Mogami, and M. Tsuda, "Ca2+ waves in keratinocytes are transmitted to sensory neurons: The involvement of extracelllular ATP and P2Y2 receptor activation," *Biochem. J.*, vol. 380, pp. 329–338, 2004.

[39] J. Long, M. Junkin, P. K. Wong, J. Hoying, and P. Deymier, "Calcium wave propagation in networks of endothelial cells: Model-based theoretical and experimental study," *PLoS Comput. Biol.*, vol. 8, no. 12, p. e1002847, 2012.

[40] S. Rdiger, "Stochastic models of intracellular calcium signals," *Phys. Report*, vol. 534, no. 2, pp. 39–87, 2007.

[41] S. Rdiger *et al.*, "Hybrid stochastic and deterministic simulations of calcium blips," *Biophys. J.*, vol. 93, no. 1, pp. 1847–1857, 2007.

[42] P. G. Reas and B. Ballaro, "Reaction-diffusion equations for simulation of calcium signalling in cell systems," *Revista Biol.*, vol. 97, pp. 443–468, 2004.

[43] A. C. Heren, M. S. Kuran, H. B. Yilmaz, and T. Tugcu, "Channel capacity of calcium signalling based on inter-cellular calcium waves in astrocytes," in *Proc. 3rd IEEE Int. Workshop Mol. Nano Scale Commun.*, 2013, pp. 792–797.

[44] T. Nakano and J.-Q. Liu, "Information transfer through calcium signaling," in *Nano-Net*. New York, NY, USA: Springer, 2009, vol. 20, pp. 29–33.

[45] J.-Q. Liu and T. Nakano, "An information theoretic model of molecular communication based on cellular signaling," in *Proc. 2nd Bio Inspired Models Netw. Inf. Comput. Syst.*, Dec. 2007, pp. 316–321.

[46] J. Harris and Y. Timofeeva, "Intercellular calcium waves in the fire-diffuse-fire framework: Green's function for gap-junctional coupling," *Phys. Rev.*, vol. 82, no. 1, p. 051910, 2010.

[47] M. Koenigsberger, R. Sauser, M. Lamboley, J.-L. Beny, and J.-J. Meister, "Ca2+ dynamics in a population of smooth muscle cells: Modeling the recruitment and synchronization," *Biophys. J.*, vol. 87, pp. 92–104, 2004.

[48] P. A. Appleby, S. Shabir, J. Southgate, and D. Walker, "Cell-type-specific modelling of intracellular calcium signalling: A urothelial cell model," *J. Roy. Soc.*, vol. 10, no. 86, p. 20130487, 2013.

[49] A. Araque and M. Navarrete, "Glial cells in neuronal network function," *Philosoph. Trans. Roy. Soc.*, vol. 365, no. 1551, pp. 2375–2381, 2010.

[50] M. Lavrentovich and S. Hemkin, "A mathematical model of spontaneous calcium(II) oscillations in astrocytes," *J. Theor. Biol.*, vol. 251, pp. 553–560, 2008.

[51] S. Zeng, B. Li, S. Zend, and S. Chen, "Simulation of spontaneous Ca2+ oscillations in astrocytes mediated by voltage-gated calcium channels," *Biophys. J.*, vol. 97, pp. 2429–2437, 2009.

[52] N. M. Kumar and N. B. Gilula, "The gap junction commmunication channel," *Cell*, vol. 84, pp. 381–388, 1997.

[53] W. R. Loewenstein, "Junctional intercellular communication: The cell-to-cell membrane channel," *Physiol. Rev.*, vol. 61, pp. 829–913, 1981.

[54] P. P. Mehta, A. Hotz-Wagenblatt, B. Rose, D. Showlloway, and W. R. Loewenstein, "Incorporation of the gene for a cell–cell channel protein into transformed cells leads to normalization of growth," *J. Phys. Chem.*, vol. 124, pp. 207–225, 1991.

[55] S. Baigent, J. Stark, and A. Warner, "Modelling the effect of gap junction nonlinearities in systems of coupled cells," *J. Theor. Biol.*, vol. 186, pp. 223–239, 1997.

[56] F. F. Bukaukas, A. Bukauskiene, M. V. L. Bennett, and V. K. Verselis, "Gating properties of gap junction channels assembled from connexin 43 and connexin 43 fused with green fluorescent protein," *Biophys. J.*, vol. 81, pp. 137–152, 2013.

[57] V. Viliunas, R. Weingart, and P. R. Brink, "Formation of heterotypic gap junction channels by connexins 40 and 43," *Circ. Res.*, vol. 86, pp. E42–E49, 2000.

[58] A. P. Moreno, J. G. Laing, E. C. Beyer, and D. C. Spray, "Properties of gap junction channels formed of connexin 45 endogenously expressed in human hepatoma (SKHep1) cells," *Amer. J. Physiol.*, vol. 268, pp. 356–365, 2000.

[59] V. Viliunas, "Biophysical properties of connexin-45 gap junction hemichannels studied in vertebrate cells," *J. Gener. Physiol.*, vol. 119, pp. 147–164, 2002.

[60] T. Nakano and J.-Q. Liu, "Design and analysis of molecular relay channels: An information theoretic approach," *IEEE Trans. NanoBiosci.*, vol. 9, no. 3, pp. 213–221, Sep. 2010.

[61] M. T. Barros, S. Balasubramaniam, B. Jennings, and Y. Koucheryavy, "Transmission protocols for calcium signaling based molecular communications in deformable cellular tissues," *IEEE Trans. Nanotechnol.*, vol. 13, no. 4, pp. 779–788, Jul. 2014.

[62] M. T. Barros, S. Balasubramaniam, and B. Jennings, "Using information metrics and molecular communication to detect cellular tissue deformation," *IEEE Trans. Nanobiosci.*, vol. 13, no. 3, pp. 278–288, Sep. 2014.
[63] M. T. Barros, S. Balasubramaniam, and B. Jennings, "Adaptive transmission protocol for molecular communications in cellular tissues," in *Proc. IEEE Conf. Commun.*, 2014, pp. 3981–3986.
[64] J. Lallouette, M. D. Pitta, E. Ben-Jacob, and H. Berry, "Sparse short-distance connection enhance calcium wave propagation in a 3D model of astrocytes networks," *Front. Comput. Neurosci.*, vol. 8, no. 45, pp. 1–18, 2014.
[65] D. T. Gillespie, "Exact stochastic simulation of coupled chemical reactions," *J. Phys. Chem.*, vol. 81, no. 25, pp. 2340–2361, 1977.
[66] M. Pierobon and I. F. Akyildiz, "A physical end-to-end model for molecular communication in nanonetworks," *IEEE J. Sel. Areas Commun.*, vol. 28, no. 4, pp. 602–611, May 2010.
[67] M. J. Moore, T. Suda, and K. Oiwa, "Molecular communication: Modelling noise effects on information rates," *IEEE Trans. NanoBioSci.*, vol. 8, no. 2, pp. 169–180, Jun. 2009.
[68] P. Abshire and A. G. Andreou, "Capacity and energy cost of information in biological and silicon photoreceptors," *Proc. IEEE*, vol. 89, no. 7, pp. 1052–1064, Jul. 2001.

Michael Taynnan Barros (S'14) was born in Campina Grande, Paraíba, Brazil. He received the B.Tech. degree in telematics from the Federal Institute of Education, Science, and Technology, Paraíba (IFPB), João Pessoa, Brazil, and the M.Sc. degree in computer science from the Federal University of Campina Grande (UFCG), Campina Grande, Brazil. He is currently pursuing the Ph.D. degree in telecommunication software at the Telecommunications Software and Systems Group (TSSG), Waterford Institute of Technology (WIT), Waterford, Ireland. Currently, he is a Postgraduate Researcher with TSSG. He has authored more than 30 papers in international journals and conferences. His research interests include dynamic optical networks, vehicular ad hoc networks, routing, IP traffic classification, QoS-DiffServ aware networks, molecular communication, nanonetworks, and bioinspired techniques. He is a Reviewer for many journals and participated as Technical Program Committee and Reviewer for various international conferences.

Sasitharan Balasubramaniam (SM'14) received the Bachelor's degree in electrical and electronic engineering from the University of Queensland, Brisbane, Qld., Australia, the Master's degree in computer and communication engineering from the Queensland University of Technology, Brisbane, Qld., Australia, and the Ph.D. degree from the University of Queensland, Brisbane, Qld., Australia, in 1998, 1999, and 2005, respectively. Currently, he is a Senior Research Fellow with the Nano Communication Centre, Department of Electronic and Communication Engineering, Tampere University of Technology, Tampere, Finland. Previously, he was a Research Fellow with the Telecommunication Software and Systems Group, Waterford Institute of Technology, Waterford, Ireland, where he worked on a number of Science Foundation Ireland projects. He has authored over 70 papers and actively participates in a number of Technical Programme Committee for various conferences. His research interests include bioinspired communication networks, and molecular communications. He was the TPC Co-Chair for the ACM NANOCOM 2014 and the IEEE MoNaCom 2011, both conferences which he cofounded. Currently, he is an Editor for the IEEE INTERNET OF THINGS JOURNAL and *Nano Communication Networks* (Elsevier).

Brendan Jennings (M'05) received the B.Eng. and Ph.D. degrees from Dublin City University, Dublin, Ireland, in 1993 and 2001, respectively. He is the Head of the Graduate Studies with Waterford Institute of Technology, Waterford, Ireland, where he is a Senior Researcher within the Emerging Network Laboratory, Telecommunications Software & Systems Group. Within the past three years, he has spent periods as a Visiting Researcher at KTH—Royal Institute of Technology, Stockholm, Sweden, and with EMC^2 Research Europe, Cork, Ireland. His research interests include in network management, cloud computing, and nanoscale communications.

Chapter 5

Transmission Protocols for Calcium Signaling based Molecular Communications in Deformable Cellular Tissues

Journal Title:	IEEE Transactions on Nanotechnology
Article Type	Regular Paper
Complete Author List	Michael Taynnan Barros, Sasitharan Balasubramaniam, Brendan Jennings and Yevgeni Koucheryavy
Keywords	Molecular Communication; Calcium Singling; Transmission Protocols; Deformable Tissue
Status	Published: vol.13, no.4, pp.779,788, July 2014. doi: 10.1109/TNANO.2014.2321492

IEEE TRANSACTIONS ON NANOTECHNOLOGY, VOL. 13, NO. 4, JULY 2014 779

Transmission Protocols for Calcium-Signaling-Based Molecular Communications in Deformable Cellular Tissue

Michael Taynnan Barros, *Student Member, IEEE*, Sasitharan Balasubramaniam, *Senior Member, IEEE*, Brendan Jennings, *Member, IEEE*, and Yevgeni Koucheryavy, *Senior Member, IEEE*

***Abstract*—Molecular communications is a new paradigm that enables nanomachines to communicate within a biological environment. One form of molecular communications is calcium (Ca^{2+}) signaling, which occurs naturally in living biological cells. Ca^{2+} signaling enables cells in a tightly packed tissue structure to communicate at short ranges with neighboring cells. The achievable mutual information of Ca^{2+} signaling between tissue embedded nanomachines is investigated in this paper, focusing in particular on the impact that the deformation of the tissue structure has on the communication channel. Based on this analysis, a number of transmission protocols are proposed; nanomachines can utilize these to communicate using Ca^{2+} signaling. These protocols are *static time-slot configuration*, *dynamic time-slot configuration*, *dynamic time-slot configuration with silent communication*, and *improved dynamic time-slot configuration with silent communication (IDTC-SC)*. The results of a simulation study show that *IDTC-SC* provides the maximum data rate when tissues experience frequent deformation.**

***Index Terms*—Calcium signaling, deformable tissue, molecular communications, transmission protocols.**

I. Introduction

THE ongoing development of sophisticated nanomachines is having a profound impact on a number of industries, including healthcare, biotechnology, and the military. While the size of the nanomachines has led to a number of important benefits, this has been accompanied by certain issues, notably their limited processing capabilities and functionality. In recent years, *nano communications* has emerged as a possible solution to enhance the functionality provided by nanomachines, in particular by interconnecting devices into *nanonetworks* [1]–[3]. Two forms of nano communications have been explored: *electromagnetic nano communications* [4], [5] and *molecular communications* [6]–[9]. Here, we focus on the latter. In molecular communications, information is represented by molecules that are transported between communicating peers via a pure biological process.

In recent years, researchers have investigated and proposed numerous techniques for molecular communications; these techniques can be broadly classified as being passive or active. Passive molecular communications uses diffusion to propagate information molecules from the transmitter to the receiver. Techniques include free-diffusion systems [10]–[12] and calcium (Ca^{2+}) signaling [13], [14]. In contrast, active molecular communications techniques involve an external entity carrying the information molecules to their destination. Techniques include the use of a cytoskeleton [15], membrane nanotubes [16], catalytic nanomotors [17], [18], and bacterial nanonetworks [19], [20]. In this paper, we investigate the Ca^{2+} signaling passive technique.

Although the Ca^{2+}-signaling-based molecular communications has been studied for 1-D arrays of cells [21], analysis of its behavior in a cellular tissue environment has been lacking. Of particular concern are the impact of recurrent signals and the impact of tissue deformation. Recurrent signals occur as Ca^{2+} ions are propagated through the cell gap junctions[1]—this usually leads to spatially fluctuating noise in the molecular communications channel. Tissue deformation can also lead to impairments of the communication channel—cells have a deformable body that can take on various shapes under force, and, since in a tissue cells are interconnected, changes in cell shape will percolate through the entire tissue. As the cells change their shape, this affects the quantity of Ca^{2+} that is diffused from the cell and thus the overall channel mutual information.

We first investigate the behavior of the Ca^{2+} signaling in a three-layered cellular tissue, analyzing the channel performance under varying time-slot lengths for bit transmission, as well as under varying concentration of the Ca^{2+} ions at the receiver and transmitter. This is followed by an analysis of the channel performance as the tissue undergoes deformation. Results from this analysis are in turn utilized in the development of new transmission protocols for nanomachines that seek to maximize the channel performance as the tissue dynamically deforms. We propose

Manuscript received October 16, 2013; revised January 31, 2014; accepted April 14, 2014. Date of publication May 1, 2014; date of current version July 2, 2014. This work was partially funded by 1) the Irish Higher Education Authority under the Programme for Research in Third Level Institutions cycle 5, which is cofunded by the European Regional Development Fund, via the Telecommunications Graduate Initiative (http://www.tgi.ie), 2) via the Science Foundation Ireland funded FAME strategic research cluster (Grant 08/SRC/I1403), and 3) via the FiDiPro program of Academy of Finland (Nano communication Networks), 2012–2016. The review of this paper was arranged by Associate Editor C. A. Moritz.

M. T. Barros and B. Jennings are with the Telecommunication Software & Systems Group, Waterford Institute of Technology, Waterford, Ireland (e-mail: mbarros@tssg.org; bjennings@tssg.org).

S. Balasubramaniam and Y. Koucheryavy are with the Nano Communications Center, Department of Electronics and Communication Engineering, Tampere University of Technology, Tampere 33720, Finland (e-mail: sasi.bala@tut.fi; yk@cs.tut.fi).

Color version of one or more of the figures in this paper are available online at http://ieeexplore.ieee.org.

Digital Object Identifier 10.1109/TNANO.2014.2321492

[1]Gap junctions refers to the cell-to-cell interconnections. The cellular cytoplasms of neighbor cells are directly connected through these junctions.

four protocols: *static time-slot configuration (STC)*, *dynamic time-slot configuration (DTC)*, *dynamic time-slot configuration with silent communication (DTC-SC)*, and *improved dynamic time-slot configuration with silent communication (IDTC-SC)*. For *STC*, the time slots for a bit transmission are static. However, in the case of *DTC*, the time slots are dynamically assigned depending on the state of tissue deformation. For *DTC-SC*, communication through silence is introduced, wherein start and stop bits are transmitted to convey specific information between the transmitter and receiver nanomachine. The last protocol, *IDTC-SC*, seeks to improve on *DTC-SC* by incorporating message block subdivision. We compare the four protocols through analytical modeling, evaluating the impact on data rate (*DR*) as we vary the time-slot lengths, degree of tissue deformation, and information bits. Our results indicate that *IDTC-SC* improves the *DR* dramatically in comparison to the other three protocols.

This paper is organized as follows. Section II presents the basic model for Ca^{2+} signaling and its use in molecular communications. Section III presents our tissue model and the analysis of the behavior of Ca^{2+} signaling in a three-layered tissue structure. Section IV evaluates the signaling behavior under varying tissue deformations, while Section V presents an analysis on the types of noise that can occur in deformed and regular tissue structures. Section VI presents the four different transmission protocols that could be utilized in deformable tissue structures. Finally, Section VII concludes this paper.

II. Calcium-Based Molecular Communications

This section provides the theoretical background of Ca^{2+} signaling in a single cell. This will be followed by a description of the molecular communications system model that utilizes Ca^{2+} signaling between the cells in the tissue, as well as the simulation model that is used throughout the paper.

A. Calcium Signaling Analytical Model

Goldbeter *et al.* [22] developed an analytical model of Ca^{2+} signaling formulated as a set of differential equations. Equations (1) and (2) describe the behavior of the cytosolic Ca^{2+} concentration (Z), as well as the Ca^{2+} pool concentration (Y) [22]. This pool has an influx magnitude $v_1\beta$, where β represents the saturation function of the receptors and v_1 represents the rate of Ca^{2+} release. The components of the equations as well as their roles, illustrated in Fig. 1, include: 1) v_0: Ca^{2+} leakage from the extracellular space into the cellular cytosol; 2) v_2: transport of Ca^{2+} ions from the cellular cytosol to the endoplasmatic reticulum, define by (3); 3) v_3: release of Ca^{2+} from the cellular endoplasmatic reticulum into the cytosol; 4) $k_f Y$: Ca^{2+} leakage from the endoplasmatic reticulum to the cytosol; and 5) kZ: transport of Ca^{2+} ions from the cytosol to the extracellular space

$$\frac{dZ}{dt} = v_0 + v_1\beta - v_2 + v_3 + k_f Y - kZ \tag{1}$$

$$\frac{dY}{dt} = v_2 - v_3 - k_f Y. \tag{2}$$

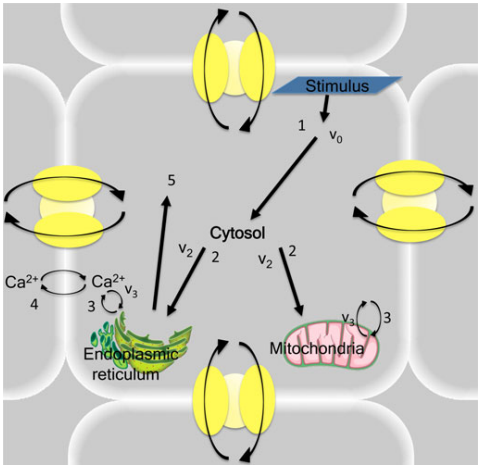

Fig. 1. Stages of the Ca^{2+} signaling process: (1) Process starts from the stimulation and extracellular leakage of Ca^{2+} ions into the cytosol. (2) Transport the Ca^{2+} ions from the cellular store (or cytosolic space) to the endoplasmic reticulum. (3) Release of Ca^{2+} ions from the endoplasmic reticulum into the cytosol, where the release will also include the leakage of Ca^{2+} ions (4). Lastly, (5) Ca^{2+} ions are transported from the cytosol to the extracellular space.

However, before the Ca^{2+} ions are diffused to the neighboring cells, the ions will first need to be activated through the IP_3 receptors, which is an internal cellular secondary channel that leads to self-amplification. This process will increase the cytosolic Ca^{2+} concentration to be ready for diffusion. The following equations represent the Ca^{2+} self-amplification mechanism from the Ca^{2+} pool due to the activation of the IP_3 receptors

$$v_2 = V_{M2}\frac{Z^n}{K_2^n + Z^n} \tag{3}$$

$$v_3 = V_{M3}\frac{Y^m}{K_R^m + Y^m}\cdot\frac{Z^p}{K_A^p + Z^p} \tag{4}$$

where V_{M2} and V_{M3} are the rate constants; K_2, K_R, and K_A are the threshold constants; and n, m, and p are the Hill coefficients [22].

B. Molecular Communications Utilizing Calcium Signaling

The molecular communications model that utilizes Ca^{2+} signaling is illustrated in Fig. 2. The original model for a digital molecular communications system in a single array of cells was proposed by Nakano and Liu [21]. However, in this paper, we extend this model to a multilayered cellular tissue, as illustrated in Fig. 3. The model consists of a transmitter nanomachine *Tx*, relay cells, and a receiver nanomachine *Rx*. The bit transmission starts when the Ca^{2+} ions are stimulated at the *Tx*, which will eventually lead to its release to the neighboring cells. The quantity of Ca^{2+} ions that are released to the neighboring cells will be βv_1. The relay cells will in turn propagate the Ca^{2+}

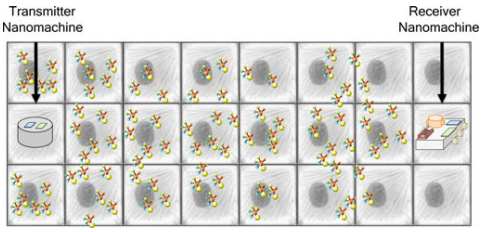

Fig. 2. Utilization of Ca^{2+} signaling for molecular communications in a tissue. Our scenario application assumes that nanomachines (receiver and transmitter) are embedded in the cells and are able to stimulate the Ca^{2+} ions for signaling. This model is introduced by Nakano and Liu [21].

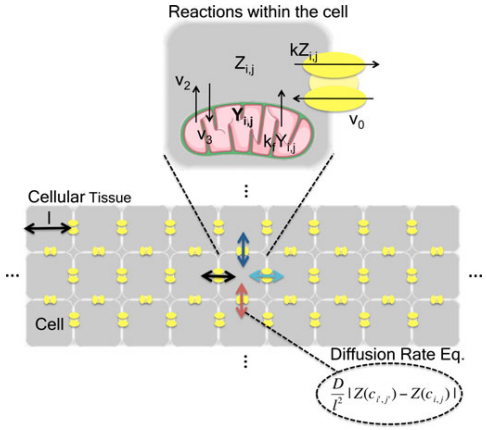

Fig. 3. Depiction of a three-layered cellular tissue, where each layer contains an array of cells. Both the reactions within cells and the diffusion process to neighboring cells are shown.

signal toward the receiver nanomachine. To extend the model in [21], we need to account for the diffusion of Ca^{2+} molecules into *all* of a cell's neighbors. For a tissue that consists of a matrix of $I \times J$ cells, where $c_{i,j}$ ($i = 1 \ldots I$ and $j = 1, \ldots J$) denotes an arbitrary cell in the tissue, a concentration difference is expressed as [21]

$$Z_{\text{Diff}} = \frac{D}{l^2}(Z(c_{i',j'}) - Z(c_{i,j})) \tag{5}$$

where $c_{i,j}$ and $c_{i',j'}$ are neighboring cells, D is the diffusion coefficient, l is the length of the cell, and Z_{Diff} is the difference in Ca^{2+} concentration between the cells.

In the receiver *Rx*, the detection of the Ca^{2+} ions will depend on the activation process. The following equation describes the receiver activation process:

$$k_a \frac{Z^q}{K^q + Z^q} \tag{6}$$

where k_a, K, and q are, respectively, the maximum receiver activation rate, the saturation constant for the cytosolic Ca^{2+} concentration, and the Hill coefficient. The transition between the inactive to the active state is dependent on the binding of the q molecules of Ca^{2+} ions.

C. Simulation Model

We simulate the Ca^{2+} signaling in a multilayer cellular tissue using the model specified above through a series of time steps. At each step, our simulator executes a Gillespie algorithm [23] to select a random cell and randomly select an internal reaction of that cell based on probability P_R. The P_R is uniformly distributed over the sum of all values of Z_{Diff}. Therefore, P_R favors a cell $c_{i,j}$ with a high quantity of Ca^{2+} that is ready to diffuse to its neighbors. Once the cell $c_{i,j}$ is selected, one of the 12 reaction processes will be randomly selected and executed. The end of each reaction process will update the concentration of the free cytosolic Ca^{2+} ions ($Z_{i,j}$), the Ca^{2+} ions within the endoplasmic reticulum ($Y_{i,j}$), the number of molecules detected at the destination as well as the probabilities of all other reactions.

The simulation time steps are discretized into time slots for a single bit transmission, where we assume that both the *Rx* and the *Tx* are fully synchronized. The synchronization means that the *Rx* as well as the *Tx* will have the same clock timing and will be aware of each bit transmission in the slot. The modulation process used in our simulation model is based on *ON–OFF Keying*, where the *Tx* stimulates Ca^{2+} when a bit 1 is to be sent or emits nothing for bit 0. We also assume that there is equal probability for each bit to be transmitted. For each simulation run at the beginning of each time slot, the *Tx* will alternate its state based on the previous state, starting with no emission of Ca^{2+}, and subsequently producing a sequence of 0 and 1 s . This process will continue repeatedly until the end of the simulation. The tissue of cells is 40 μm in length with each cell's diameter set to 0.5 μm [24], which is roughly the size and the shape of a typical epithelial mammalian cell (therefore, there are 80 cells/layer of the tissue). In our simulation scenario, the *Tx* is positioned at the center of the 2-D cellular tissue, and the receiver is positioned in the same layer but at a certain distance *Dx* away from the *Tx*. In line with [21], we used the following values for the model parameters: $v_0 = 1$ (μM/s), $v_1 = 100$ (1/s), Z = 100 (nM), k = 4.2 (1/s), $k_f = 1$ (1/s), $V_{M2} = 50$ (μM/s), $V_{M3} = 500$ (μM/s), $K_2 = 1$ (μM), $K_R = 2$ (μm), $K_A = 0.9$ (μM), $m = n = 2$, $p = 4$, $D = 10$ (μm^2/s) $l = 0.5$ (μm), $k_a = 2.5$ (μM/s), $K = 0.6$ (nm), $q = 4$, $k_{ia} = 0.5$ (μM/s), $W = 500$ (nM).

III. Mutual Information on a Calcium-Signaling-Based Molecular Communications

By considering a multilayer cellular tissue, we can better analyze the communications performance between two given endpoints in the tissue, taking account of the impact that noise resulting from neighboring cell layers may have on the communications channel. Using results generated with our simulator, we now describe the use of *mutual information* $I(X;Y)$ to analyze the quantity of information transmitted between the *Tx*

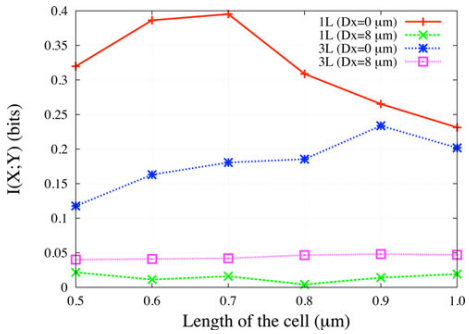

Fig. 4. *I(X;Y)* (in bits) for both the three and single layered (3L and 1L) cellular tissue as a function of the cell length. This also includes varying the distance between the *Tx* and the *Rx* between 0 and 8 μm.

(X) and *Rx* (Y). The mutual information can be represented through the following equations:

$$I(X;Y) = \sum_{y \in Y} \sum_{x \in X} p(x)p(y \mid x) \log_2 \frac{p(y \mid x)}{p(y)} \quad (7)$$

$$p(x) = P(x = x_0 \wedge x = x_1) \quad (8)$$

$$p(y) = P(y = y_0 \wedge y = y_1) * p(y/x) \quad (9)$$

$$p(y = y_0 \mid x = x_0) = 1 - p(y = y_1 \mid x = x_0) \quad (10)$$

$$p(y = y_0 \mid x = x_1) = 1 - p(y = y_1 \mid x = x_1). \quad (11)$$

Probabilities $p(x)$ and $p(y)$ represent the internal cellular states of the *Tx* and the *Rx*, respectively. Both the *Tx* and the *Rx* will have two states: 0 or 1. On the sender side, state 1 implies the release of the Ca^{2+} ions, and state 0 otherwise. In the *Tx* side, state 1 implies the reception of molecules which activates the *Rx*, and state 0 otherwise. In the simulations, the *Tx* transmits sequences of 0's and 1's serially. The *Rx* state is determined based on the signals received. If what is received is noise, then the state is 0 and if the signal is a considerable amount of Ca^{2+}, the state is 1. The probabilities are calculated at the end of the simulation.

Fig. 4 presents the mutual information $I(X;Y)$ comparison between the single and three layer cellular tissue cases as the distance Dx between the transmitter nanomachine Tx and the receiver nanomachine Rx is varied. It also shows the impact of varying the length (diameter) of the cells that make up the path between the *Tx* and *Rx*—changes in a cell's length impact on the number of reactions inside that cell, leading to varying Ca^{2+} diffusion levels. As shown in the figure, the quantity of information decreases as the distance between the *Tx* and the *Rx* increases. We can also observe that there is an optimum point for single tissue layer with cell lengths between 0.6 and 0.7 μm and distance of 0 μm between the *Tx* and the *Rx*, which shows the highest mutual information. On the other hand, for the same Dx in the three-layered cellular tissue, we observe that the quantity of information increases as the cell length

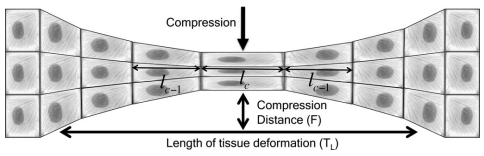

Fig. 5. Tissue structure under force.

increases up to 0.9 μm, falling down at higher lengths. However, once we increase the Dx to 8 μm, the three-layered cellular tissue has higher information transmitted compared to the single layer tissue. This indicates that the quantity of recurrent Ca^{2+} ions (which are the ions that are diffused into the environment) that are reflected from neighboring cells in the top and bottom layer of the cellular tissue positively impacts on the end-to-end quantity of information transmitted. The results demonstrate the impact of Ca^{2+} diffusion on a lattice of cells compared to a 1-D array of cells. In the subsequent sections, the reason for this impact will be further discussed and analyzed.

IV. Impact of Tissue Deformation on Mutual Information

In this section, we will first describe the background on the tissue deformation, and this will be followed by a description of its effect on the communication channel.

A. Tissue Deformation

A tissue has a flexible structure, which allows it to have different shapes when under the influence of force. Intuitively, we would expect that such deformation will impact on the information transmitted for molecular communications, which are modeled and investigated in this section.

The impact of force applied to the tissue is investigated as follows. We first consider the impact of tissue deformation (under increasing force) and its effect on the area of cells that are being deformed—as illustrated in Fig. 5. As previously discussed, the length of the cells on the path from the *Tx* to the *Rx* impacts on the diffused quantity of Ca^{2+}. Since we generalize the shape of each cell as a square, by applying a force at the middle of the tissue, we can assume that the cells will change their shape into approximately a trapezium. The impact of this approximation is quite low, since our model is based only on the length of the cell and not in its shape. Based on the location that the force is applied to the tissue, the cells in the center of the tissue will have the largest increase in length, with the magnitude of this increase falling off as the distance from the applied point of force increases. This effect is illustrated in Fig. 5. Assuming that the force is applied to the center of the tissue, we compute the changes in the length of the other cells of the tissue; these lengths are then used to determine the flow of Ca^{2+} using the model described in Section II-A.

We apply simple concepts from geometry to calculate the length of the cell. Our scenario in this paper is based on a single type of compression, which is illustrated in Fig. 5. Since the

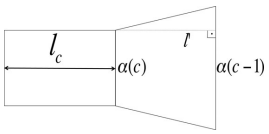

Fig. 6. Impact of center cell deformation on the neighboring cell, where a trapezium shape can be observed.

deformation of the cells is highly correlated and the origin of deformation is at the center of the cellular tissue, we start by calculating the length of the center cell in the tissue. The length and height of each cell are denoted as l, and the length of the central cell is denoted as l_c. Based on a tissue with N_L number of layers and the compression distance (length of the deformation of the tissue) of F, the value of l_c is calculated as follows:

$$l_c = \frac{l^2 N_L}{l N_L - 2F}. \tag{12}$$

The effects of the deformation starting from the center cell are illustrated in Fig. 6. During deformation, the area of the cell does not change. All the cells are assumed to be in a 2-D domain. Therefore, based on the calculation of l_c, we are also able to calculate the new height of the center cell $\alpha(c) = \frac{l^2}{l_c}$. The height of the center cell will in turn provide a value for one base of the trapezium-shaped cell, where the calculation for the bottom base of the cells can be represented as

$$\alpha(c-i) = \frac{l^2}{l_c} + \sum_{i=1}^{|z-(c-1)|} \frac{F}{T_L} \tag{13}$$

where $(c-i)$ represents the cell's position along the tissue, and T_L represents the length of the tissue that is under deformation. Equation (13) approximates the lower base of the trapezium-shaped cell where the lower base $\alpha(c-i)$ is larger than the higher base $\alpha(c)$ by a factor of $\frac{F}{T_L}$. Therefore, the bases of the trapezium-shaped cell will slowly increase as the position of the cell $(c-i)$ increases outwards toward the tissue boundary. Using the values of $\alpha(c)$ and $\alpha(c-i)$, we then calculate the deformed length l_{c-i} of cell $(c-i)$, which is on the basis of the area of a trapezium as follows:

$$l_{c-i} = \frac{2l^2}{\alpha(c-i) + \alpha(c)}. \tag{14}$$

B. Comparative Analysis of Deformed and Regular Cellular Tissue

We now build on the relationships that we have established in the previous sections, using them to investigate the impact that tissue deformation has on the end-to-end communication channel. In particular, we investigate: 1) the quantity of noise from the neighboring cells in the cellular tissue and its impact on the communication between the *Tx* and *Rx*; and 2) the system behavior when force is applied to the tissue and how the deformation impacts on the Ca^{2+} signaling.

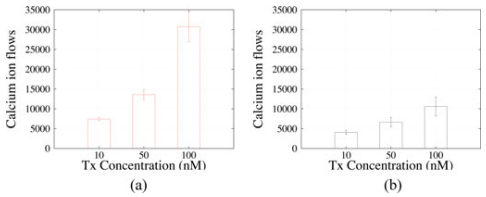

Fig. 7. Ca^{2+} ion flows as a function of *Tx* concentration for a three-layered cellular tissue. The time-slot length is 10s and the *Rx* concentration is 500 nM. (a) Regular tissue. (b) Deformed tissue.

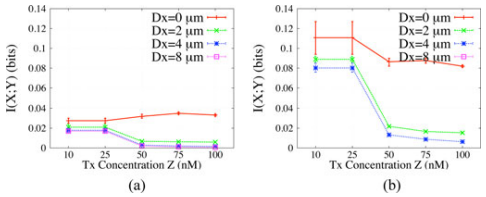

Fig. 8. *I(X;Y)* as a function of the *Tx* concentration for a three-layered cellular tissue with varying distances *Dx* between the *Tx* and the *Rx*. The time-slot length is 10 s, the *Tx* concentration is 50 nM and the *Rx* concentration is 500 nM. (a) Regular tissue. (b) Deformed tissue.

The first parameter considered in our analysis is the concentration of Ca^{2+} information molecules that are emitted by the *Tx*, which we refer to as the *Tx concentration*. Similarly, we also evaluate the impact of varying the *Rx concentration*. One important parameter of the system is the time period during which the *Tx* emits Ca^{2+} ions, which we refer to as the *time-slot* length.

In each experiment, we executed ten simulation runs, where we changed the random seed of each run to compute the 90% confidence interval. Our analysis mainly concentrates on the mutual information *I(X;Y)* for bits transmitted between the *Tx* and the *Rx*.

1) Quantity of Ca^{2+} Ion Flows Between Cells: An important factor in affecting the information transmitted through the channel is the quantity of Ca^{2+} ion flows between the cells in the tissue. As presented in the results (see Fig. 7), the quantity of Ca^{2+} ion flows increases as we increase the concentration at the *Tx*. However, we can see that the deformed tissue has a much smaller quantity of flows compared to the regular tissue. This is attributed to the varying size of the cells in different parts of the tissue that are under compression. In certain regions, cells will have varying sizes which lead to a lower quantity of Ca^{2+} ion efflux from the cells. The manner the tissue is deformed contributes to this—in our experiments, the compression acts to sometimes decrease the size of the distance between the *Tx* and the *Rx*.

2) Sensitivity Analysis of Tx Concentration: Fig. 8 presents the mutual information *I(X;Y)* comparison between a regular and deformed tissue as function of *Tx* concentration for a three-layered cellular tissue. In this analysis, the time-slot length of

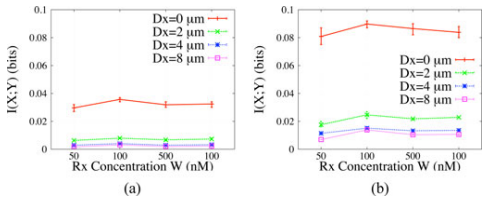

Fig. 9. *I(X;Y)* as a function of the *Tx* concentration for a three-layered cellular tissue with varying *Rx* concentration. The time-slot length is 10 s and the *Tx* concentration is 50 nM. (a) Regular tissue. (b) Deformed tissue.

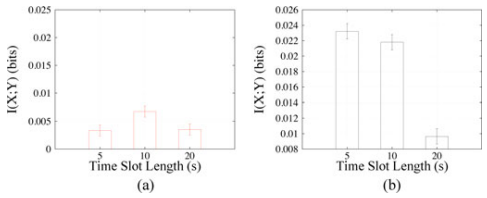

Fig. 10. *I(X;Y)* as a function of the time-slot length for a three-layered cellular tissue, with *Rx* concentration of 500 nM and the *Tx* concentration of 50 nM. (a) Regular tissue. (b) Deformed tissue.

10 s and the *Rx* concentration of 500 nM are the fixed parameters. As expected, the increase in distances between the *Tx* and the *Rx* tends to decrease the number of bits transmitted. However, an interesting observation is the rise in mutual information *I(X;Y)* once the tissue is deformed. We can attribute this to the pipe-effect, which drives the Ca^{2+} ions to flow toward one specific direction. In particular, since the neighboring cells around the *Tx* have smaller length, we can also assume minimum noise will be contributed by those cells. Another interesting point is the concentration value at the *Tx*, where we can see that at low values our mutual information *I(X;Y)* is the highest.

3) Sensitivity Analysis of Rx Concentration: Fig. 9 presents the mutual information of *I(X;Y)* analysis as we vary the quantity of Ca^{2+} concentration at the *Rx*. For all the experiments, we fixed the time-slot length at 10 s and the *Tx* concentration at 50 nM. Similar to the variations in the *Tx* concentration, we observe that increasing the distances also dramatically decreases *I(X;Y)*. However, the difference is marginal as we vary the concentration at the *Rx*. This could be due to the fact that the sensitivity of the concentration at the *Rx* will not get further stimulated when we fix the concentration from the *Tx*. Similar to the results from the previous section, we can observe that the mutual information increases as we compress the tissue, and this is again due to the fact that there is confined physical channel space to allow the ions to flow from the *Tx* to the *Rx*.

4) Sensitive Analysis of Tx Time-Slot Duration: We now investigate the impact that transmission time-slot duration will have on the mutual information *I(X;Y)*. From Fig. 10, we observe that the increase in time-slot length does not guarantee an increase in the mutual information for the regular tissue,

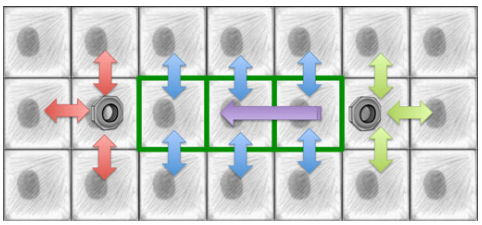

Fig. 11. Spatial illustration of different types of noise: source noise (red), destination noise (green), system noise (blue), and the recurrent noise (purple). Direct pipe-effect for the cellular tissue is shown as the green border.

where we can see an optimal point when the time slot is 10s . For the deformed tissue, we observe an increase in the mutual information—due to the pipe-effect—which has a positive impact for all the time-slot lengths in comparison to the regular tissue structure. An interesting observation is the fact that a smaller time-slot length results in higher mutual information. This can be attributed to two factors: the physical compressed channel of the tissue and the quantity of noise. As described earlier, the compressed length of neighboring cells will lead to lower diffusion of Ca^{2+}, which in turn leads to lower noise in the environment. This is also coupled with the fact that there will be less noise emitting from the cells of the higher and lower layers. Therefore, there is a high correlation between the amount of concentration, as well as the quantity of noise in the environment. This is particularly the case when the time-slot duration is lower.

V. Spatial Noise Analysis

As discussed above, the performance of Ca^{2+} signaling molecular communications is impacted by both the noise from neighboring cells and tissue deformation under force. In the former case, the noise in the system results from the noise in the form of leftover Ca^{2+} ions from a previous transmission. Due to the spatial characteristic of the tissue and the mechanism of Ca^{2+} stimulation from neighboring cells, we identify different types of noise that impact on the channel, as illustrated in Fig. 11 and outlined as follows:

1) *Recurrent noise:* Since Ca^{2+} signaling is a cascading process between neighboring cells, a stimulation of one cell will lead to diffusive stimulation of other cells. Therefore, after the refractory process from a cell emitting Ca^{2+} ions, we find that this cell will get stimulated a bit later on due to the recurrent Ca^{2+} signals that are reflected from the cells on the boundary of the tissue. Refractory process is a recovery time needed by the cells after the stimulation and release of Ca^{2+} ions. As indicated in Fig. 11, this noise affects the direct path between the *Tx* and the *Rx*.
2) *Source noise:* This noise is due to the recurrent Ca^{2+} signals that come from the cells surrounding the *Tx*.
3) *Destination noise:* This noise is due to the recurrent Ca^{2+} signals that come from the cells surrounding the *Rx*.

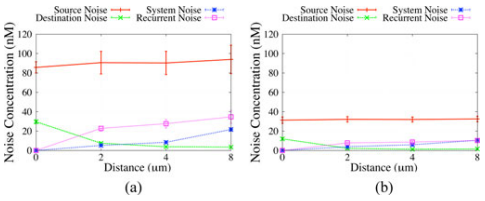

Fig. 12. Noise concentration with respect to varying distances for a three-layered cellular tissue. We include the comparison for the four identified types of noise: source, destination, recurrent, and system. The time-slot length is 10 s, *Tx* concentration is 50 nM, and the *Rx* concentration is 500 nM. (a) Regular tissue. (b) Deformed tissue.

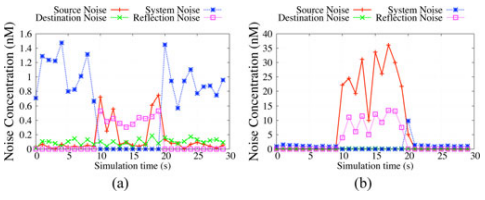

Fig. 13. Temporal analysis for the four noise types in a regular tissue. The time-slot length is 10 s, *Rx* concentration is 500 nM, and *Dx* is 8 μm. (a) *Tx* concentration $=$ 10 nM. (b) *Tx* concentration $=$ 100 nM.

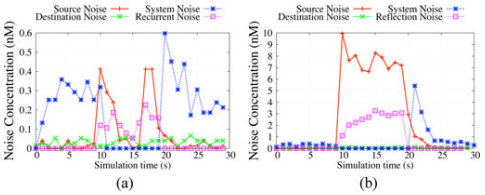

Fig. 14. Temporal analysis for the four noise types in a deformed tissue. The time-slot length is 10 s, *Rx* concentration is 500 nM, and *Dx* is 8 μm. (a) *Tx* concentration $=$ 10 nM. (b) *Tx* concentration $=$ 100 nM.

4) *System noise:* Besides the noise resulting from the transmission of bits from the *Tx*, there is also the system noise—"regulatory" ions emitted from each cell as part of their normal functioning. The concentration of Ca^{2+} ions for such system noise is usually a very small quantity compared to the other types of noise.

The impact of each type of noise with respect to varying distances for both the regular and deformed tissue is shown in Fig. 12. The results show that different noise types have varying impact on the channel in terms of concentration. The highest concentration of noise is the source noise for both the regular and deformed tissue. We note that the level of recurrent noise is much lower in deformed tissue—due to the pipelining effect discussed above. This explains the higher quantity of mutual information during deformation compared to the regular tissue. Figs. 13 and 14 present the quantity of noise from a temporal perspective. We can once again observe that the highest level of noise is from the source noise and that there is an overall reduction in noise for the deformed tissue compared to the regular tissue. We note that the deformed tissue with the *Tx* concentration of 100 nM shows the peak noise duration for approximately 10 s.

VI. Transmission Protocols

Our analysis to this point has shown that there are different noise characteristics in the cellular tissue, and this is highly dependent on the spatial structure of the tissue due to deformation, time slots used for transmission, as well as the concentration of the Ca^{2+} at the *Tx*. We have observed that the concentration at the *Rx* does not dramatically change the mutual information for the end-to-end channel. However, a major factor we have found that impacts the mutual information is the time-slot duration used for the Ca^{2+} stimulation, as evident from Fig. 10. We can see that there are optimal time-slot durations and these differ between the regular and deformed tissues. Therefore, this presents opportunities for the development of transmission protocols at the *Tx* nanomachine to improve the channel *DR*, depending on the compression state of the tissue. In this section, we propose four transmission protocols: *STC*, *DTC*, *DTC-SC*, and *IDTC-SC*. *DR* is the particular metric that we used to compare the different protocols for our analysis.

A. Static Time-Slot Configuration

This is the simplest transmission protocol, where the time-slot lengths are set to static values for each bit transmission. The *DR* is represented as $\frac{1}{T_b}$, where T_b is the time-slot duration.

B. Dynamic Time-Slot Configuration

Given that the state of tissue deformation affects the optimum time slot, the *DTC* protocol dynamically reconfigures the time-slot duration depending on the deformation level of the tissue. We assume that using this approach, the *Tx* nanomachine can detect the quantity of source noise to infer the deformation level. As shown in Fig. 12, the variation in the quantity of source noise between the regular and deformed tissue is on the order of two and a half times. Since we assume a three-layered cellular tissue, the optimum time slots of 5 s(T_{BC}) and 10 s(T_{BR}) for regular and deformed tissue, respectively, are used for the *DTC*. For the total transmission duration ΔT, we assume that we know the probability of compression $P(c)$ (this probability refers to the frequency of tissue compression). The *DR* for the *DTC* protocol can, therefore, be represented as

$$DR = \frac{1}{\Delta T P(c) T_{BC} + \Delta T (1 - P(c)) T_{BR}}. \quad (15)$$

C. Dynamic Time-Slot Configuration With Silent Communication

Communication by silence has previously been investigated in wireless sensor networks [25], and more recently in molecular communications [26]. In the technique, the *silence* period between successive signals is itself used to convey information. A start signal is first transmitted from the *Tx*, and when this is

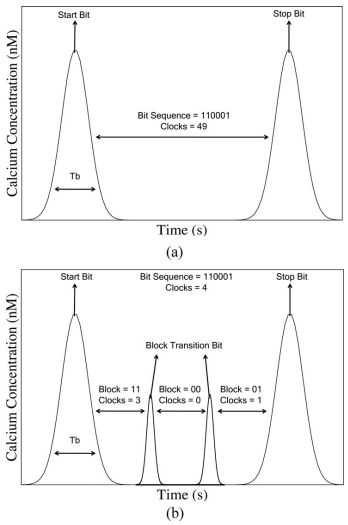

Fig. 15. Illustration of the DTC-SC and the IDTC-SC Transmission Protocols. (a) The DTC-SC transmission protocol. (b) The IDTC-SC transmission protocol.

received at the *Rx*, a counter is invoked. This counter will continue to count until a stop signal arrives at the *Rx*. This means that only two signals will be required for the information transmission. Therefore, T_b is only limited to the duration of the start signal (the stop signal is not considered, since this is transmitted in parallel to when the clock is running at the receiver). The operation of *DTC-SC* is illustrated in Fig. 15. For n number of bits to be transmitted, the *DR* for the *DTC-SC* protocol is represented as (this equation is modified from [26])

$$DR = \frac{n}{T_B + \frac{2^n - 1}{f_c}} \tag{16}$$

where f_c is the clock frequency of the counter at the receiver nanomachine. As shown in the equation, the *DR* is dependent on the duration of the time slot for transmitting the start signal and the duration for the counting process at the receiver. Similar to the *DTC*, T_b will depend on the state of the tissue, where T_{BC} is used when there is a deformation and T_{BR} is used when the tissue state is regular.

D. Improved Dynamic Time-Slot Configuration With Silent Communication

IDTC-SC seeks to improve over the *DTC-SC* by first dividing the information into blocks (see Fig. 15(b) for an illustration). For each block, a transition bit is transmitted by the transmitter to indicate transmission of a new block. Using this configuration can provide further opportunity to reduce the number of clock counts at the *Rx*, while ensuring that the *DR* is high. In order to realize this, it will require that different signals are transmitted for the start and stop bit, as well as the block transition bit. For this, we can send Ca^{2+} signals of different concentration, where the receiver will be required to have the capability of distinguishing the different signals. The *DR* for the *IDTC-SC* protocol is represented as

$$DR = \frac{n * Bs}{T_B + \frac{(\frac{n}{Bs}) * (2^{Bs} - 1)}{f_c}}. \tag{17}$$

TABLE I
PARAMETERS STANDARD VALUES

Variable	Value
Δt	300 s
T_{BC}	5 s
T_{BR}	10 s
$P(c)$	0.5
B_s	2
f_c	500 (Hz)
n	100

Similar to the *DTC-SC*, the value of the time slot T_b will be either T_{BC} or T_{BR} depending on the state of the tissue. B_s is the block size in number of bits. This protocol takes a hybrid approach that combines signaling as well as counting at the *Rx*. As illustrated in Fig. 15(b), sending the same digital bits as in Fig. 15(a) in three blocks will only require each block to have a small number of clock counts.

Fig. 16 presents numerical analysis of the four protocols. The values of the system variables used are shown in Table I. In Fig. 16(a), we analyze the *DR* for the different protocols as the number of transmitted bits varies. We see that the increase in the number of transmitted bits will lead to *IDTC-SC* having the highest *DR* (the f_c is set at 500 Hz). An interesting observation, which is a general observation valid even for other communication systems, is the fact that *DTC-SC* does not perform as well as the other protocols. The reason for this is because the waiting time for the clock counting process at the receiver is longer than transmitting bits in time slots using either *DTC* or *STC*. However, the *IDTC-SC* integrates the two strategies and is able to find the right balance where the counting process for short blocks is faster than sending the bits in sequences of time slots such as in *DTC* or *STC*. Therefore, the use of silence in molecular communications is most ideal for *super-slow* networks, such as bacteria communication in [26]. In Fig. 16(b), we compare the performance of the four transmission protocols as we vary the duration of compression (the percentage indicates the time that the tissue is under compression). The reason we see that the *IDTC-SC* has the highest *DR* is because as we increase the duration of compression, we minimize the quantity of noise, as our previous analysis has shown. However, this also ensures that each time slot will have shorter durations, and at the same time minimizes the clock frequency for the *Rx*. Our confirmation of the optimal time slot is once again shown in Fig. 16(c), where we see that as we increase the time-slot lengths, the *DR* starts to drop. Although the *DR* does decrease, we also once again see that the *IDTC-SC* has a higher performance compared

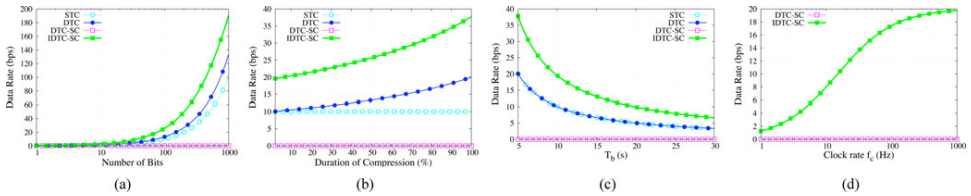

Fig. 16. Comparison analysis for the *STC*, *DTC*, *DTC-SC*, and the *IDTC-SC* transmission protocols, for (a) varying number of bits for transmission, (b) varying the duration of compression in the tissue, (c) varying the time-slot length, and (d) varying the clock rate.

to the other protocols. In Fig. 16(d), we see that as the clock frequency increases, this only impacts on the *IDTC-SC*. This can be attributed to the shorter time-slot duration and higher number of information blocks that can be transmitted in each time slot.

VII. Conclusion

In this study, we analyze the use of Ca^{2+} signaling for molecular communications in a cellular tissue environment. We first analyze the natural properties of Ca^{2+} signaling in a three-layered cellular tissue compared to a single layer, which has been investigated previously. This was followed by an analysis of a regular and deformed cellular tissue. Our analysis shows that while concentration of Ca^{2+} at the transmitter and receiver nanomachine does impact on the mutual information, an important parameter is the time-slot duration used for information transmission. Since the structure of the tissue impacts on the duration of the time slot that is used for the transmission, we propose four protocols to improve the *DR* for Ca^{2+}-signaling-based molecular communications. Our numerical analysis suggests that the *IDTC-SC* protocol significantly outperforms the other protocols in terms of *DR* as we vary the number of bits for transmission, total transmission duration, and the quantity of compression in the tissue deformation.

References

[1] D. Kilinc and O. B. Akan, "An information theoretical analysis of nanoscale molecular gap junction communication channel between cardiomyocytes," *IEEE Trans. Nanotechnol.*, vol. 12, no. 2, pp. 129–136, Mar. 2013.

[2] B. D. Unluturk, D. Malak, and O. B. Akan, "Rate-delay tradeoff with network coding in molecular nanonetworks," *IEEE Trans. Nanotechnol.*, vol. 12, no. 2, pp. 120–128, Mar. 2013.

[3] I. F. Akyildiz, F. Brunetti, and C. Blazquez, "Nanonetworks: A new communication paradigm," *Comput. Netw.*, vol. 52, pp. 2260–2279, 2008.

[4] B. Gulbahar and O. B. Akan, "A communication theoretical modeling of single-layer graphene photodetectors and efficient multireceiver diversity combining," *IEEE Trans. Nanotechnol.*, vol. 11, no. 3, pp. 601–610, May 2012.

[5] J. M. Jornet and I. F. Akyildiz, "Joint energy harvesting and communication analysis for perpetual wireless nanosensor networks in the terahertz band," *IEEE Trans. Nanotechnol.*, vol. 11, no. 3, pp. 570–580, May 2012.

[6] I. F. Akyildiz and J. M. Jornet, "The internet of nano-things," *IEEE Wireless Commun.*, vol. 17, no. 6, pp. 58–63, Dec. 2010.

[7] M. Kuran, T. Tugcu and B. O. Edis, "Calcium signaling: Overview and research directions of a molecular communication paradigm," *IEEE Wireless Commun.*, vol. 19, no. 5, pp. 20–27, Oct. 2012.

[8] I. Akyildiz, F. Fekri, R. S. C. R. Forest, and B. K. Hammer, "Monaco: Fundamentals of molecular nano-communication networks," *IEEE Wireless Commun.*, vol. 19, no. 5, pp. 12–18, Oct. 2012.

[9] B. Atakan, S. Balasubramaniam, and O. B. Akan, "Body area nanonetworks with molecular communications in nanomedicine," *IEEE Commun. Mag.*, vol. 50, no. 1, pp. 28–34, Jan. 2012.

[10] M. Pierobon and I. F. Akyildiz, "Diffusion-based noise analysis for molecular communication in nanonetworks," *IEEE Trans. Signal Process.*, vol. 59, no. 6, pp. 2532–2547, Jun. 2011.

[11] M. Pierobon and I. F. Akyildiz, "Noise analysis in ligand-binding reception for molecular communication in nanonetworks," *IEEE Trans. Signal Process.*, vol. 59, no. 9, pp. 4168–4182, Sep. 2011.

[12] A. Guney, B. Atakan, and O. B. Akan, "Mobile ad hoc nanonetworks with collision-based molecular communication," *IEEE Trans. Mobile Comput.*, vol. 11, no. 3, pp. 353–366, Mar. 2012.

[13] T. Nakano, T. Suda, M. Moore, R. Egashira, A. Enomoto, and K. Arima, "Molecular communication for nanomachines using intercellular calcium signaling," in *Proc. IEEE 5th Conf. Nanotechnol.*, 2005, pp. 478–481.

[14] A. C. Heren, M. S. Kuran, H. B. Yilmaz, and T. Tugcu, "Channel capacity of calcium signalling based on inter-cellular calcium waves in astrocytes," in *Proc. IEEE Int. Conf. Commun. Workshop*, 2013, pp. 792–797.

[15] A. Enomoto, M. Moore, T. Nakano, R. Egashira, T. Suda, A. Kayasuga, H. Kojima, H. Sakakibara, and K. Oiwa, "A molecular communication system using a network of cytoskeleton filaments," in *Proc. Nano Sci. Technol. Inst.-Nanotech*, 2006, pp. 725–728.

[16] J. Hurtig, D. T. Chiu, and B. Onfelt, "Intercellular nanotubes: Insights from imaging studies and beyond," *Wiley Interdiscipl. Rev.: Nanomed. Nanobiotechnol.*, vol. 2, no. 3, pp. 260–276, 2010.

[17] M. Gregori and I. Akyildiz, "A new nanonetwork architecture using flagellated bacteria and catalytic nanomotors," *IEEE J. Sel. Areas Commun.*, vol. 28, no. 4, pp. 612–619, May 2010.

[18] M. Gregori, I. Llatser, A. Cabellos-Aparicio, and E. Alarcón, "Physical channel characterization for medium-range nanonetworks using catalytic nanomotors," *Nano Commun. Netw.*, vol. 1, no. 2, pp. 102–107, 2010.

[19] P. Lio and S. Balasubramaniam, "Opportunistic routing through conjugation in bacteria communication nanonetwork," *Nano Commun. Netw.*, vol. 3, pp. 36–45, 2012.

[20] L. C. Cobo and I. F. Akyildiz, "Bacteria-based communication in nanonetworks," *Nano Commun. Netw.*, vol. 1, pp. 244–256, 2010.

[21] T. Nakano and J.-Q. Liu, "Design and analysis of molecular relay channels: An information theoretic approach," *IEEE Trans. Nanobiosci.*, vol. 9, no. 3, pp. 213–221, Sep. 2010.

[22] A. Goldbeter, G. Dupont, and M. J. Berridge, "Minimal model for signal-induced Ca2+ oscillations and for their frequency encoding through protein phosphorylation," *Proc. Nat. Acad. Sci. USA*, vol. 87, pp. 1461–1465, 1990.

[23] D. T. Gillespie, "Exact stochastic simulation of coupled chemical reactions," *J. Phys. Chem.*, vol. 81, no. 25, pp. 2340–2361, 1977.

[24] R. V. Krsti, " Surface epithelia. Simple cuboidal epithelium. Example: Distal tubule of the nephron," in *General Histology of the Mammal*. Berlin, Germany: Springer-Verlag, 1985, pp. 24–25.

[25] Y. Zhu and R. Sivakumar, "Challenges: Communication through silence in wireless sensor networks," in *Proc. ACM Mobicom 11th Annu. Int. Conf. Mobile Comput. Netw.*, 2005, pp. 140–147.

[26] B. Krishnaswamy, C. M. Henegar, J. P. Bardill, D. Russakow, G. L. Holst, B. K. Hammer, C. R. Forest, and R. Sivakumar, "When bacteria talk: Time elapse communication for super-slow networks," in *Proc. IEEE Int. Conf. Commun.*, 2013, pp. 6348–6353.

Michael Taynnan Barros (S'14) was born in Campina Grande-PB, Brazil, in 1990. He received the M.Sc. degree in computer science from the Federal University of Campina Grande, Campina Grande, and the B.Tech. degree in telematics from the Federal Institute of Education, Science and Technology of Paraiba, Campina Grande. He joined the Telecommunications Software and System Group, Waterford Institute of Technology, Waterford, Ireland, in 2012, as a Ph.D. student.

His experience concentrates on dynamic optical networks, vehicular ad hoc networks, routing, Ip traffic classification, and QoS-DiffServ aware networks with more than 30 papers published. He is also a reviewer for several international journals and conferences. His research interests include nanonetworks, molecular communications, and bioinspired techniques.

Sasitharan Balasubramaniam (SM'14) received the Bachelor's degree in electrical and electronic engineering from the University of Queensland, Brisbane, Australia, in 1998, the Master's degree in computer and communication engineering from the Queensland University of Technology, Brisbane, in 1999, and the Ph.D. degree from the University of Queensland in 2005.

He is currently a Senior Research Fellow at the Nano Communication Centre, Department of Electronic and Communication Engineering, Tampere University of Technology, Tampere, Finland. Previously, he was a Research Fellow at the Telecommunication Software & Systems Group, Waterford Institute of Technology, Waterford, Ireland, where he worked on a number of Science Foundation Ireland projects. He has published more than 70 papers and actively participates in a number of technical programme committee for various conferences. His current research interests include bioinspired communication networks and molecular communications.

Dr. Balasubramaniam was the TPC Co-Chair for ACM NANOCOM 2014 and IEEE MoNaCom 2011, both conferences which he cofounded. He is currently an Editor for the IEEE INTERNET OF THINGS journal and *Elsevier Nano Communication Networks*.

Brendan Jennings (M'05) received the B.Eng. and Ph.D. degrees from Dublin City University, Dublin, Ireland, in 1993 and 2001, respectively.

He is the Director of Research with the Telecommunications Software & Systems Group (http://www.tssg.org) at the Waterford Institute of Technology, Waterford, Ireland. He also leads the TSSG Emerging Networks Laboratory, which addresses manageability aspects of computing and communications environments. His research interests include network management, cloud computing, and molecular communications. Further information is available at http://brendanjennings.net.

Yevgeni Koucheryavy (SM'09) received the Ph.D. degree from the Tampere University of Technology (TUT), Tampere, Finland, in 2004.

Prior joining TUT, he spent five years in the industry with R&D LONIIS, St. Petersburg, Russia, where he held various technical and managerial positions. He is an Invited Expert for International Telecommunication Union for Telecommunication and the Skolkovo Foundation (Russia) and acts as an External Reviewer for the state funding agencies of several European countries. He is currently a Professor with the Department of Communications Engineering, TUT. His current research interests include heterogeneous wireless communications and systems, network and services performance evaluation, internet of things, and machine-to-machine communications.

Chapter 6

Using Information Metrics and Molecular Communications to Detect Cellular Tissue Deformation

Journal Title:	IEEE Transactions on Nanobioscience
Article Type	Regular Paper
Complete Author List	Michael Taynnan Barros, Sasitharan Balasubramaniam and Brendan Jennings
Keywords	Molecular Communication; nanonetworks; calcium signaling, information theory, tissue deformation
Status	Published: v. 13, p. 278-288, September 2014. doi: 10.1109/TNB.2014.2351451

278 IEEE TRANSACTIONS ON NANOBIOSCIENCE, VOL. 13, NO. 3, SEPTEMBER 2014

Using Information Metrics and Molecular Communication to Detect Cellular Tissue Deformation

Michael Taynnan Barros*, *Student Member, IEEE*, Sasitharan Balasubramaniam, *Senior Member, IEEE*, and Brendan Jennings, *Member, IEEE*

***Abstract*—Calcium-signaling-based molecular communication has been proposed as one form of communication for short range transmission between nanomachines. This form of communication is naturally found within cellular tissues, where Ca^{2+} ions propagate and diffuse between cells. However, the naturally flexible structure of cells usually leads to the cells dynamically changing shape under strain. Since the interconnected cells form the tissue, a change in shape of one cell will change the shape of the neighboring cells and the tissue as a whole. This will in turn dramatically impair the communication channel between the nanomachines. We propose a process for nanomachines utilizing Ca^{2+} based molecular communication to infer and detect the state of the tissue, which we term the *Molecular Nanonetwork Inference Process*. The process employs a threshold based classifier that identifies its threshold boundaries based on a training process. The inference/detection mechanism allows the destination nanomachine to determine: i) the type of tissue deformation; ii) the amount of tissue deformation; iii) the amount of Ca^{2+} concentration emitted from the source nanomachine; and iv) its distance from the destination nanomachines. We evaluate the use of three information metrics: mutual information, mutual information with generalized entropy and information distance. Our analysis, which is conducted on two different topologies, finds that mutual information with generalized entropy provides the most accurate inferencing/detection process, enabling the classifier to obtain 80% of accuracy on average.**

***Index Terms*—Molecular communication, nanonetworks, calcium signaling, information theory, tissue deformation.**

I. Introduction

MOLECULAR COMMUNICATION is a new communication paradigm for nanoscale communication [1]–[3]. By enabling communication to be performed at the nanoscale within a biological environment numerous novel applications can be developed to complement the already mature field of nanotechnology. An obvious field of application is in healthcare, where more improved diagnostics and monitoring processes can be achieved at fine granular scale and also at an early stage. In recent years, numerous models have been proposed for molecular communication, including diffusion-based systems [4]–[6], bacteria nanonetworks [7], and Forster Resonance Energy Transfer (FRET) [8], [9].

One particular form of diffusion-based molecular communication is through **Calcium signaling** (Ca^{2+}) [10]. Ca^{2+} signaling provides short-range communication between biological cells, where information is encoded and modulated through the concentration of Ca^{2+} ions. Numerous research efforts have targeted the use of Ca^{2+} for molecular communication, in particular for nanomachines that may interface to tissues within organs [11], [12].

While utilizing natural Ca^{2+} signaling for communication is appealing, there are numerous challenges. Firstly, Ca^{2+} signaling is a highly stochastic signaling process that involves a number of chemical reactions that occur stochastically. Secondly, since Ca^{2+} signaling is one common communication mechanism in the tissue, the reliability of the signaling process is highly reliant on the state of the physical tissue structure. Tissues in their natural form have highly flexible structures that can change and deform depending on various external forces, which in turn could affect the Ca^{2+} ions propagation. This latter challenge is the motivation of this paper: we aim to develop an approach that can enable the nanomachines embedded in a tissue to infer the current state of the molecular nanonetwork. The inferencing process, which is conducted by the destination nanomachine, will infer the state of the tissue based on statistics collected from communication between the different nanomachines. These states may include i) the quantity of deformation, ii) type of deformation, iii) the concentration of the Ca^{2+} emitted from the nanomachines, as well as iv) the distances between the source and destination nanomachines. We propose a **Molecular Nanonetwork Inference Process**, which uses information metrics in combination with threshold based classifiers during the training phase to detect and infer the state of the tissues. The three information metrics we evaluate are: *mutual information*, *mutual information with generalized entropy* and *information distance*. Initially we investigate the properties of these metrics for a single-hop communication between the nanomachines, in order to determine the importance of the

Manuscript received August 16, 2013; revised June 02, 2014; accepted July 08, 2014. Date of publication August 28, 2014; date of current version September 23, 2014. *Asterisk indicates corresponding author.*

*M. T. Barros is with the Telecommunication Software & Systems Group (TSSG), Waterford Institute of Technology (WIT), Waterford, Ireland.

B. Jennings is with the Telecommunication Software & Systems Group (TSSG), Waterford Institute of Technology (WIT), Waterford, Ireland.

S. Balasubramaniam is with the Nano Communications Center (NCC), Department of Electronics and Communication Engineering, Tampere University of Technology (TUT), Tampere, Finland. (e-mail: mbarros@tssg.org, sasi.bala@tut.fi, bjennings@ieee.org).

Color versions of one or more of the figures in this paper are available online at http://ieeexplore.ieee.org.

Digital Object Identifier 10.1109/TNB.2014.2351451

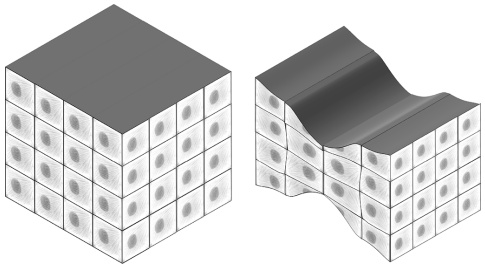

Fig. 1. Illustration of tissue deformation: when localized force is applied to cells this is propagated through the tissue so that all cells experience structural changes. (a) No compression. (b) Dual compression.

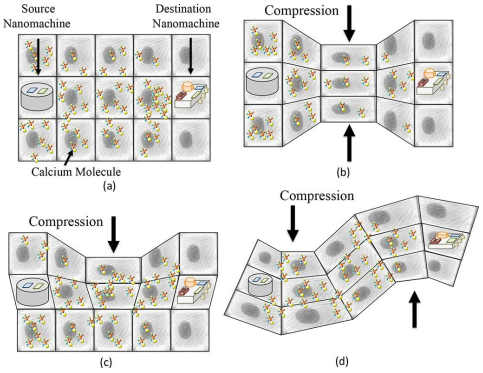

Fig. 2. Communication disruption due to tissue deformation, (a) *normal* tissue structure, (b) *double-sided* compression, (c) *single-sided* compression and (d) *S shape* deformation.

data variance and its impact on inferencing accuracy. This is followed by an analysis of the classifier for two different nanomachine topologies that are embedded into a tissue.

This paper is organized as follows. Section II presents the problem statement of tissue deformation and its impact on molecular communication systems. Section III presents the basic model for calcium signaling based molecular communication, which serves as the model used in our simulations. Section IV presents our proposed classifier of channel state information. Section V presents the three information metrics used in our proposed classifier. Section VI presents the performance of the metrics over a single-hop molecular communication system based on calcium signaling. Section VII presents the accuracy analysis of the proposed approach for two different topologies. Section VIII presents a discussion about the nanomachines realization for future envisioned applications. Finally, Section IX concludes the paper.

II. Problem Statement

In this section we discuss the properties of tissue deformation, and how this could impact on the Ca^{2+} signaling within the tissue.

Since the majority of tissue structures are constructed from a tight formation of interconnected cells, a change in the structure of a cell could impact the tissue as a whole. The changes in shapes of cells can largely be attributed to their structure and internal composition. Fig. 1 illustrates an example of a tissue undergoing structural change as a result of compression. Example factors that can influence the cell shape changes includes physical movement, chemotaxing cells or mitotic cleavage [13]. During mitotic cleavage, the stretching process of a cell will compress the neighboring cells [14]. In [15], a study was conducted on the deformation of cells resulting from the movements in the joint's cartilage. In particular, the focus of the study was on the *Tibiofemoral* joint and its mechanical loading impact on cells of the musculoskeletal system.

The deformation of the tissue can affect the performance of molecular communication, in particular communication that is performed through diffusion of molecules inside the cellular tissue. Masselter and Speck [16] investigate how tissue deformation spatially modulates *angiogenic* and *angiogenesis* signals. This is due to the physical forces applied to the developing tissues. For example, during vascular development, the deformation caused by such forces has a huge impact on the Ca^{2+} signaling and the overall behavior of the cell. Fig. 2 illustrates an example of communication disruption that could occur due to different types of tissue deformation, including: *double-sided* tissue compression [Fig. 2(b)], *single-sided* tissue compression [Fig. 2(c)] and compression in multiple spots, which we refer to it as *"S"* shape deformation [Fig. 2(d)]. Since Ca^{2+} signaling diffuses the molecules between tightly packed cells within a tissue, the communication capacity is largely dependent on the spatial volume of the cells, which affects the process of invoking Ca^{2+} signaling, as the signals are propagated through the tissue. Therefore, any physical force that impacts on the spatial volume, will in turn affect the communication capacity.

III. Calcium Based Molecular Nano Network

In this section, we present the simulation model of the Ca^{2+} signaling process between the cells within the tissue that we consider in our study. The Ca^{2+} signaling process, illustrated in Fig. 3, is conducted through diffusion of ions that are propagated through the cell gap junctions. There are multiple complex chemical reactions that occur in sequence and in parallel, where the signaling process includes stimulation, storage, as well as the release of Ca^{2+} ions from the intracellular store. As the Ca^{2+} ions are diffused through the gap junction, the ions will invoke the neighboring cell's intracellular store, which in turns leads to repeated signaling process that propagates to the neighboring cells, known as intercellular signaling.

A. Calcium Signaling Analytical Model

Our simulation model of the Ca^{2+} signaling process is based on the analytical model proposed by Goldbeter *et al.* [17]. For each cell, the (1) and (2) below describe the behavior of the *cytosolic* Ca^{2+} concentration (Z) as well as the *intracellular* store concentration (E). The components of the (1) and (2) are: 1) v_0: Ca^{2+} leakage from the extracellular space into the cellular cytosol; 2) v_2: transport of Ca^{2+} from the cellular cytosol to the endoplasmic reticulum; 3) v_3: release of Ca^{2+} from the cellular

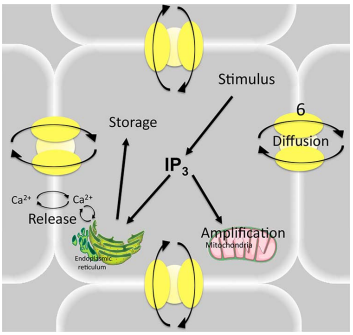

Fig. 3. Illustration of the stimulation, storage, and release of ions in the Ca^{2+} signaling process, which gets diffused to the neighboring cells through the gap junction.

endoplasmic reticulum into the cytosol; 4) $k_f E$: Ca^{2+} leakage from the endoplasmic reticulum to the cytosol; 5) kZ: transport of Ca^{2+} from the cytosol to the extracellular space. At the same time, the intracellular pool also has a magnitude for the influx $(v_1\beta)$, where β is the saturation function of the internal Ca^{2+} receptors in the cell. Both equations represent the Ca^{2+} behaviour within the cell, where this leads to oscillations as they are diffused between the cells.

$$\frac{dZ}{dt} = v_0 + v_1\beta - v_2 + v_3 + k_f E - kZ, \quad (1)$$

$$\frac{dE}{dt} = v_2 - v_3 - k_f E. \quad (2)$$

However, before the Ca^{2+} ions are diffused to the neighboring cells, the ions will first need to be activated through the IP_3 receptors, where this activation will lead to self-amplification. These processes are represented in (3) and (4).

$$v_2 = V_{M2}\frac{Z^n}{K_2^n + Z^n}, \quad (3)$$

$$v_3 = V_{M3}\frac{E^m}{K_R^m + E^m} \cdot \frac{Z^p}{K_A^p + Z^p}, \quad (4)$$

where V_{M2} and V_{M3} are rate constants; K_2, K_R and K_A are threshold constants; and n, m and p are the Hill coefficients.

Finally, the (5) represents the destination activation process as it receives the Ca^{2+} ions. For the destination nanomachine, the transition between the inactive and active state is dependent on the binding rate of the Ca^{2+} ions, v_4, which is represented as:

$$v_4 = k_a\frac{Z^q}{K^q + Z^q}, \quad (5)$$

where k_a, K and q are respectively, the maximum destination activation rate, saturation constant for the cytosolic Ca^{2+} concentration and the Hill coefficient.

B. Simulation of the Calcium Signaling Model

In order to simulate the Ca^{2+} signaling for a cellular tissue, we extended the original model in [18]. Fig. 4 depicts our model

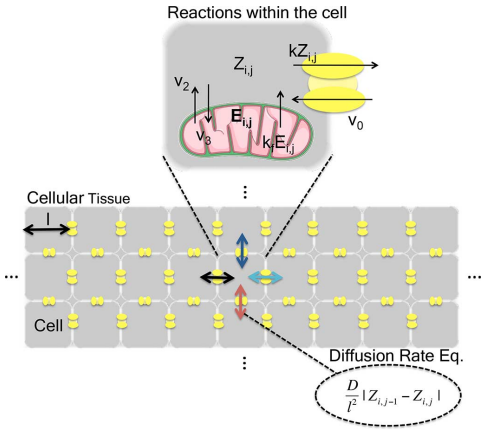

Fig. 4. Illustration of a three-layered cellular tissue, where each layer contain an array of cells. Both the reactions within the cells and the diffusion process to the neighboring cells are shown.

for a cellular tissue. We model the tissue as a 2D lattice structure, where each cell invokes the (1)–(4) to determine the state of the Ca^{2+} ions as it propagates between the cells. We consider a tissue as a matrix of $I \times J$ cells. Let $c_{i,j}$, where $i = 1 \ldots I$ and $j = 1, \ldots J$, denote an arbitrary cell in the tissue. Each cell $c_{i,j}$ also maintains diffusion reactions, which are responsible for the cell-to-cell propagation of Ca^{2+}, and is represented as:

$$Z_{\text{Diff}}(i,j,n,m) = \frac{D}{l^2}(|Z_{n,m} - Z_{i,j}|), \quad (6)$$

where $n \in (i-1, i+1)$, $m \in (j-1, j+1)$, D is the diffusion coefficient and l is the length of the cell.

We assume that the nanomachines are embedded in the tissue and are able to stimulate the diffusion of Ca^{2+} ions for communication. We simulate the Ca^{2+} signaling in the tissue by evaluating the equations presented above at discrete simulated time steps. At each step, our simulator randomly selects a cell, where a randomly selected reaction is executed, in line with the Gillespie algorithm [19]. The selection of the random cell is based on a probability P_R, which is uniformly distributed over the sum of all values of $Z_{\text{Diff}}(i,j,n,m)$. The P_R favors a cell with a high Ca^{2+} concentration, in order to select the cell for diffusion of Ca^{2+} ions into the neighbouring cell. One of the internal reactions of the cell will be randomly executed once the cell $c_{i,j}$ is selected. For each time step, the concentration of the free cytosolic Ca^{2+} ions $(Z_{i,j})$, the Ca^{2+} ions within the endoplasmic reticulum $(E_{i,j})$, as well as the number of molecules detected at the destination nanomachine are updated. When the diffusion is triggered, we assume that the gap junctions are opened.

The communication process is based on the *On-Off Keying (OOK)* modulation technique, where we assume that both the source and destination nanomachines are synchronized. In the OOK modulation technique, when a bit 1 is to be sent, the nanomachine stimulates Ca^{2+} of a particular concentration. However, in the event a bit 0 is to be transmitted, the source nanomachine will be silent for that time slot.

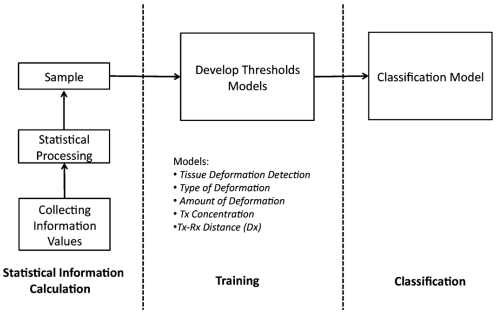

Fig. 5. Flowchart of the Molecular Nanonetwork Inference Process.

The values for the parameters used for the simulation are based on the values used in [18], which are as follows: $v_0 = 1$ (μm/s), $v_1 = 100$ (1/s), Z $= 100$ (nm), k $= 4.2$ (1/s), $k_f = 1$ (1/s), $V_{M2} = 50$ (μm/s), $V_{M3} = 500$ (μm/s), $K_2 = 1$ (μm), $K_R = 2$ (μm), $K_A = 0.9$ (μm), m $=$ n $= 2$, p $= 4$, l $= 0.5$ (μm), $k_a = 2.5$ (μm/s), K $= 0.6$ (nm), q $= 4$, $k_{ia} = 0.5$ (μm/s), D $= 10$ (μm2/s), W $= 500$ (nM).

IV. Inferring Tissue Deformation With the Molecular Nanonetwork Inference Process

As introduced earlier, we seek to have a destination nanomachine (Rx) collects information regarding the communication between it and different source nanomachines (Tx), and analyze the data to infer the state of the molecular nanonetwork. In Fig. 5, a flowchart describes the steps that are used in our Molecular Nanonetwork Inference Process. The three phases are the *statistical information calculation*, then *training*, followed by the *classification*. A single-hop communication system is set up in order to collect information values in the *statistical information calculation*. This information values are mainly based on information theory metrics for communication systems evaluation, or in short, information metrics. We explore three different information metrics: mutual information, mutual information with generalized entropy and information distance. This is responsible for tracking the differences in channel abnormalities. Then, the data is statically treated and grouped into sample, which are sent afterwards to the *training* phase. In this phase threshold models are then developed based on the collected samples, including: tissue deformation detection, type of deformation, amount of deformation, Tx Concentration and $Tx-Rx$ distance (Dx). Only after that is the classification phase performed, where it is possible to detect channel abnormalities online. We now outline these three phases.

A. Statistical Information Calculations

In the statistical information calculation phase we use information metrics to process the collected measurement data, which is converted into samples using statistical processing. Information metrics are further explored in Section V. We assume that for n transmissions from a number of nanomachines, we collect a set ψ of information metric values. This is followed by using the confidence intervals to statistically treat the data, which can be represented as:

$$ci(n,\psi) = m(\psi) \pm U_{\rho/2}\left(\frac{\delta(\psi)}{n}\right), \tag{7}$$

where $m(\cdot)$ is the mean of sampled values, $\delta(\cdot)$ is the standard deviation over a set of values, $\rho = 1-(B/100)$ where B is the confidence level, and finally $U_{\rho/2}$ is the standard normal table value. All the threshold information, which are the confidence intervals for all n transmissions, will be converted into a sample. In the case that we want to identify the type of deformation, we need to train the model with a number of samples that is equal to the number of deformation types.

B. Training Process

The training process involves determining the thresholds and boundaries that are used for the classification of the collected data. We define a decision function $f(\cdot)$, which enables the classifier to determine if the new collected data is placed in the right category. The function $f(\cdot)$ is represented as:

$$f(\chi) = \begin{cases} 1, & \chi \in [-ci(n,\psi), +ci(n,\psi)] \\ -1, & \chi \notin [-ci(n,\psi), +ci(n,\psi)], \end{cases} \tag{8}$$

where χ represents the new collected data.

C. Classification Process

Once the training process is completed, the next stage is the classification process. Here, new information collected at the destination will be compared to the threshold models that have been developed previously. This model will have unique characteristics that will be used to identify all listed channel state information that was introduced earlier. The classifier will be a set of decision functions f, whose cardinality will be equal to the product of the number of samples and the number of nanomachines in each sample. At the end of each transmission, the collected data will be analyzed by the classifier, and in the event that the function returns a non-negative value, this will indicate as the correct inference.

V. Information Metrics

In this section, we will describe the three different information metric algorithms that are used in our training process.

We use digital bit transmission with OOK modulation, investigated in [18], [20], [21]. The transmission is based on the state of the source nanomachine (x), where a bit one transmission releases Ca^{2+} ions of a particular concentration in the channel $(x = x_1)$, while a bit zero results in no ion emission $(x = x_0)$. The same is for the destination nanomachine state (y), where either it can be receiving Ca^{2+} ions representing bit 1 $(y = y_1)$ or bit 0 $(y = y_0)$. The X and Y are the set of states for both the source and destination nanomachines.

A. Mutual Information

The *mutual information* $I(X;Y)$ is used to determine the mutual dependence between two random variables, and is represented through the following equations:

$$\begin{aligned} I(X;Y) &= H(X) - H(X \mid Y) \\ &= \sum_{y \in Y} \sum_{x \in X} p(x) p(y \mid x) \log_2 \frac{p(y \mid x)}{p(y)}, \end{aligned} \tag{9}$$

$$\begin{cases} p(x) = P(x = x_0 \wedge x = x_1), \\ p(y) = P(y = y_0 \wedge y = y_1) * p(y/x), \\ p(y = y_0 \mid x = x_0) = 1 - p(y = y_1 \mid x = x_0), \\ p(y = y_0 \mid x = x_1) = 1 - p(y = y_1 \mid x = x_1). \end{cases} \tag{10}$$

In our analysis, we utilize the mutual information $I(X;Y)$ to analyze the quantity of information that is transmitted from a source nanomachine to a destination nanomachine. The probabilities $p(x)$ and $p(y)$ represents the probability of each state on the source nanomachine or the destination nanomachine, respectively.

B. Mutual Information With Generalized Entropy

Another metric used in information theory to measure the uncertainty over a random variable is the *Generalized Entropy*. The difference in comparison to the Shannon entropy is an increases in the number of dimensions for the data analysis. The metric belongs to family of functions that quantifies the diversity, uncertainty, and/or the randomness of a system, and it is largely used to detect the distances between different probability density functions. We then add this dimension to mutual information The generalized entropy is defined as follows:

$$H_\alpha(x) = \frac{1}{1-\alpha} \log_2 \left(\sum_{i=1}^{n} p_i^\alpha \right), \tag{11}$$

where p_i are the probabilities of $\{x_1, x_2, \ldots, x_n\}$, $p_i \geq 0$,

$$\sum_{i=1}^{n} p_i = 1, \quad \alpha \geq 0, \alpha \neq 1. \tag{12}$$

When $\alpha = 0$ or the probabilities of $\{x_1, x_2, \ldots, x_n\}$ are all the same, we have the maximum information entropy which is represented as follows:

$$H_0(x) = \log_2 n, \tag{13}$$

which indicates high divergence between the probability density functions.

When $\alpha = 1$, the $H_\alpha(x)$, as in (14), Generalized Entrophy converges to the Shannon entropy:

$$H_1(x) = -\sum_{i=1}^{n} p_i \log_2 p_i. \tag{14}$$

We use generalized entropy in combination with the mutual information (15), to amplify the values to different dimensions. Basically, the usual mutual information formula is used but with generalized entropy. In this way, we believe that the classifier will detect the channel characteristics with more accuracy, since this metric is highly recommended in detecting differences in probability density functions.

$$I_\alpha(X;Y) = H_\alpha(X) - H_\alpha(X \mid Y) \tag{15}$$

C. Information Distance

Information distance is another metric that is used to measure the relationship between stochastic variables. This metric, proposed by Bennett *et al.* [22], is commonly applied to pattern recognition between different classes, which fits to our proposed classifier. It provides a measure of the divergence between X and Y and is represented as:

$$\Delta_\alpha(X \mid \mid Y) = \frac{1}{\alpha - 1} \log_2 \left(\sum_{i=1}^{n} x_i^\alpha y_i^{1-\alpha} \right), \quad \alpha \geq 0. \tag{16}$$

We consider that the information distance is always nonnegative with $\alpha \geq 0$. Therefore, based on $\alpha = 0$ and $\alpha = 1$, we have the following equations:

$$\Delta_0(X \mid \mid Y) = -\log_2 \left(\sum_{i=1}^{n} y_i \right), \quad \alpha = 0 \tag{17}$$

$$\Delta_1(X \mid \mid Y) = \sum_{i=1}^{n} (x_i \log_2 (x_i \, y_i)), \quad \alpha = 1 \tag{18}$$

which is also known as the Kullback-Leibler divergence [23], [24].

VI. Application of Information Metrics to Calcium Signaling Based Molecular Communication

Using the simulation model described in Section III-B, we now analyze the performance for the three different information metrics in a single-hop nanonetwork embedded in a cellular tissue. The objective of the analysis is to observe the pattern of data collected from the molecular nanonetwork, in order to determine the quantity of divergence and variance in the data that can be used in the classification process.

We consider a subset of parameters from our model for the analysis. The first parameter considered is the concentration of the information molecules encoded in the Ca^{2+} ions that are emitted by the source nanomachine, which we refer to as the *Tx* concentration. Also the variation of the distances *Dx* between the *Tx* and the receiver (denoted *Rx*) is included in our analysis. Another important parameter of the system is the time during which the *Tx* releases the Ca^{2+} ions, which we refer to as the *time-slot* length. The tissue structure considered in our analysis is a three layer lattice of cells that is 40 μm long, with each cell being 0.5 μm long. In our simulation scenario the *Tx* is positioned in the very center of the 2D cellular tissue lattice, and the destination will be positioned in the same layer but with varying distance apart. In each simulation, we executed ten runs to compute the 90% confidence interval.

A. Mutual Information

In this subsection, we investigate the impact of different deformation types on the mutual information of the end-to-end communication channel.

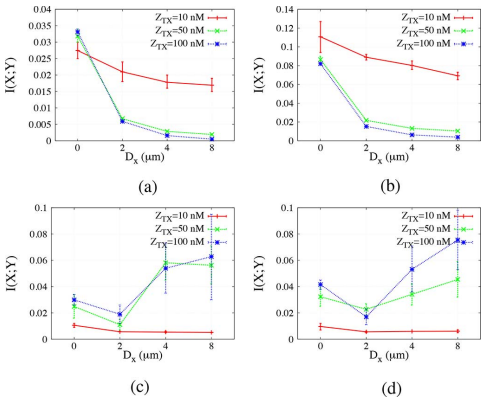

Fig. 6. Information rate as a function of the *Tx* concentration for a five-layered tissue of cell with varying distance *Dx* analysis. The *time-slot* length is 10 seconds, the *Tx* concentration is 50 (nM) the *Rx* concentration is 500 (nM). (a) Normal tissue. (b) *Double-sided* compression. (c) *Single-sided* compression. (d) *S shape* compression.

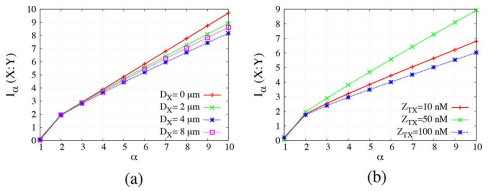

Fig. 7. Mutual Information with generalized entropy metric for a five-layered tissue of cells with a single-hop transmission. The *time-slot* length is 10 seconds and the *Rx* concentration is 500 (nM). (a) Mutual information with respect to varying distances between the nanomachines. The *Tx* concentration is fixed at $100nM$. (b) Mutual information with respect to varying source nanomachine Ca^{2+} concentration. The distance between the nanomachines is set at 4 μm.

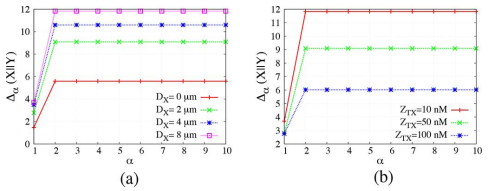

Fig. 8. Information Distance metric for a five-layered tissue of cells with single-hop transmission. The *time-slot* length is 10 seconds and the *Rx* concentration is 500 (nM). (a) Information distance with respect to varying distances between the nanomachines. The *Tx* concentration is fixed with $100nM$. (b) Information distance with respect to varying source nanomachine Ca^{2+} concentration. The distance between the nanomachines is set at 4 μm.

Fig. 6 presents the mutual information comparison for the tissue under no compression, as well as the three types of compression presented in Fig. 2 (*double-sided* compression, *single-sided* compression, and S-shaped compression). The analysis is with respect to the varying *Tx* concentration of a five-layered cellular tissue. In this analysis, the fixed parameters are the time-slot length of 10 seconds, and the *Rx* concentration of 500 (nM). An interesting observation in Fig. 6(a)/(b) is that as we increase the distance D_x, the mutual information $I(X;Y)$ starts to decrease. However, the double-sided compression does have a higher mutual information $I(X;Y)$. The reason that the uncompressed tissue has a lower mutual information $I(X;Y)$ is because the Ca^{2+} ions are subjected to freely move in a larger area. However, once the compression occurs, this space is confined leading to higher quantity of Ca^{2+} reaching the destination. However, the *single-sided* compression and the S shaped compression has an opposite effect, where we see that the mutual information $I(X;Y)$ increases as we increase the distance. Once again this could be attributed to the nature of the compression, which could create a dedicated pipe to support directed Ca^{2+} ions flows between the source and destination nanomachines. However, an interesting result is the identical mutual information $I(X;Y)$ for certain concentration and distance D_x. For example, in the case of no compression, there is negligible difference for *Tx* concentration of 50 or 100 (nM). Similarly, for the *single-sided* and S-shaped compression, there is negligible difference in mutual information $I(X;Y)$ for the same *Tx* concentration. Therefore, this presents a weakness in using mutual information as a metric for classifying or determining the quantity of concentration at the *Tx*.

B. Mutual Information With Generalized Entropy Metric

Fig. 7 presents the result of the mutual information $I(X;Y)$ for a single-hop communication between a source and destination nanomachine in a five-layered tissue. In Fig. 7(a) we first analyze the varying distances D_x between the nanomachines with respect to varying α. In Fig. 7(b) we analyze the mutual information $I(X;Y)$ for different T_x concentration as we increase the value of α. The results of both graphs shows that as we increase the alpha value, we start to get higher divergence in the information of the tissue state. This indicates that a higher accuracy can be achieved as we increase the value of α; however, this comes at the cost of increased computational complexity.

C. Information Distance

For the same number of layers (five) in the tissue, and also for a single-hop analysis, the results for the information distance is presented in Fig. 8. The results shows that information distance converges after $\alpha = 2$. This means that for $\alpha = 2$, we are able to obtain the highest divergence of data analysis. This provides an added benefit to our proposed application, where we can encounter nanomachines that have limited processing capabilities. Therefore, a classifier with the lowest possible value of α keeps the computational complexity low, an interesting feature for low-processing devices like nanomachines.

D. Variance Analysis of the Information Metrics

We now analyze and compare the variance of the different information metrics. The variance provides an indication of the threshold range, where a long range threshold provides the classifier with greater accuracy in inferring the state of the tissue. First, in Fig. 9, we analyze the variance with respect to varying the distance D_x. As we can observe, information distance with an $\alpha = 2$ leads to a reasonably high variance compared to the generalized metric (including the generalized entropy with a high value of α). This is due to the fact that when the α is increased, the difference between the different probability density

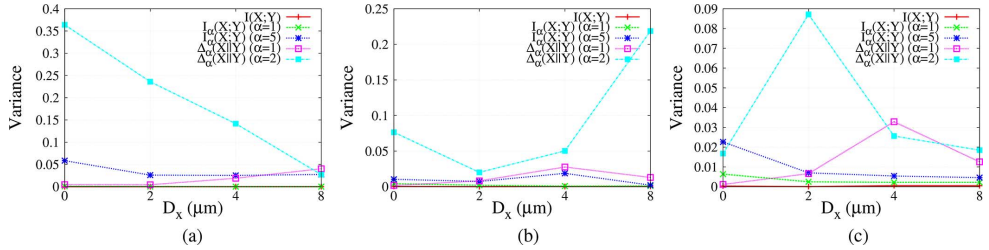

Fig. 9. Variance analysis with respect to varying distance between nanomachines for a five-layered tissue of cells with a single-hop transmission. The time slot length is set at 10 seconds, the *Tx* concentration is $50nM$, and the *Rx* concentration is 500 (nM). (a) Normal tissue with no compression. (b) Tissue with *one-side* compression. (c) Tissue with a *S-type* compression.

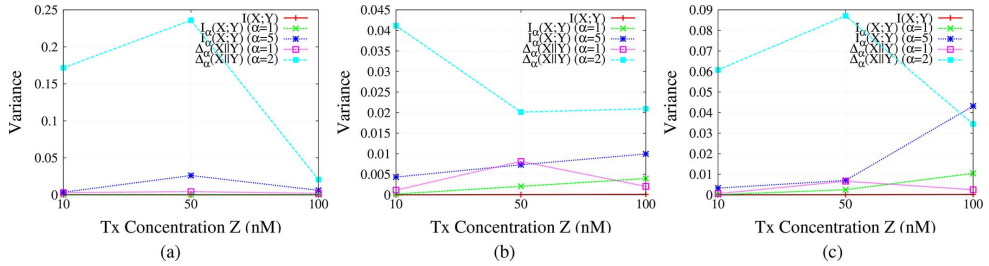

Fig. 10. Variance analysis with respect to varying source nanomachine Ca^{2+} concentration for a five-layered tissue of cells with a single-hop transmission. The time slot length is set at 10 seconds, the distance *Dx* is 2 μm and the *Rx* concentration is 500 (nM). (a) Normal tissue with no compression. (b) Tissue with *one-side* compression. (c) Tissue with a *S-type* compression.

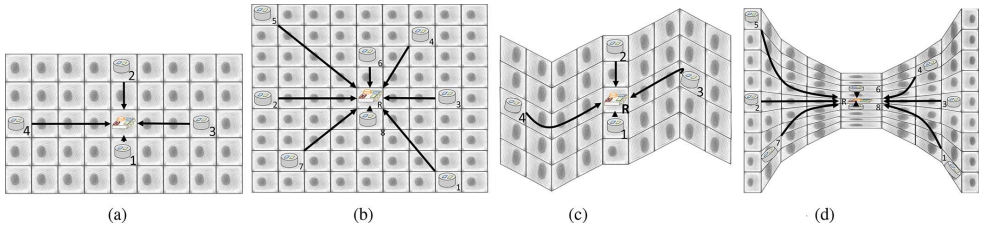

Fig. 11. Example of tissue deformation and its impact on the changes in the nanonetwork topologies. (a) Topology 1: 5 nodes. (b) Topology 2: 9 nodes. (c) *S-shape* deformation on Topology 1. (d) *Double-sided* deformation on Topology 2.

TABLE I
TOPOLOGY 1

Node	Z (nM)	D_x (μm)
1	10	0
2	100	2
3	50	4
4	10	8

TABLE II
TOPOLOGY 2

Node	Z (nM)	D_x (μm)
1	50	8.94
2	10	8
3	50	4
4	50	4.47
5	50	11.31
6	100	2
7	50	5.66
8	10	0

functions will also increase. Now analyzing the variance with respect to varying the Tx concentration, Fig. 10, we observe the same results with exactly for the same reason. Just by increasing the data dimension the variance tends to increase as well. These results suggest that the information distance metrics should lead to good classification process. However, we will also see in the performance evaluation below, that the mutual information with generalized entropy performed equally as good or better than the information distance, albeit at higher computational cost.

VII. Analysis of the Inference Process

In this section we analyze the performance of the proposed Molecular Nanonetwork Inference Process. Our aim is to evaluate the effectiveness of the different information metrics, and how they will be impacted for different topologies of nanomachines. We consider two different star topologies, depicted in Fig. 11; in Topology 1 there are 4 source nanomachines and

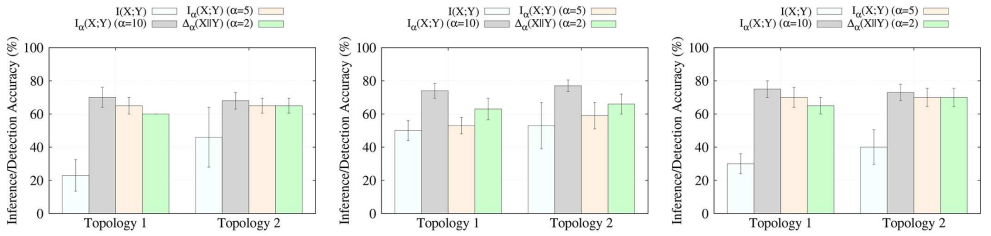

Fig. 12. Accuracy of inferring the type of deformation for Topologies 1 and 2. The *time-slot* length is 10 seconds and the *Rx* concentration is 500 (nM). (a) Average for all compressing types. (b) Tissue with a *one-side* compression. (c) Tissue with a *S type* compression.

1 destination nanomachine, while in Topology 2 there are 8 source nanomachines and 1 destination nanomachine. The details of the distance between the source nanomachines and destination nanomachines D_x and the concentration of Ca^{2+} for each source nanomachine for both topologies are presented in Tables I and II.

The simulation algorithm operates as follows: We implemented a round robin scheduling algorithm which will determine which nanomachine will transmit in each time slot. Each nanomachine will be labeled with a random number (from one to the maximum number of nanomachines), and the transmitting starts from the lowest to the highest assigned number. In this case, each nanomachine will transmit in a different time lapse. We assume that each source nanomachine will perfectly identify its transmission time for each time slot to avoid any transmission collisions. There are in total 10 simulation runs, where during each run we change the seed, and we compute the 90% confidence interval of each set of results. Our analysis will mainly concentrate on the accuracy of the classifier using different information metrics.

A. Tissue Deformation Detection

In our first evaluation we analyze the accuracy of the tissue deformation detection for both topologies. We simulated two different types of deformation: *single-sided* and S shape deformation. For both topologies and information metrics, we obtained 100% accuracy in detecting the presence of deformation. This was an expected result because the probability density function of the deformed tissues is very different compared to the distribution of a normal tissue under no deformation. We observed this in Section VI when we analyzed the mutual information $I(X;Y)$—for different types of deformation we get very different patterns compared to the normal tissue. The reason for this is because the system is highly sensitive to the changes in the diameter of the cell, which will determine the quantity of diffusion, where less diffusion is associated with increased deformation.

B. Inferring Deformation Types

In this section we analyze the classifier's ability to accurately detect the type of deformation in the tissue. As shown in Fig. 12, the highest accuracy is achieved by the generalized entropy with $\alpha = 10$ for Topology 1. The mutual information $I(X;Y)$, on the other hand, resulted in the worst performance. This is attributed to the low divergent probability distribution function, which results in the mutual information suffering from poor accuracy. Therefore, this result confirms the fact that the accuracy of the generalized entropy with high values of α performs better compared to other approaches.

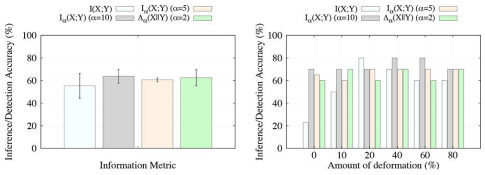

Fig. 13. Accuracy of detecting the amount of compression in a *one-side* type deformation. We use a single hop transmission in a three-layered tissue. The time slot length is 10 seconds, the *Tx* concentration is 10 and 50 (nM), the destination nanomachine distances are set at 0 and 4 μm, and the *Rx* concentration is 500 (nM). (a) Overall. (b) Varying the amount of deformation from 0 to 80% of the tissue.

The same results are also shown in Fig. 12 for Topology 2, where the mutual information with generalized entropy ($I_\alpha(X;Y)(\alpha = 10)$) resulted in the highest level of accuracy. One interesting point here, we may note, is that pure mutual information $I(X;Y)$ jumps from 34% (Topology 1) to 58% (Topology 2) in accuracy detection. The reason for this improved performance is due to the higher number of source nanomachines. The increase in the number of nanomachines supports the classifier during the training phase to develop more accurate thresholds, since the number of nanomachines equals the number of training samples.

C. Inferring the Quantity of Deformation

In this section we investigate the accuracy in inferring the quantity of deformation on the tissue. The inferencing process should infer the quantity of deformation by relating to the percentage in length that a tissue is being compressed. For example, consider a three-layered tissue of cells, were each cell's diameter is 0.5 μm. If the classifier infers that the deformation is of 40%, this means that there is 40% compression over the 1.5 μm height of the whole tissue. In this analysis, we used only *single-sided* compression and a single-hop transmission with two different configurations (configuration 1: Tx concentration

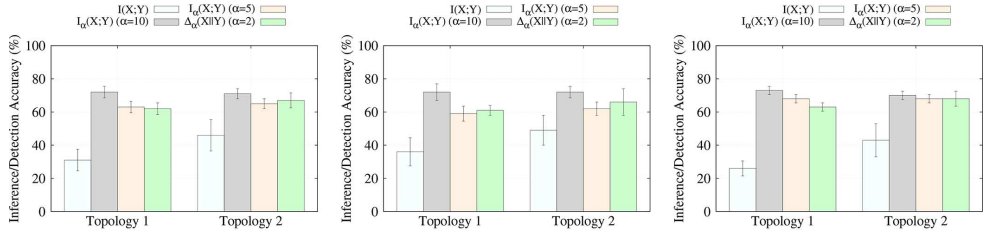

Fig. 14. The Inference/Detection accuracy for source nanomachine concentration and distance information for both Topologies 1 and 2. (a) Normal tissue. (b) Tissue with a *single-side* compression. (c) Tissue with a "*S*" type compression.

of 10 (nM) and D_x of 0 (μm); configuration 2: Tx concentration of 10 (nM) and D_x of 4 (μm)). The amount of deformation is from zero (no compression) to 80%.

The mutual information with generalized entropy $I_\alpha(X;Y)$ for both values of α achieve the best results as shown in Fig. 13. This is followed by the information distance $\Delta_\alpha(X \parallel Y)$ and the mutual information $I(X;Y)$. We can note that the values for accuracy are close, which means that the distributions were highly divergent from each other. As described earlier, the system is highly sensitive to cell length changes when the tissue is compressed. Therefore, irrespective of the compression quantity, the divergence will always be high and unique, resulting in efficient classification that can enable high levels of inference accuracy.

However, when we decompose the results to the varying amount of deformation as shown in Fig. 13, we can observe some interesting results. The mutual information with generalized entropy $I_\alpha(X;Y)$ did not always achieve the highest levels of accuracy for all deformation quantity. At certain percentage of deformation, the divergence of the probability density function is so wide that using lower values of α can achieve decent accuracy. An example of this is the result of the mutual information $I(X;Y)$ at 20% deformation, results in the highest inferencing accuracy.

D. Inferring the Ca^{2+} Concentration and Distance of the Source Nanomachines

Besides the state of compression on the tissue, an important information to infer by the destination nanomachine is the information of the different source nanomachines. This is crucial in molecular communication, in particular when the various source nanomachines are distributed randomly in the tissue. Useful applications of this could be disease detection in specific parts of the tissue, where the source nanomachines could act as nanosensors. Therefore, inferring their distance D_x as well as the amount of Ca^{2+} concentration emitted from the source nanomachines (*Tx* concentration) could provide useful information. In particular, accurately inferring these information under various tissue deformation could be quite challenging. Fig. 14 present the inferring accuracy for the three different types of deformation for Topologies 1 and 2.

The mutual information with generalized entropy $I_\alpha(X;Y)(\alpha = 10)$, once again, presents the highest levels of accuracy over all other metrics. This is observed in both topologies as shown in Fig. 14. Obviously, when the probability density functions are not too divergent, the use of lower values of α leads to lower levels of accuracy. However, it is interesting to note that in some case there are similar performance even when the value of α increases [Fig. 14(a) and (c)]. We may safely say that in such cases the use of other information metrics might be sufficient, since lower values of α results in lower complexity.

When the number of nanomachines increases, the difference in performance of the information metrics is not very high (Topology 2). This interesting insight is based on the increased accuracy of the mutual information metric. The number of nanomachines is exactly the number of samples that the source nanomachine has to build the thresholds during the training phase. Therefore, if the number of nanomachines is higher it is expected that the probability density function will have more divergence, which will increase the accuracy level of the mutual information.

VIII. Discussion

In this section, we are going to discuss the example nanomachines that we can envision in our molecular nanonetwork embedded in a tissue, as well as potential applications for the Molecular Nanonetwork Inference Process.

A. Nanomachines

Nanomachines are devices composed of nano components that are able to perform limited functionalities [1]. The nanomachines can either be produced naturally from biological components and systems or assembled artificially. A good example of natural nanomachines are cellular organisms, which are constructed from sophisticated nanoscale biological components. As we have shown in the communication system within the tissue, the cells within the tissue can represent the source, destination, as well as the relay nanomachines. However, artificial manipulation (e.g., synthetic biology) of these biological components has gained attention, where specific functionalities can be integrated into the cells. Therefore, a cell-based nanomachine may include a dedicated engineered genetic circuit [25] that senses and releases the Ca^{2+} ions (this could represent the source nanomachines). In the case of artificially assembled nanomachines, these devices can be implemented using *nano-electromechanical systems* (*NEMS*) technology. The nanomachine we envision embedded into the tissue could externally activate the Ca^{2+} ions, and one example is through the use of

needles or force probes [26], [27]. The destination nanomachine could be developed from NEMS that sense molecules produced around the neighboring cells, or utilize a process of harvesting molecules.

B. Applications

Numerous research efforts in recent years have been dedicated to technologies that enable *tissue engineering*. Tissue engineering combines methods of engineering and life science in the control and design of tissues that can lead to organ construction [28], [29]. This technology provide alternative treatment for patients with organ and tissue failure, treatments that can alleviate issues relating to increasing costs of current treatments and the shortage of organ donors [28], [30]. Embedding nanonetworks into the organs constructed from tissue engineering, could provide new dimensions for advanced patient care. Langer [31], commented that the use of sensors embedded into tissues for monitoring and detecting illnesses can lead to *Smart Organs*. Another possible real life application is with *breast compression estimation*. Mammography volume is associated with *breast cancer*, and works like [32] use simulations for breast compression estimation and rarely human body data. Breast cancer research is impaired due to unethical issues of frequent radiation exposure on humans. That is an ideal scenario for the utilization of the method proposed in this paper, in which human body data can be obtained with a minimally invasive approach. At the same time, the vision of *virtual physiological human* (*VPH*) is to develop a technological framework that can support integrative biological functions in the cells, tissue, organs, as well as entire systems within the human body [33]. Therefore, by combining advanced services in cloud computing and the technological framework of VPH, we can utilize the Molecular Nanonetwork Inference Process to monitor the conditions within the Smart Organs as well as detect early signs of diseases.

IX. Conclusion

We presented a technique that relies on information metrics and molecular communication to infer the state of the nanonetwork embedded in the tissue; we term this technique a Molecular Nanonetwork Inference Process. Central to the process is a classifier that is able to detect the presence of tissue deformation, the type of tissue deformation, the degree of deformation, the source nanomachine concentration and the source nanomachine distance from the destination nanomachine. Classifer thresholds are generated after a training phase using information theoretic metrics. We compared three different information metrics: *Mutual Information*, *Mutual Information with Generalized Entropy*, and *Information distance*. First, we compared all the information metrics in a regular single-hop transmission in a cellular tissue. Our analysis shows that the different metrics results in various divergence and sparsity of data, which in turn affects the accuracy of the classifier's thresholds. This is followed by evaluating the proposed classifier in a simulation model of a calcium signaling molecular communication system, and we perform simulations for two different topologies. We could observe in all the results that with a average level of accuracy of 80% the use of mutual information with the generalized entropy in the classifier outperforms the other information metric techniques.

Acknowledgment

This work was partially funded by: i) the Irish Higher Education Authority under the Programme for Research in Third Level Institutions (PRTLI) cycle 5, which is co-funded by the European Regional Development Fund (ERDF), via the Telecommunications Graduate Initiative (http://www.tgi.ie); ii) via Science Foundation Ireland funded FAME strategic research cluster (grant no. 08/SRC/I1403); and iii) via the Academy of Finland FiDiPro program, "Nanocommunication Networks," 2012–2016, and the Academy Research Fellow program, (project no. 284531).

References

[1] I. F. Akyildiz, F. Brunetti, and C. Blzquez, "Nanonetworks: A new communication paradigm," *Comput. Netw.*, vol. 52, pp. 2260–2279, 2008.

[2] I. Akyildiz, F. Fekri, R. Sivakumar, C. R. Forest, and B. K. Hammer, "Monaco: Fundamentals of molecular nano-communication networks," *IEEE Wireless Commun.*, vol. 19, no. 5, pp. 12–18, 2012.

[3] T. Nakano, M. Moore, A. Enomoto, and T. Suda, "Molecular communication technology as a biological ICT," in *Biological Functions for Information and Communication Technologies*. New York: Springer, 2011, ch. 2, pp. 49–86.

[4] M. Pierobon and I. F. Akyildiz, "Diffusion-based noise analysis for molecular communication in nanonetworks," *IEEE Trans. Signal Process.*, vol. 59, pp. 2532–2547, 2011.

[5] M. Pierobon and I. F. Akyildiz, "Capacity of a diffusion-based molecular communication system with channel memory and molecular noise," *IEEE Trans. Inf. Theory*, vol. 59, no. 2, pp. 942–954, 2013.

[6] I. Llatsera, I. Pascual, N. Garralda, A. Cabellos-Aparicio, M. Pierobon, E. Alarcon, and J. Sole-Pareta, "Exploring the physical channel of diffusion-based molecular communication by simulation," in *Proc. IEEE Global Telecommun. Conf.*, 2011.

[7] S. Balasubramaniam and P. Lio, "Multi-hop conjugation based bacteria nanonetworks," *IEEE Trans. NanoBiosci.*, vol. 12, no. 1, pp. 47–59, 2013.

[8] M. Kuscu and O. B. Akan, "A physical channel model and analysis for nanoscale molecular communications with forster resonance energy transfer (FRET)," *IEEE Trans. Nanotechnol.*, vol. 11, no. 1, pp. 200–207, 2012.

[9] M. Kuscu, D. Malak, and O. B. Akan, "An information theoretical analysis of broadcast networks and channel routing for fret-based nanoscale communications," in *Proc. IEEE Int. Conf. Commun. (ICC)*, 2012, pp. 6167–6171.

[10] T. Nakano, T. Suda, T. Koujin, T. Karaguchi, and Y. Hiraoka, "Molecular communication through gap junction channels: System, design, experiment, and modelling," in *Proc. 2nd Bio-Inspired Models Netw., Inf., Comput. Syst.*, 2007.

[11] T. Nakano, T. Suda, M. Moore, R. Egashira, A. Enomoto, and K. Arima, "Molecular communication for nanomachines using intercellular calcium signaling," in *Proc. 5th IEEE Conf. Nanotechnol.*, 2005.

[12] T. Nakano, M. J. Moore, F. Wei, A. V. Vasilakos, and J. Shuai, "Molecular communication and networking: Opportunities and challenges," *IEEE Trans. NanoBiosci.*, vol. 11, pp. 135–148, 2012.

[13] A. Nagasaki, E. L. de Hostos, and T. Q. Uyeda, "Genetic and morphological evidence for two parallel pathways of cell-cycle-coupled cytokinesis in dictyostelium," *J. Cell Sci.*, vol. 115, no. 10, pp. 2241–2251, 2002.

[14] A. Werner, A. Disanza, N. Reifenberger, G. Habeck, J. Becker, M. Calabrese, H. Urlaub, H. Lorenz, B. Schulman, G. Scita, and F. Melchior, "Scffbxw5 mediates transient degradation of actin remodeller eps8 to allow proper mitotic progression," *Nat. Cell. Biol.*, vol. 15, no. 2, pp. 179–188, Feb. 2013.

[15] S. C. Sibole and A. Erdemir, "Chondrocyte deformations as a function of tibiofemoral joint loading predicted by a generalized high-throughput pipeline of multi-scale simulations," *PLoS ONE*, vol. 7, no. 5, p. e37538, May 2012.

[16] T. Masselter and T. Speck, "Quantitative and qualitative changes in primary and secondary stem organization of aristolochia macrophylla during ontogeny: Functional growth analysis and experiments," *J. Exper. Botany*, vol. 59, no. 11, pp. 2955–2967, 2008.

[17] A. Goldbeter, G. Dupont, and M. J. Berridge, "Minimal model for signal-induced Ca^{2+} oscillations and for their frequency encoding through protein phosphorylation," *Proc. Natl. Acad. Sci. USA*, vol. 87, pp. 1461–1465, 1990.

[18] T. Nakano and J.-Q. Liu, "Design and analysis of molecular relay channels: An information theoretic approach," *IEEE Trans. NanoBiosci.*, vol. 9, pp. 213–221, 2010.

[19] D. T. Gillespie, "Exact stochastic simulation of coupled chemical reactions," *J. Phys. Chem.*, vol. 81, no. 25, pp. 2340–2361, 1977.

[20] M. T. Barros, S. Balasubramaniam, B. Jennings, and Y. Koucheryavy, "Transmission protocols for calcium signaling based molecular communications in deformable cellular tissues," *IEEE Trans. Nanotechnol.*, vol. 13, no. 4, pp. 779–788, 2014.

[21] M. T. Barros, S. Balasubramaniam, and B. Jennings, "Error control for calcium signaling based molecular communications," in *Proc. 47th Annu. Asilomar Conf. Signals, Syst., Comput.*, 2013.

[22] C. H. Bennett, P. Gacs, M. Li, P. M. B. Vitanyi, and W. H. Zurek, "Information distance," *IEEE Trans. Inf. Theory*, vol. 44, no. 4, pp. 1407–1423, 1998.

[23] S. Kullback and R. A. Leibler, "On information and sufficiency," *Ann. Math. Stat.*, vol. 22, no. 1, pp. 79–86, 1951.

[24] Y. Xiang, K. Li, and W. Zhou, "Low-rate ddos attacks detection and traceback by using new information metrics," *IEEE Trans. Inf. Forensics Security*, vol. 6, no. 2, pp. 426–437, 2011.

[25] H. Kobayashi, M. Kaern, M. Araki, K. Chung, T. Gardner, C. Cantor, and J. J. Collins, "Programmable cells: Interfacing natural and engineered gene networks," *Proc. Natl. Acad. Sci.*, vol. 101, no. 22, pp. 8414–8419, 2004.

[26] G. C. Churchill, M. M. Atkinson, and C. F. Louis, "Mechanical stimulation initiates cell-to-cell calcium signaling in ovine lens epithelial cells," *J. Cell Sci.*, vol. 109, no. 1, pp. 355–365, 1996.

[27] J. Long, M. Junkin, P. K. Wong, J. Hoying, and P. Deymier, "Calcium wave propagation in networks of endothelial cells: Model-based theoretical and experimental study," *PLoS Comput. Biol.*, vol. 8, no. 12, Dec. 2012.

[28] B. Mason, J. Califano, and C. Reinhart-King, "Matrix stiffness: A regulator of cellular behavior and tissue formation," in *Engineering Biomaterials for Regenerative Medicine*, S. K. Bhatia, Ed. New York: Springer, 2012, pp. 19–37.

[29] R. Skalak and C. F. Fox, *Tissue Engineering*. New York: Alan R. Liss, 1988.

[30] R. Langer and J. P. Vacanti, "Tissue engineering," *Science*, vol. 260, no. 5110, pp. 920–926, 1998.

[31] BBC, "Tissue engineering: Grow your own smart organs" [Online]. Available: http://www.bbc.com/future/story/20131016-smart-organs-for-everyone

[32] T.-C. Shih, J.-H. Chen, D. Liu, K. Nie, L. Sun, M. Lin, D. Chang, O. Nalcioglu, and M.-Y. Su, "Computational simulation of breast compression based on segmented breast and fibroglandular tissues on magnetic resonance images," *Phys. Med. Biol.*, vol. 55, no. 14, pp. 4153–4168, 2010.

[33] B. S. Brook, P. Khol, and J. R. King, "Towards the virtual physiological human: mathematical and computational case studies," *Philos. Trans. Roy. Soc. A*, vol. 369, no. 1954, pp. 4145–4148, 2011.

Michael Taynnan Barros (S'14) was born in Campina Grande, Brazil. He received his M.Sc. degree in computer science at the Federal University of Campina Grande (UFCFG), Brazil, and B.Tech. degree in telematics at the Federal Institute of Education, Science and Technology of Paraiba (IFPB), Brazil. He joined the Telecommunications Software and System Group (TSSG) at the Waterford Institute of Technology (WIT) in 2012, working as a postgraduate researcher towards his Ph.D. degree. His experience concentrates on dynamic optical networks, vehicular ad-hoc networks, routing, IP traffic classification, QoS-diffserv aware networks, and molecular communications, publishing more than 30 papers. He is also a reviewer for several journals and participated as technical programme committee and reviewer for various international conferences. His interests are in nanonetworks, molecular communications, and bio-inspired techniques.

Sasitharan Balasubramaniam (SM'14) received his B.S. (electrical and electronic engineering) and Ph.D. degrees from the University of Queensland, Australia, in 1998 and 2005, respectively, and M.S. (computer and communication engineering) degree in 1999 from the Queensland University of Technology, Australia. He is currently a Senior Research Fellow at the Nano Communication Centre, Department of Electronic and Communication Engineering, Tampere University of Technology, Finland. Previously, he was a Research Fellow at the Telecommunication Software & Systems Group, Waterford Institute of Technology, Ireland, where he worked on a number of Science Foundation Ireland projects. He has published over 80 papers and actively participates in a number of technical programme committee for various conferences. He was the TPC co-chair for ACM NANOCOM 2014 and IEEE MoNaCom 2011, both conferences which he co-founded. He is currently an editor for the IEEE Internet of Things journal and Elsevier *Nano Communication Networks*. His current research interests includes bio-inspired communication networks, as well as molecular communications.

Brendan Jennings (M') received the B.Eng. and Ph.D. degrees from Dublin City University, Ireland, in 1993 and 2001 respectively. He is the Director of Research with the Telecommunications Software & Systems Group (http://www.tssg.org), Waterford Institute of Technology, Ireland. He also leads the TSSG Emerging Networks Laboratory, which addresses manageability aspects of computing and communications environments. His research interests are in network management, cloud computing and molecular communications. Further information is available at http://brendanjennings.net.

Chapter 7

Adaptive Transmission Protocol for Molecular Communications in Cellular Tissues

Journal Title:	The IEEE Conference on Communication (ICC 2014)
Article Type	Regular Paper
Complete Author List	Michael Taynnan Barros, Sasitharan Balasubramaniam, Brendan Jennings and Yevgeni Koucheryavy
Keywords	Molecular Communication; nanonetworks; calcium signaling, information theory, tissue deformation
Status	Published: 2014. doi: doi: 10.1109/ICC.2014.6883943

Adaptive Transmission Protocol for Molecular Communications in Cellular Tissues

Michael Taynnan Barros*, Sasitharan Balasubramaniam‡§, Brendan Jennings* and Yevgeni Koucheryavy‡§

*TSSG, Waterford Institute of Technology, Ireland
‡Nano Communications Center (NCC), Finland
§Department of Electronics and Communication Engineering, Tampere University of Technology (TUT), Finland
Email: mbarros@tssg.org, bjennings@ieee.org, sasi.bala@tut.fi, yk@cs.tut.fi

***Abstract*—One form of molecular communications for short range transmission between nanomachines is Calcium Signaling. This form of signaling is commonly found in cellular tissues, which consist of tightly packed cells, whereby Ca^{2+} ions propagate and diffuse between the cells. However, the natural flexible structure of cells usually leads to them dynamically changing shapes under certain strains and forces. Since the interconnected cells form a tissue, changes in the shape of one cell will change the shape of neighboring cells and the tissue as a whole. This may in turn significantly impair the communication channel between the nanomachines (which we assume to be embedded within the cells). In order to counter this problem, we propose an adaptive transmission protocol for Ca^{2+} signaling based molecular communications in cellular tissues. The protocol operates in two phases. The first phase utilizes information metrics to infer the state of the tissue; second phase then involves the determination of the most appropriate time-slot for bit transmission. In this way, we aim to improve the information rate by using a time slot length that is appropriate for the prevailing type of tissue deformation. Through simulation studies we show that, for two types of deformation and two different topologies, our protocol can improve the information rate performance by 15%.**

***Index Terms*—Molecular Communication, Nanonetworks, Calcium Signaling, Information Theory, Tissue deformation.**

I. Introduction

Recent years has seen considerable research efforts on how best to facilitate communication between nano-scale devices. Of particular interest in this field is *Molecular Communications*, which aims to utilize existing biological systems to create nanoscale networks [1], [2], [3], [4]. One form of molecular communication utilizes existing molecular signaling known as Calcium Signaling (Ca^{2+}). In this form of nanonetwork, nano devices are embedded into the cells within the tissue and invoke Ca^{2+} ions that diffuse through the neighboring cells in order to propagate information to other nanodevices[5], [6].

While Ca^{2+} signaling provides an interesting approach for molecular communication, there are a number of challenges. Firstly, since the Ca^{2+} ions propagate and diffuse through the neighboring cells, this could lead to recurrent signaling the may result in excessive noise. This will be an issue in the event of large number of nano devices. Secondly, the natural form of Ca^{2+} signaling is highly dependent on the spatial shape of the cells. As the cells change shape this leads to different quantities of Ca^{2+} ions that diffuse out from the cell. Therefore, the capacity of the communication channel is highly dependent on the quantity of tissue deformation. The cellular tissue can be deformed due to a number of reasons: movement or repairs that lead to cells that proliferate or differentiate. At the same time, we can also assume that different types of cellular tissue deformation can affect the performance of the communication channel in different ways. In order to counter this challenge, we adopt an approach in which we first infer the current state of compression of the tissue, and, using this information, adapt the time slot length (which we denote Tb) that is used to emit a single transmitted bit. In this paper we show that it is possible to achieve an optimal value of information rate using different values of Tb for different types of cellular tissue deformation. We propose an adaptive communication protocol, the *Adaptive Time-slot Protocol (ATP)*, that first detects the cellular tissue state and then adjusts the Tb to achieve the highest information rate. Our simulation study shows that ATP can significantly increase the information rate in comparison to a non-adptive approach. Our evaluation includes simulating different topology sizes (e.g. different number of nano devices), where our classifier performs well with higher quantities of nodes.

This paper is organized as follows. §II presents the problem statement of tissue deformation and its impact on molecular communication systems. §III specifies our proposed ATP for Ca^{2+} signaling based molecular communications in cellular tissues. It includes an analysis of the most appropriate metric to use for inferencing of channel state. §IV describes the results of a simulation study to evaluate the information rate of ATP in comparison to a non-adaptive protocol for two different topologies. Finally, §V concludes the paper.

II. Problem Statement

In this section we discuss the properties of tissue deformation, and how this could impact on Ca^{2+} signaling within a tissue.

A. Tissue Deformation

Since the majority of tissue structures are constructed from a tight formation of interconnected cells, a change in the structure of a cell could trigger a structural change in neighboring cells, changes which propagate through the tissue as a

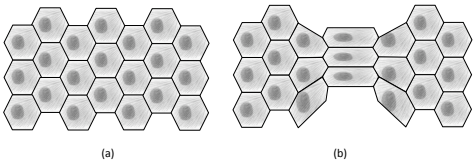

Fig. 1: Example of tissue deformation, (a) normal cell shape, (b) expansion of cell under compression.

whole (see Fig. 1). Thus, the majority of cells can undergo shape changes, in particular under certain strain and forces. The changes in shapes of cells can largely be attributed to their structure and internal composition. These component structures within the cells are mainly the cytoskeleton [7], which are distributed throughout the cells and have a flexible structure that maintains the cell shapes. Figure 1 illustrates an example of cell structural change under a certain load. Example factors that can influence the cell shape changes include physical movement, chemotaxing cells or mitotic cleavage [8]. During mitotic cleavage, the stretching process of a cell will compress the neighboring cells [9]. Sibole and Erdemir [10] describe a study conducted on the deformation of cells resulting from the movements in the joint's cartilage. In particular, their focus was on the *Tibiofemoral* joint and its mechanical loading impact on cells of the musculoskeletal system.

B. Communication Disruption

The deformation of the tissue could in turn affect the performance of molecular communications, in particular communications that is performed through diffusion of molecules between tightly packed cells. Masselter and Speck [11] investigated how tissue deformation spatially modulates angiogenic signals and angiogenesis. This is due to the physical forces applied to the developing tissues. For example, during the vascular development, the deformation caused by such forces has a huge impact on the Ca^{2+} signaling and the overall behavior of the cell. Fig. 2 illustrates an example of communication disruption that could occur due to different types of tissue deformation, including: *double-sided* tissue compression (Fig. 2(b)), *single-sided* tissue compression (Fig. 2(c)) and compression in multiple spots, which we may refer to it as *"S"* shape deformation (Fig. 2(d)). Since Ca^{2+} signaling diffuses the molecules between tightly packed cells within a tissue, the communication capacity is largely dependent on the spatial volume of the cells, which affects the process of invoking Ca^{2+} signaling, as the signals are propagated through the tissue. Therefore, any physical force that impacts on the spatial volume, will in turn affect the information rate.

C. Optimal Time-slot

In our scenario application, nanomachines are embedded into the tissue and transmit information in pre-defined time

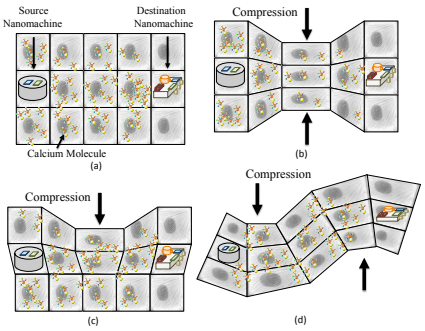

Fig. 2: Communication disruption due to tissue deformation, (a) regular tissue, (b) *double-sided* compression, (c) *single-sided* compression and (d) *"S" shape* deformation.

slots (Tb). For each time slot, a single bit is transmitted. Since the volume of Ca^{2+} ions that diffuse is highly dependent on the spatial property of the cells and tissue, the compression may determine an optimum time-slot duration.

For the four different types of compression presented in Fig. 2, we evaluate the optimum time-slot duration Tb; the results are presented in Fig. 3. The first observation we can make is that as we vary the time-slot duration for the different compression types, we start to observe that there are optimum points in the mutual information (denoted $I(X;Y)$). In the case of a regular tissue with no compression (Fig. 3(a)), we can observe that the optimum duration for the time slot is at 10s. The results from our analysis also shows that the compression of all types usually leads to higher end-to-end mutual information. In the case of *Double-sided* compression (Fig. 3(b)), the mutual information is highest when the time slot is the lowest. The main reason for this is reflected in Fig. 2(b) where we see that the double compression leads to a dedicated pipe between the source and destination nanomachines. This means that there is a directed channel to direct the flow of Ca^{2+} ions, leading to lower diffusion and higher concentrations arriving at the destination. The case of the *Single-sided* compression is slightly similar to the performance of the regular tissue (Fig. 3(c)), where the optimum time-slot is at 10s. Double-sided compression had an optimal value at 5s. This is due to the fact that the spatial changes of the tissue is very similar. However, as we move to the *S shape* compression, we can observe that the optimum duration is at 10s, with a performance that is very close to the double compression. Once again this could be attributed to the channel effect show in Fig. 2(d), leading to higher quantity of Ca^{2+} ions flows between the source and destination nanomachine.

Therefore, from our analysis we can observe that as we compress the tissue differently and at the same time vary the time-slot Tb duration, we have different mutual information.

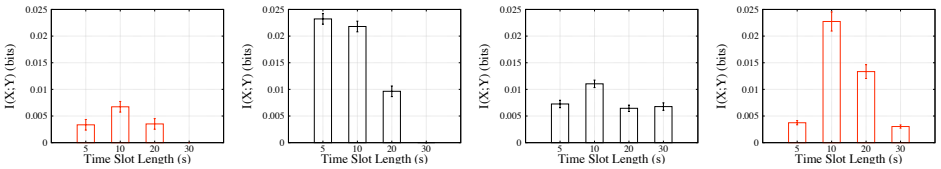

(a) Regular tissue (b) *Double-sided* compression (c) *Single-sided* compression (d) *S shape*

Fig. 3: *I(X;Y)* as a function of the time-slot length for a three layered cellular tissue, with *Rx* of $500nM$ and the *Tx* concentration of $50nM$.

This is the basis of our proposed *ATP* protocol, where we will need an approach that can help infer the tissue compression state, in order for us to adapt the time-slot accordingly in order to maximize the channel capacity.

III. ATP Protocol Specification

Due to the variable condition described in the previous section, we propose in this section the components of the *ATP* protocol, which is illustrated in Figure 4. The aim of the protocol is to be able to adapt the time-slot Tb based on the current state of the tissue. By adapting Tb we hope to achieve maximum information rate in our Ca^{2+} signaling based molecular communications [12]. The proposed protocol is divided into two parts, which includes the *Inferencing stage*, which is followed by the Tb *adaptation* stage. The *Inferencing Stage* includes: *Statistical Information Calculations*, *Training* and the *Classification process*. §III-A will present the full details of the algorithms that we have utilize to infer the state of the tissue. The process involves collecting information from the communication behavior between the source and destination nanomachines, and then utilizing information metrics to perform the inferencing process. Once the inferencing process has converged, and the state of the tissue is known, the nanomachines will be able to adjust the time-slot Tb for the bit transmission.

A. Inferencing channel state

We now describe the tissue inferencing process, which infers the type and degree of deformation. We assume that a central destination nanomachine receives all the information from the different source nanomachines, and analyzes the data to infer the state of the tissue deformation. Although this could lead to high computation, our approach could enable the destination nanomachine to feed all information to an external device, which in turn could feed this to an external device to perform the statistical information calculation. Based on the the *Statistical Information Calculation* process within the *Inferencing stage*, we use information theory metrics to process the collected measurement data, where we convert the data into samples using statistical processing. The details of the different information metrics will be discussed below.

We assume that for n transmissions from i number of nodes, we collect a set ψ of information metric values. This is

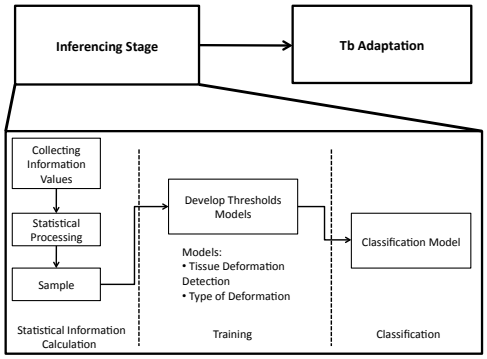

Fig. 4: The stages of the ATP protocol

followed by using the confidence intervals to statistically treat the data, which can be represented as:

$$ci(n,\psi) = m(\psi) \pm Z_{\rho/2}(\frac{\delta(\psi)}{n}) \quad (1)$$

where $m(.)$ is the mean of the sampled values, $\delta(.)$ is the standard deviation over a set of values, $\rho = 1 - (\beta/100)$ where β is the confidence level, and finally $Z_{\rho/2}$ is the Z table value. All the threshold information, which are the confidence intervals for all n nodes, will be converted into a sample. In the case that we want to identify the type of deformation, we need to train the model with a number of samples that is equal to the number of deformation types.

This part of the algorithm is very important because this phase is directly related to the performance of the proposed protocol. The nanomachines will only be able to adjust well to the condition of the channel if they are well trained. In this way the sample data have a higher importance, because samples with higher data divergence will results in a better adaptation of the system. In our experiments we used a sample data that contains all possible configuration of the communication system. The training phase will also map the best performance in each type of deformation.

Now, we will describe the three different information metric algorithms that are used in our training process.

1) Mutual Information: The *mutual information* $I(X;Y)$ is used to determine the mutual dependence between two variables, and is represented through the following equation:

$$I(X;Y) = \sum_{y \in Y} \sum_{x \in X} p(x)p(y|x) \log_2 \frac{p(y|x)}{p(y)} \tag{2}$$

$$p(x) = P(x = x_0 \wedge x = x_1) \tag{3}$$
$$p(y) = P(y = y_0 \wedge y = y_1) * p(y/x) \tag{4}$$
$$p(y = y_0|x = x_0) = 1 - p(y = y_1|x = x_0) \tag{5}$$
$$p(y = y_0|x = x_1) = 1 - p(y = y_1|x = x_1) \tag{6}$$

In our analysis, we utilize the mutual information $I(X;Y)$ to analyze the quantity of information that is transmitted from a source nanomachine to a destination nanomachine. The probabilities $p(x)$ and $p(y)$ represents the probability a digital bit is transmitted and successful received, respectively.

2) Mutual Information with Generalized Entropy: This metric is commonly used in information theory to measure the uncertainty over a random variable. The difference between the *Generalized Entropy* in comparison to the *Shannon entropy* is an increases in the number of dimensions for the data analysis. The metric belongs to a family of functions that quantifies the diversity, uncertainty, and/or the randomness of a system, and it is largely used to detect the distances between different probability density function. The generalized entropy is represented as follows:

$$H_\alpha(x) = \frac{1}{1-\alpha} \log_2 (\sum_{i=1}^{n} p_i^\alpha) \tag{7}$$

where p_i are the probabilities of $\{x_1, x_2, ..., x_n\}$, $p_i \geq 0$,

$$\sum_{i=1}^{n} p_i = 1, \alpha \geq 0, \alpha \neq 1 \tag{8}$$

The generalized entropy is used in combination with the mutual information (Eq. 9), in order to amplify and separate the samples to a different dimension. Therefore, this should enable the classifier to accurately detect the state of the tissue with increased accuracy, since the metric can detect sensitive differences in the probability density functions.

$$I(X;Y) = H_\alpha(X) - H_\alpha(X|Y) \tag{9}$$

3) Information Distance: Besides the generalized metric and the mutual information, information distance is another metric that is used to measure the uncertainty of the random variables. This metric was proposed by Bennett et al. [13] and is commonly applied to pattern recognition between different classes. The information distance is a measure of the divergence between two random variables X and Y and is represented as:

$$D_\alpha(X||Y) = \frac{1}{\alpha - 1} \log_2 (\sum_{i=1}^{n} x_i^\alpha y_i^{1-\alpha}), \alpha \geq 0. \tag{10}$$

B. Training Process

The training process involves determining the thresholds and boundaries that are used for the classifications of the collected data. We define a decision function $f(.)$, which enables the classifier to determine if the new collected sample is placed in the right category. The function f is represented as:

$$f(x) = \begin{cases} 1 & , x \in [-ci(n,\psi), +ci(n,\psi)] \\ -1 & , x \notin [-ci(n,\psi), +ci(n,\psi)] \end{cases} \tag{11}$$

where x represents the new collected sample.

C. Classification Process

Once the training process is completed, the next stage is the classification process. Here, a new information input in the destination will be compared to the threshold models that have been developed iteratively. This model will have unique characteristics that will be used to identify all listed channel state information that was introduced earlier. The classifier will be a set of decision function f whose cardinality will be equal to the product of the number of samples and the number of nanomachines in each sample. At the end of each transmission, the collected data will be analyzed by the classifier, and in the event that the function returns a non-negative value, this will indicate as the correct inference.

D. Accuracy Performance

1) Tissue Deformation Detection: In our first evaluation we analyze the accuracy of the tissue deformation detection for two topologies. We consider two different star topologies in our analysis (*Topology 1* (Fig. 6), and *Topology 2* (Fig. 7)). In Topology 1 there are 4 source nanomachines and 1 destination nanomachine, while in Topology 2 there are 8 source nanomachines and 1 destination nanomachine. For both topologies, the nanomachines are placed randomly within the tissue, and at the same time the Ca^{2+} concentration of the source nanomachines are also randomly selected. The details of the distance between the source nanomachines and destination nanomachines D_x and the concentration of Ca^{2+} for each source nanomachine in Topologies 1 and 2, are presented in Tables I and II, respectively. We simulated two different types of deformation: *single-sided* and "S" shape deformations. For both topologies and information metrics, we obtained 100% accuracy in the detection process. This was an expected result because the probability density function of the deformed tissues is very different compared to the distribution of a regular tissue. The reason for this is because the system is highly sensitive to the changes in the diameter of the cell. The diameter of the cell will determine the quantity of diffusion, where less diffusion is associated to increased deformation.

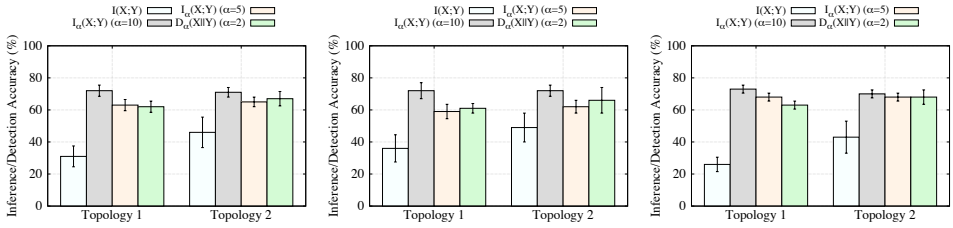

(a) Overall (b) Tissue with a one side compression (c) Tissue with a S type compression

Fig. 5: Inference accuracy of tissue deformation types for Topologies 1 and 2. The time-slot length is 10 seconds and the Rx concentration is 500 (nM).

TABLE I: Setup of Topology 1

Node	Z (nM)	D_x (μm)
1	10	0
2	100	2
3	50	4
4	10	8

TABLE II: Setup of Topology 2

Node	Z (nM)	D_x (μm)
1	50	8.94
2	10	8
3	50	4
4	50	4.47
5	50	11.31
6	100	2
7	50	5.66
8	10	0

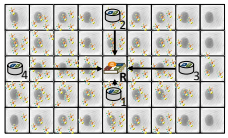

Fig. 6: Topology 1: 5 nanomachines (4 source and 1 destination).

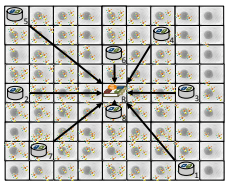

Fig. 7: Topology 2: 9 nanomachines (8 source and 1 destination).

2) Inferencing Deformation Types: In this section we analyze the classifier's ability to accurately detect the type of deformation in the tissue (Fig. 5). As shown in Fig. 5, the highest accuracy value is achieve by the generalized entropy with $\alpha = 10$ for Topology 1, in which α is the order of entropy that determines the dimensions of the data analysis. This result confirms the fact that the accuracy of the generalized entropy with high values of α performs better compared to other approaches. The same results are also shown in Fig. 5 for Topology 2, where the mutual information with generalized entropy ($I_\alpha(X;Y)(\alpha = 10)$) resulted in the highest level of accuracy. This is attributed to the low divergence in the probability density function, which results in the mutual information performing with poor accuracy. In the proposed protocol, we assume that the nanomachines will have sufficient processing capabilities, then we chose the mutual information with generalized entropy ($I_\alpha(X;Y)(\alpha = 10)$) as our information metric.

IV. ATP Protocol Evaluation

In this section, we analyze the performance of the proposed channel state inferencing process. Our objective is to evaluate the performance of a molecular communication nanonetwork that adapts the bit duration transmission using the proposed *ATP* protocol.

We used the same simulation model mentioned in §II-C with the two topologies presented in §III-D. Then we implemented a round robin scheduling algorithm which will determine which nanomachine will transmit in each time slot. Each nanomachine will be labeled with a random number (from one to the maximum number of nanomachines), and the transmission starts from the lowest to the highest assigned number. In this case, each nanomachine will transmit in a different time lapse. We assume that each source nanomachine will perfectly identify its transmission time for each time-slot to avoid any transmission collisions. The simulation scenario mixes the compression process, where half the period will be based on the *double-sided* compression while the remaining period will have the "S" shape compression. There are in total 10 simulation runs, where during each run we change the seed, and we compute the confidence interval of each set of results with a 90% confidence interval. Our analysis will mainly concentrate on the accuracy of the classifier using different information metrics approaches described earlier. We present the setup for the training phase in Table III.

As a benchmark comparison, we compare the ATP protocol to *Static (STC)* time-slot durations of 5s and 10s. As shown in Fig. 8, the highest information rate is achieve by the *ATP* protocol for Topology 1. The STC, on the other hand, and even with two different values of Tb, resulted in the worst performance. Therefore, this result confirms that using an adaptive approach achieves higher information rates. The same

TABLE III: Training Setup

Variable	Value
Training Time	100 min
Number of Samples	200
Number of data sets	12
Ca^{2+} concentration values	{10, 50,100} nM
D_x values	{0,2,4,8} μm
Tb values	{5,10,20,30} s

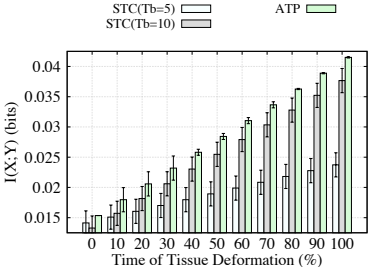

Fig. 8: Performance comparison between static time-slots *STC* (5 and 10s) and the adaptive *ATP* protocol, for Topology 1.

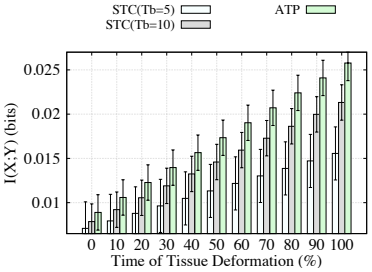

Fig. 9: Performance comparison between static time-slots *STC* (5 and 10s) and the adaptive *ATP* protocol, for Topology 2.

pattern is presented in the results for Topology 2, in which with the increase in the number of nanomachines, we can see a higher difference between the proposed adaptive approach versus the STC approach. This is attributed to the adaptability of the Tb duration when the tissue changes its state.

V. Conclusion

In this paper, we propose and analyse a communications protocol that adapts the bit transmission duration for a molecular communication system based on the Ca^{2+} signaling that is dependent on the type and level of tissue deformation caused by application of force. The proposed approach, which we term the *Adaptive Time-slot Protocol (ATP)*, has two stages. The first stage is the inferencing stage, which uses information metrics to infer the type of compression on the tissue. The second stage adapts the time-slot duration for the bit transmission based on the inferencing results. Our analysis found that as we apply different compression types of the tissue, there is an optimal time-slot duration for the bit transmission. We evaluated the protocol using two different star topologies of nanomachines that are embedded into a tissue, with multiple types of compression. The results from our simulation show an average increase in performance of 15% for the ATP protocol compared to a static time-slot protocol.

Acknowledgments

This work was partially funded by the Irish Higher Education Authority under the Programme for Research in Third Level Institutions (PRTLI) cycle 5, which is co-funded by the European Regional Development Fund (ERDF), via the Telecommunications Graduate Initiative (http://www.tgi.ie), the Science Foundation Ireland (SFI) via FAME (grant no. 08/SRC/I1403), as well as the FiDiPro program of Academy of Finland "Nano communication Networks," 2012-2016.

References

[1] I. F. Akyildiz and J. M. Jornet, "The internet of nano-things," *IEEE Wireless Communications*, vol. 17, pp. 58 –63, 2010.

[2] M. Kuran, T. Tugcu, and B. O. Edis, "Calcium signaling: overview and research directions of a molecular communication paradigm," *IEEE Wireless Communications*, vol. 19, no. 5, pp. 20–27, 2012.

[3] I. Akyildiz, F. Fekri, R. S. C. R. Forest, and B. K. Hammer, "Monaco: fundamentals of molecular nano-communication networks," *IEEE Wireless Communications*, vol. 19, no. 5, pp. 12–18, 2012.

[4] B. Atakan, S. Balasubramaniam, and O. B. Akan, "Body area nanonetworks with molecular communications in nanomedicine," *IEEE Communications Magazine*, vol. 50, pp. 28 –34, 2012.

[5] M. T. Barros, S. Balasubramaniam, B. Jennings, and Y. Koucheryavy, "Transmission protocols for calcium signaling based molecular communications in deformable cellular tissues," *Manuscript sumbitted for journal publication*, 2014.

[6] M. T. Barros, S. Balasubramaniam, and B. Jennings, "Error control for calcium signaling based molecular communications," in *47th Annual Asilomar Conference on Signals, Systems, and Computers*, 2013.

[7] L. Yang *et al.*, "Modelling cellular deformations using the level set formalism," *BMC Systems Biology*, vol. 2, pp. 1–16, 2008.

[8] A. Nagasaki, E. L. de Hostos, and T. Q. Uyeda, "Genetic and morphological evidence for two parallel pathways of cell-cycle-coupled cytokinesis in dictyostelium," *Jounal of Cell Science*, vol. 115, no. 10, pp. 2241–2251, 2002.

[9] A. Werner, A. Disanza, N. Reifenberger, G. Habeck, J. Becker, M. Calabrese, H. Urlaub, H. Lorenz, B. Schulman, G. Scita, and F. Melchior, "Scffbxw5 mediates transient degradation of actin remodeller eps8 to allow proper mitotic progression," *Nat Cell Biol*, vol. 15, no. 2, pp. 179–188, 02 2013.

[10] S. C. Sibole and A. Erdemir, "Chondrocyte deformations as a function of tibiofemoral joint loading predicted by a generalized high-throughput pipeline of multi-scale simulations," *PLoS ONE*, vol. 7, no. 5, p. e37538, 05 2012.

[11] T. Masselter and T. Speck, "Quantitative and qualitative changes in primary and secondary stem organization of aristolochia macrophylla during ontogeny: functional growth analysis and experiments," *Journal of Experimental Botany*, vol. 59, no. 11, pp. 2955–2967, 2008.

[12] M. T. Barros, S. Balasubramaniam, and B. Jennings, "Integrating information metrics and molecular communications for inferencing and detecting cellular tissue deformation," *Manuscript sumbitted for journal publication*, 2014.

[13] C. H. Bennett, P. Gacs, M. Li, P. M. B. Vitanyi, and W. H. Zurek, "Information distance," *IEEE Transactions on Information Theory*, vol. 44, no. 4, pp. 1407–1423, 1998.

Chapter 8

Set Point Regulation of Asytrocytes' Intracellular Ca^{2+} Signalling in the Tripartite Synapses

Journal Title:	IEEE Transactions on Nanobioscience
Article Type	Regular Paper
Complete Author List	Michael Taynnan Barros, Subhrakanti Dey and Sasitharan Balasubramaniam
Keywords	Molecular Communication; Tripartite Synapses; Ca^{2+} Signalling; Astrocytes
Status	Submitted

Set Point Regulation of Astrocyte Intracellular Ca^{2+} Signalling in Tripartite Synapses

Michael Taynnan Barros, *Student Member*, IEEE, Subhrakanti Dey, *Senior Member*, IEEE,
Sasitharan Balasubramaniam, *Senior Member*, IEEE

***Abstract*—Tripartite synapse is a three way communication process between a pre-synaptic neuron, a post-synaptic neuron and an astrocyte cell. Synapses are transmitted based on the gliotransmitters concentration in the channel, which is important for the signalling quality in this three way communication between cells using Ca^{2+} signalling. Abnormal concentration of gliotransmitters can lead to a number of neurodegenerative diseases, including: Alzheimer's, Parkinson's, Epilepsy, Schizophrenia and Depression. In this paper we investigate a technique that can control the root cause of the abnormal concentration of gliotransmitters, and this is through the Ca^{2+} signalling. The paper investigates the use of feed-forward feedback control technique to control the quantity of IP_3 that determines the concentration of Ca^{2+} emitted from intracellular signalling. The application of the control model showed that the quantity of Ca^{2+} signalling can be stabilised. The paper focuses on two applications of the control model. The first application is to maintain the stability of the Ca^{2+} concentration in order to prevent neurodegenerative diseases (extreme high or low concentration can result in disease progression). The second application is to improve the data rate performance for molecular communication that utilises Ca^{2+} signalling. In the case of the molecular communication application, the control model showed that the refractory periods from Ca^{2+} can be maintained to lower the noise propagation resulting in shower time-slots for bit transmission. The proposed approach can lead to novel solutions for biotechnology development, where synthetic biology can be used to program the control functionality into the cells.**

***Index Terms*—Molecular Communication, Tripartite Synapses, Ca^{2+} Signalling, Astrocytes.**

I. Introduction

The field of biological and medical science in recent years has witnessed the impact from multi-disciplinary research efforts that utilize engineering concepts and theory. Examples of this impact includes new approaches for smart drug delivery systems [1], [2] and tissue engineering [3], [4], [5], which has seen fields of nanobiotechnology and information technology brought together. More recently, telecommunication engineers are investigating biological communication processes that can be either used to understand the signalling process and to correct and adapt them to minimise disease progression, or developing artificial communication system at the nanoscale. The latter research topic is known as *Molecular Communication* [6], [7], [8], and its potential applications includes sensor and actuator nanonetworks for the human body, as well as new forms of environmental monitoring for smart cities.

A particular communication process that has attracted the attention of the molecular communication community is within the human brain, and specifically through chemical synapses. Although a known communication process is between neuron-neuron signalling, another signalling mechanism is performed by the so-called *tripartite synapses*, which are formed by three-way communication of a pre-synaptic neuron, an astrocyte and a post-synaptic neuron [9] [10]. The signalling process starts with an increase of astrocytes' cytosolic Ca^{2+} concentration that in turn stimulates the production and release of gliotransmitters. The internal Ca^{2+} concentration is then regenerated with post-synaptic voltage influence, which allows the increase of IP_3 (a protein responsible for Ca^{2+} stimulation and production) [11], [12]. An example of gliotransmitters that are triggered by increasing the Ca^{2+} signals in astrocytes [13] is *glutamate*. Through the *Glutamate Dependent NMDA Receptors* (*GNMDAR*), the astrocytes have a major role in numerous brain processes such as plasticity, learning and memory processes [14]. Since, the GNMDAR are the primary source of Ca^{2+} signalling in the post-synaptic neuron and critical for proper functioning of brains processes, the stable regulation of Ca^{2+} signalling is very important. **Noise in the astrocytes intracellular Ca^{2+} signalling** can lead to serious diseases, including: alzheimer's, epilepsy, schizophrenia, parkinson's and depression [15], [16].

For this, our main idea involves the application of control theory to maintain stable levels of intracellular Ca^{2+} signalling process in the cytosol. The modelling of the communication process and applying control theory for Ca^{2+} signaling can provide new approaches for prevention of neurodegenerative disease [17], [18]. Besides this, the control model can also be used in developing molecular communication systems in order to ensure that when information bits are transmitted due to stimulation of Ca^{2+} ions in the tripartite synapses, this will not result in emergence of neurodegenerative diseases. This disease may emerge from extra stimulation of Ca^{2+} signalling when transmitting information between implantable nanomachines within the brain. In this paper we investigate the usage of a **feed-forward feedback** control mechanism to perform indirect astrocytes' cytosolic Ca^{2+} concentration regulation. Since proteins are more easily stimulated, IP_3 is then used as a regulation point where its control will lead to the accurate stimulation of Ca^{2+} ions [19], [20].

M. T. Barros is with the Telecommunication Software & Systems Group (TSSG), Waterford Institute of Technology (WIT), Ireland.

S. Balasubramaniam is with the Nano Communications Center (NCC), Department of Electronics and Communication Engineering at Tampere University of Technology (TUT), Finland.

S. Dey is with the Signal and Systems group, Department of Engineering Sciences at the Uppsala University, Sweden.

E-mail: mbarros@tssg.org, sasi.bala@tut.fi,subhra.dey@signal.uu.se

The main contributions of the paper are:

- *Regulation of Ca^{2+} Signalling in Astrocytes* - The proposed technique is able to control Ca^{2+} ion levels in the cytosol of astrocytes. A mathematical framework was developed to calculate the desired Ca^{2+} levels based on a given desired IP_3 level and also stability of the system (the system in this context is the point of communication between the astrocyte and neuron inter-cellular signalling). Finally, a disturbance analysis investigated the benefits of having a feed-forward component in the control design.
- *Cellular Disease Prevention Technique* - The proposed control technique is able to stabilise Ca^{2+} levels inside the cells. The stable regulation of Ca^{2+} levels in astrocyte cells will also affect the release of glutamate in the tripartite synapses and, therefore, improve synaptic transmission quality. This approach is an alternative technique for preventing neurodegenerative diseases compared to the use of drugs.
- *Improve Data Rate Performance in Molecular Communication* - The proposed approach can be used to control the simulation of Ca^{2+} ions that is used for molecular communication between implantable nanomachines that communicate through networks of astrocyte and neuron cells. The use of Ca^{2+} signalling for molecular communication can result in high quantity of noise propagating through the tissue, resulting in low data rates. However, the control model proposed in this paper can control sufficient quantity of Ca^{2+} propagation that will result in minimum amount of noise, which in turn will increase the data rate. The proposed control model can also be used to develop new modulation techniques for Ca^{2+}-signalling-based molecular communication.

The paper is organized as follows. §II introduces the tripartite synapses and the intracellular Ca^{2+} signalling model for astrocytes. §III presents the oscillation behaviour of regular Ca^{2+} signalling process and the problem statement. §IV presents the feed-forward feedback control technique for astrocytes' cytosolic Ca^{2+} concentration regulation followed by a stability analysis. §V presents the results and analysis of the application of the control technique for elimination of Ca^{2+} signalling oscillations, disturbance, disease prevention and data rate improvements. §VI present a discussion about the future envisioned applications. Finally, §VII. concludes the paper.

II. Tripartite Synapses

Fig 1 shows an accurate illustration of the tripartite synapses, in which the concentration of *gliotransmitters* in the region that connects both neuron and the astrocyte cells is linked to the quality of the synapse transmission. Researchers were able to identify the importance of the astrocytes in the tripartite synapses [10], and the communication process is illustrated in Fig 2. The tripartite synapses starts with the stimulation of the Ca^{2+} ion production in the astrocytes. The IP_3 concentration is increased from the stimulation and this will trigger the release of Ca^{2+} ions to the cytosol from the endoplasmic reticulum. High quantity of Ca^{2+} ions will provoke the release of *glutamate* [1] to the synaptic channel. Glutamate is also released from the pre-synaptic neuron invoking Ca^{2+} concentration increase in the astrocytes. These glutamate molecules go back to the pre-synaptic terminal either to inhibit or assist further glutamate release. Therefore, the intracellular Ca^{2+} signalling in astrocytes of the tripartite synapses dynamically regulates synaptic transmission. Based on this, we focus on root of this sequential communication process by concentrating on the intracellular Ca^{2+} signalling process in astrocytes.

The intracellular Ca^{2+} signalling in astrocytes model consist of state equations for the Ca^{2+} concentration in the cytosol (C) (Eq. 1), kinetics of IP_3 receptors (h) (Eq. 2) as well as the IP_3 concentration (I) (Eq. 3). This model is proposed in [21], and a visual illustration of the model is presented in Fig. 3. The main state equations are defined as follows:

$$\frac{dC}{dt} = \sigma_1 + \sigma_2 - \sigma_3, \tag{1}$$

$$\frac{dh}{dt} = \frac{H - h}{\tau}, \tag{2}$$

$$\frac{dI}{dt} = \frac{1}{\alpha}(i_0 - I) + \beta\mathcal{H}(E_0 - 35) \tag{3}$$

where α is the constant degradation time of IP_3 concentration, i_0 is the IP_3 concentration in equilibrium, β is the production rate of IP_3 ions, E_0 is the pre-synaptic potential and $\mathcal{H}(.)$ is the Heaviside function. *Ca^{2+}-induced Ca^{2+} release* (*CICR*) is the trigger process of Ca^{2+} ions from the *sarco(endo)plasmic reticulum* by existing Ca^{2+} ions within the cytosol. The σ_1 models the *CICR* and is defined as:

$$\sigma_1 = vm^3h^3[c_0 - (1 + C_1)C] \tag{4}$$

where v is the maximal *CICR* rate, c_0 is the total cell free Ca^{2+} concentration depending on the cytosol volume, and C_1 is the ratio between the cytosol and endoplasmic reticulum volume.

The IP_3 and Ca^{2+} ion binding process that is responsible for providing stable IP_3 kinetics is represented as:

$$m = \left(\frac{I}{I + d}\right)\left(\frac{C}{C + d_3}\right) \tag{5}$$

where d is the IP_3 dissociation constant and d_3 is the Ca^{2+} activation-dissociation constant.

The σ_2 is the leakage of Ca^{2+} ions to the cytosol from the *sarco(endo)plasmic reticum* and is represented as:

$$\sigma_2 = v_1[c_0 - (1 + C_1)C] \tag{6}$$

where v_1 is the maximal rate of Ca^{2+} ions leakage from the endoplasmic reticulum.

The efflux of Ca^{2+} from the *sarco(endo)plasmic reticulum* to the *endoplasmic reticulum* (*SERCA*) is represented as:

[1] One type of gliotransmitter, which activates certain signalling processes in the cells.

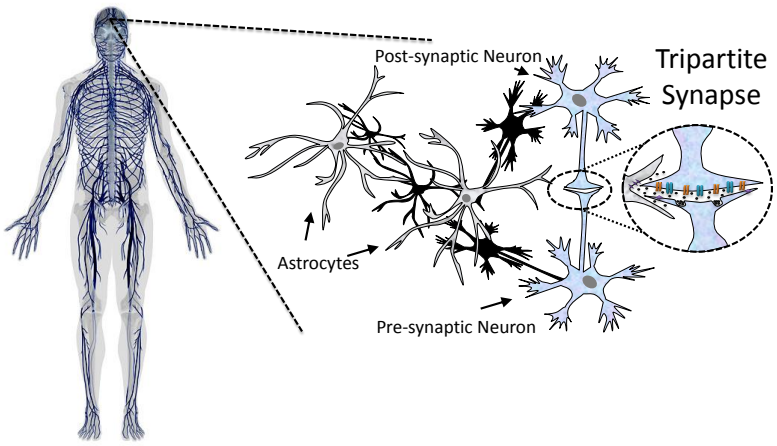

Fig. 1: Tripartite synapses overview, showing the communication process between the astrocyte cell and the pre-synaptic neuron, as well as the post-synaptic neuron. The three way communication process emits *gliotranmitters* which are molecules crucial for maintaining synaptic transmission quality.

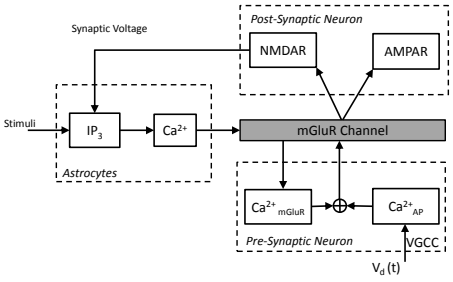

Fig. 2: Model for the Tripartite Synapses. Pre-synaptic neuron, post-synaptic neuron and the astrocyte communicates through a gliotransmitter channel that is invoked from Ca^{2+} signalling.

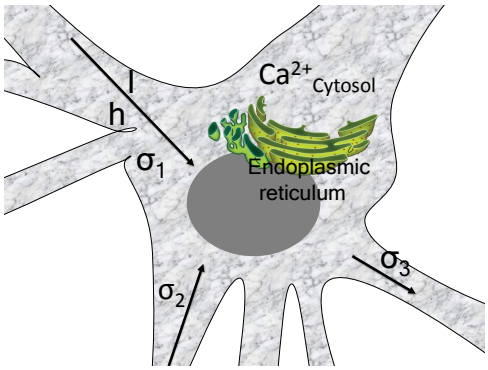

Fig. 3: Intracellular Ca^{2+} signalling model for astrocytes. The flux/efflux rates control the concentration of Ca^{2+} signalling. The σ_1 models the Ca^{2+}-induced Ca^{2+} release (*CICR*). The σ_2 is the leakage of Ca^{2+} ions to the cytosol from the *sarco(endo)plasmic reticum* (*SERCA*), and σ_3 is efflux of Ca^{2+} from the *sarco(endo)plasmic reticulum* to the *endoplasmic reticulum*.

$$\sigma_3 = \frac{v_2 C^2}{k^2 + C^2} \tag{7}$$

where v_2 is the maximal rate of SERCA uptake and k is Ca^{2+} binding affinity.

The following equations are important for modelling h:

$$H = \frac{Q}{Q + C} \tag{8}$$

$$\tau = \frac{1}{a(Q + C)} \tag{9}$$

$$Q = \frac{I + d}{I + d_2} d_1 \tag{10}$$

where d_1 is the Ca^{2+} inactivation dissociation constant, d_2 is the IP_3 dissociation constant and a is the IP_3 receptors binding rate for Ca^{2+} inhibition.

III. Problem Statement

Neurodegenerative diseases are related to the quality of the synapses in neuronal communication. Poor concentration of glutamate inside the synaptic channel will lead to poor propagation in the synapses, causing lack of memory, insomnia,

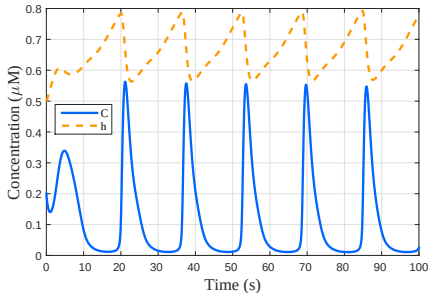

Fig. 4: Ca^{2+} oscillation with respect to time. In this illustration the IP_3 = 0.5 μM. The Ca^{2+} concentration (C - blue line) oscillates alongside with the kinetics of IP_3 receptors (h - dashed yellow line).

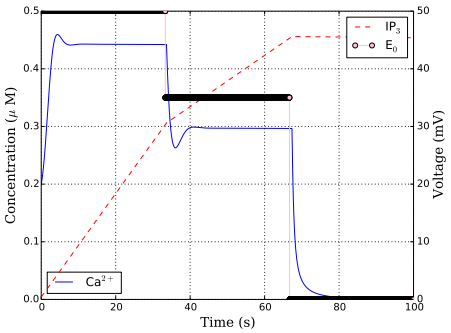

Fig. 5: Effect of both IP_3 and the E_0 on the Ca^{2+} concentration. The Ca^{2+} concentration is highly dependent on the increasing factor of IP_3 and, therefore, so is the stability.

depression which are symptoms of most neurodegenerative diseases. Current treatment to neurodegenerative diseases are based on drugs that are not effective and only helps to eliminate symptoms and not really treat them. The brain-blood barrier, imposed by the central nervous system, prevents drugs to reach the desired destination and therefore inhibiting the drugs' efficiency. Nanotechnology is a promising area that provided the idea of using nanoparticles to bypass the brain-blood barrier, which results in a new and exciting frontier for neurodegenerative treatment research.

Based on what was already presented, it is clear that controlling Ca^{2+} levels in astrocytes can indirectly control the glutamate release and potentially improve the synaptic transmission. Control of Ca^{2+} can be achieve with nanoparticles, which include: Carbon Black (CB), Titanium Dioxide (TiO2) or Zinc Oxide (ZnO) [22]. The main challenge now is to provide an analysis on the astrocytes Ca^{2+} concentration of the tripartite synapses and, therefore, create a theoretical framework that will be a base for alternative approaches in preventing neurodegenerative diseases. A regulation technique, capable of maintaining the healthy state of the tissue while also maintaining enough glutamate in the tripartite synapses, would be required in such scenario.

For this, we are looking at how to control levels of Ca^{2+} in the cytosol. More specifically, internal Ca^{2+} signalling is characterized by oscillations invoked by certain range of IP_3. Fig 4 shows the Ca^{2+} oscillation at IP_3 = 0.5 μM and when production rate of IP_3 ions (β - eqn. 3) varies from 0.1-1.5 μM/s. The elimination of such oscillatory behaviour (both of the Ca^{2+} oscillation (blue line) and the kinetics of the IP_3 oscillation (dashed yellow line)) will give a stable level of the desired Ca^{2+} concentration.

Fig 5 shows how the IP_3 can affect the intracellular Ca^{2+} signalling. Basically, increase of IP_3 in the system is desired for regular Ca^{2+} concentration levels. Since β is responsible for the IP_3 increase, we can assume that it is highly important for regulation of Ca^{2+} concentration levels. As soon as IP_3 is constant, the Ca^{2+} concentration will drop. The electrical component of the astrocytes also plays an important role (E_0 from Eq. 3). However since the synapses happen periodically, we are more interested in how to design the control when the synapses are activated.

The IP_3 is then a decisive factor for Ca^{2+} regulation, in which its increase is controlled by β. Such behaviour is going to be further explored with a mathematical model that enables the intracellular Ca^{2+} signalling control by regulating IP_3 levels.

IV. Feed-forward Feedback Control of Intracellular Ca^{2+} Signalling in Astrocytes

Since IP_3 activator nanoparticles can be inserted into the cell, e.g. Carbon Black (CB), Titanium Dioxide (TiO2) or Zinc Oxide (ZnO) [22], its regulation of Ca^{2+} concentration is more suitable for *in vivo* scenarios. The approach we are proposing may integrate nanoparticles to inhibit or activate Ca^{2+} as part of the control model.

Fig. 6 shows the flowchart of the desired Ca^{2+} signalling set point regulation, and the state feedback and feedforward control function is represented as [20]:

$$\beta = \beta_f - K_f(C - C_f), \tag{11}$$

where β_f is the desired IP_3 level, C_f is the desired Ca^{2+} concentration level and K_f is the adjustment constant. The Eq. 11 has been initially proposed for disturbance rejection in roll-to-roll manufacturing system [20]. They used the control function of an increasing factor variable that can be related to β. Also, since the nature of the problem investigated in this paper is elimination of Ca^{2+} oscillations, it was clear that such function would perfectly fit to our output control system.

A. β_f and C_f Relationship

To eliminate dependency of multiple variables a mathematical relationship between β_f and C_f is proposed. Suppose equilibrium exists with (h^o,c^o), then $\frac{dh}{dt} = 0$ at $h = h^o$ and $\frac{dC}{dt} = 0$ at $c = c^o$. Rewriting Eq. 1 and Eq. 2, we obtain:

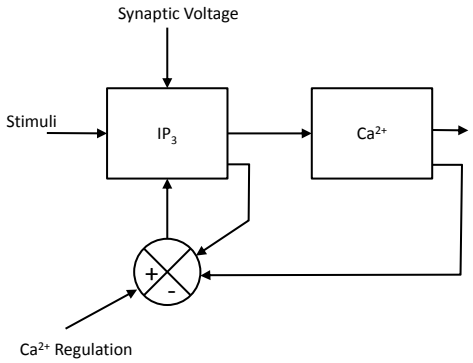

Fig. 6: Ca^{2+} regulation flowchart based on the regulation of cytosolic IP_3. The input rate of IP_3 is a function of the current cytosolic Ca^{2+} and the current IP_3 levels, which makes it both a state feedback and feed-forward control.

$$(v_1 + z_o(h^o)^3) \times (C_0 - (1 + C_1)c^o) = \frac{V_2(c^o)^2}{k^2 + (c^o)^2}, \quad (12)$$

$$h^o = \frac{Q_o}{Q_o + c^o}, \quad (13)$$

$$z_o = v\left(\frac{I_o}{I_o + d}\right)^3 \left(\frac{c^o}{c^o + d_3}\right)^3, \quad (14)$$

$$Q_o = \frac{I_o + d}{I_o + d_2} d_1. \quad (15)$$

Now for Eq. 3, assuming that $E_0 = 1$, we obtain:

$$\frac{dI}{dt} = \left(\frac{i_0}{\alpha} + \beta\right) - \frac{I}{\alpha}. \quad (16)$$

Solving Eq. 16 we thus obtain:

$$I = (i_0 + \alpha\beta)(1 - e^{\frac{-t}{\alpha}}). \quad (17)$$

As $t- > \infty$, I becomes a constant I_o, which is represented as:

$$I_o = (i_0 + \alpha\beta). \quad (18)$$

B. System Stability

Since the dynamics in Ca^{2+} signalling can lead to diseases and also tissue death, a control model for such a system is required for proper stability analysis, and this will be presented in this section.

Consider a function f and g as follows:

$$f(x) = Ax + A_2(x), g(x) = B + B_2(x) \quad (19)$$

where Ax is the linear part of $f(x)$, $A_2(X)$ contains the second and higher order terms of $f(x)$, $B = g(0)$, and $B_2(x)$ contains linear and higher order terms of $g(x)$.

Theorem 1: The system is stable if the matrix $A - BK$ is Hurwitz. *Proof*: Stability using Hurwitz matrix is defined as $Re[\lambda_i] < 0$.

In order to proof this, first we need to find the values of the matrix, which can be found in the following:

$$A = \begin{bmatrix} \frac{\partial f_1}{\partial C} & \frac{\partial f_2}{\partial C} & \frac{\partial f_3}{\partial C} \\ \frac{\partial f_1}{\partial h} & \frac{\partial f_2}{\partial h} & \frac{\partial f_3}{\partial h} \\ \frac{\partial f_1}{\partial I} & \frac{\partial f_2}{\partial I} & \frac{\partial f_3}{\partial I} \end{bmatrix}_{|c=0,h=0,i=0} \quad (20)$$

where $f_1 = \sigma_1 + \sigma_2 - \sigma_3$, $f_2 = \frac{H-h}{\tau}$ and $f_3 = \frac{1}{\alpha}(i_0 - I) + \beta\mathcal{H}(E_0 - 35)$.

Now, after solving the derivatives of matrix A we obtain,

$$A = \begin{bmatrix} -v_1(1 + C_1) & 0 & 0 \\ 0 & -a \times \frac{dd_1}{d_2} & a \times \frac{d_1(d_2 - d)}{d_2^2} \\ 0 & 0 & -\frac{1}{\alpha} \end{bmatrix} \quad (21)$$

We can define matrix BK as,

$$BK = \begin{bmatrix} 0 \\ 0 \\ 1 \end{bmatrix} \left\{ (B_f + K_f C_f) - \begin{bmatrix} K_F & 0 & 0 \end{bmatrix} \begin{bmatrix} C \\ h \\ I \end{bmatrix} \right. \quad (22)$$

Rewriting the matrix $A - BK$ we obtain:

$$\begin{bmatrix} f_1(C, h, I) \\ f_2(C, h, I) \\ f_3(I) \end{bmatrix} + \begin{bmatrix} 0 \\ 0 \\ 1 \end{bmatrix} \left\{ (B_f + K_f C_f) - \begin{bmatrix} K_F & 0 & 0 \end{bmatrix} \begin{bmatrix} C \\ h \\ I \end{bmatrix} \right\} \quad (23)$$

The simplified matrix is represented as:

$$A - BK = \begin{bmatrix} -v_1(1 + C_1) & 0 & 0 \\ 0 & -a \times \frac{dd_1}{d_2} & a \times \frac{d_1(d_2 - d)}{d_2^2} \\ -K_f & 0 & -\frac{1}{\alpha} \end{bmatrix} \quad (24)$$

We use the determinant rule to calculate the eigenvalues of $A - BK$ and thus $det\,[\lambda\Gamma - (A - BK)] = 0$. For this, consider

$$\lambda\Gamma - (A - BK) = \begin{bmatrix} \lambda + v_1(1 + C_1) & 0 & 0 \\ 0 & \lambda + a \times \frac{dd_1}{d_2} & -a \times \frac{d_1(d_2 - d)}{d_2^2} \\ K_f & 0 & \lambda + \frac{1}{\alpha} \end{bmatrix} \quad (25)$$

Finally, the eigenvalues can be computed as follows:

$$det\,[\lambda\Gamma - (A - BK)] = (\lambda + v_1(1 + C_1)) \left(\lambda + a \times \frac{dd_1}{d_2}\right) \left(\lambda + \frac{1}{\alpha}\right) = 0 \quad (26)$$

TABLE I: Simulation parameters for astrocytes.

Variable	Value
v	6s^{-1}
v_1	0.11 s^{-1}
c_0	2.0μM
C_1	0.185
v_2	0.9 Ms^{-1}
k	0.1μM
d	0.13μM
d_1	1.049 s^{-1}
d_2	0.9434$\mu M/s$
d_3	0.08234μM
a	0.2 s^{-1}
α	1/0.00014μM
i_0	0.160μM
β	0.1-1.5μM
E_0	35

Based on this the eigenvalues are: $\left(-v_1(1+C_1), -a \times \frac{dd_1}{d_2}, -\frac{1}{\alpha}\right)$. Since all eigenvalues are negative, this results in $A - BK$ as Hurwitz.

V. Analysis

We now present an analysis of the proposed regulation of Ca^{2+} concentration levels for astrocytes. The analysis is broken into four parts for a proper understanding of the system and also quantification of the application impact if this control technique is utilised. First, we start by showing how the control system will eliminate intracellular Ca^{2+} oscillations in astrocytes, solving the problem defined in Section III. This is followed by the disturbance analysis, where Gaussian noise is applied to the intracellular Ca^{2+} signalling for adding a controlled abnormal behaviour to the system and observing system effectiveness while looking at the feed-forward and feedback techniques separately. Finally, analysis of two main envisioned application are shown, which consist of a disease prevention and a data rate performance improvement for a molecular communication system that utilises Ca^{2+} signalling for transmitting information.

A. Elimination of Intracellular Ca^{2+} Oscillations

As mentioned in Section III, the elimination of the intracellular Ca^{2+} oscillation is a desired outcome of the control process. For this we solved Eqs. 1, 2 and 3 using the variables found in Table I. For the control technique, we replace the β in Eq. 3 for Eq. 11, in order to integrate the feed-forward feedback control element to the system. We chose a value of $C_f = 0.32\ \mu M$, which is a central value of the system, and computed the desired β_f with an appropriate calibration of the K_f.

A total elimination of the Ca^{2+} oscillation is obtained using the proposed mechanism and this is illustrated in Fig 7. The Eq. 11, which represents the state feedback and feed-forward control, can efficiently adjust β accordingly and maintain Ca^{2+} concentration levels throughout the time period shown. This positive results demonstrates the effectiveness and potential of utilizing the control technique to stabilize the excessive Ca^{2+} concentration that may either lead to neurodegenerative diseases or artificial molecular communication, which will be further explored in the subsections.

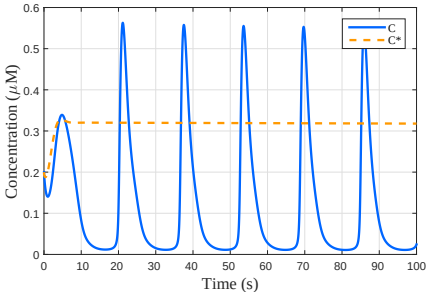

Fig. 7: Elimination of Ca^{2+} oscillation using the proposed feedback and feed-forward control technique. Regular Ca^{2+} oscillations C (straight lines) is compared to a controlled Ca^{2+} level C^* (dashed line) for IP_3 = 0.5 (μM).

B. Analysis of System Disturbance

Feed-forward control techniques are used in control theory to stabilize disturbances within a system. The presented Ca^{2+} signalling model so far is absent of any disturbances or noise component. In order to analyse the benefit of the feedback control technique with and without feed-forward separately, we integrate a noise component and determine the effectiveness of the approach to stabilize the disturbance. To achieve this, a disturbance component was added to Eq. 1, and this is through addition of Gaussian noise [23]. This additional noise will affect the Ca^{2+} level in the astrocyte cell's cytosol.

As illustrated in Fig. 8, the feed-forward control is able to main the levels of Ca^{2+} even with the additional Gaussian noise. This is obtained by the relation of the current Ca^{2+} concentration levels with the desired level, and therefore, through the adjustment of β this stability is achieved. This demonstrates that by controlling the noise effects through the control technique, excessive Ca^{2+} concentration levels from additional noise can be stabilised.

C. Maintaining Stable Ca^{2+} Concentration

While the previous section presented the case of maintaining stable Ca^{2+} concentration due to excessive noise, in this section we discuss the impact of overall fluctuations in the cytosolic concentration of the cell. The ability to maintain stability of the cytosolic Ca^{2+} concentration levels in astrocyte cells can not only maintain that healthy state of the cell but also the synaptic transmission quality in the tripartite synapses. In the event of fluctuations (extreme low or high) in the overall concentration, this can lead to a number of neurodegenerative diseases. For example, low Ca^{2+} concentration lead to cellular death and poor functioning of neurons that cause depression, whereas high Ca^{2+} concentration is linked with one of the causes of Alzheimer's disease [25], [26], [27]. For evaluation of both extreme high and low concentrations, we developed a

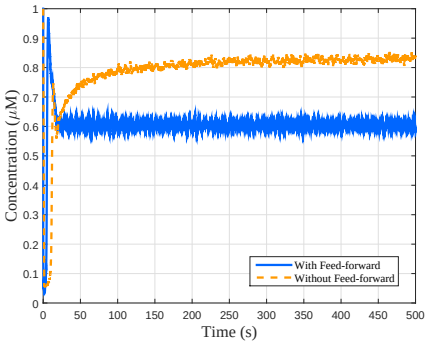

Fig. 8: The application of the Feed-forward technique to maintain the desired levels of Ca^{2+} in the astrocytes' cytosol.

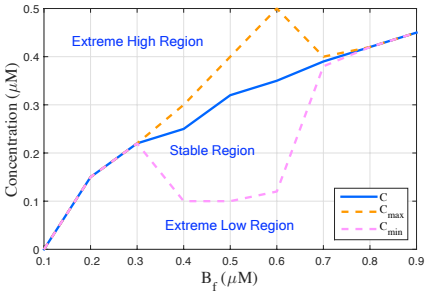

Fig. 9: Application of the control model to achieve the desired Ca^{2+} level compared to regions that can result in diseases. *Extreme high region* is any value higher than the maximum Ca^{2+} levels, *Extreme low region* is any value lower than the minimum Ca^{2+} levels, and the *stable region* is the Ca^{2+} levels in between the maximum and minimum values.

simple model that shows the effectiveness of the control technique in maintaining the stable zones of Ca^{2+} concentration levels.

We varied the $beta$ in Eq. 3 from 0.1 to 0.9 μM and compared the resulting Ca^{2+} concentration levels with the feed-forward feedback control technique. In the case of when no control is applied, the Ca^{2+} oscillations are expected. Based on the oscillations, we selected the maximum and minimum values of the final concentrations and used them to define three regions: *extreme high region*, *extreme low region*, and *stable region*. The extreme high region is any value higher than the maximum Ca^{2+} concentration levels, while the extreme low region is any value lower than the minimum Ca^{2+} concentration levels. The stable region, which represents the safe level in the Ca^{2+} concentration, is in between the extreme limits.

Regulation of Ca^{2+} concentration can effectively maintain stability in the concentration within the safe region for all IP_3 values as illustrated in Fig. 9. The C_f from Eq. 11 was selected based on the central value between the maximum and minimum values of C. The β_f was computed based on C_f and by adjusting this, the system will adjust C to be matched with C_f.

D. Data Rate of a Molecular Communication System

Molecular communication is a new communication paradigm that facilitates for nanomachines in biological environments to communicate. The Ca^{2+}-signalling-based molecular communication system has been proposed for cellular tissues, where previous works have explored its performance for various types of cells [28]. One of the issues regarding the use of Ca^{2+} signalling for molecular communication is the artificial stimulation of the ions for communication purpose, as well as the excessive noise that can result in poor data rate performance. The low data rate mainly results from the long bit transmission periods (Tb) that have to wait in order to allow the noise within the tissue to die before the following bits can be transmitted. Barros et. al. [29], [28], showed that large Tb is desired to achieve reasonable communication capacity but this results in poor data rate for most types of cells that communicate using Ca^{2+} ions. Another reason for the long bit transmission periods Tb is due to the refractory time of the Ca^{2+} oscillation. The refractory time is an inherent process found in Ca^{2+} intracellular signalling, where the concentration of the fluctuating ions are required to stabilise before they can be stimulated again. Our objective now is to see if we can integrate the proposed feed-forward feedback control technique to eliminate the refractory time.

To show the benefits of the proposed control technique for molecular communication, we present a data rate analysis of a single hop Ca^{2+} molecular communication system using astrocytes. The data rate in such system can be computed using: $(1/Tb) * Nb$, where Nb is the number of bits transmitted. We used three Tb values ($5s$, $10s$, $50s$) and compared the performance for the case when the system integrates the control model as well as without, and varying Nb in the process.

As demonstrated in Fig. 10 the elimination of the refractory time provides substantial benefit in improving the data rate for all the Tb values. On average, the refractory time takes up to five seconds to be completed. This time is needed for a complete oscillation cycle from the signalling process of the cell. However, such oscillatory process can also be eliminated with the proposed feed-forward feedback control technique. Then, higher data rate values are reached based on the usage of the refractory time for the next bit transmission. For example, with the highest values of data rate ($Tb = 5s$), without control reaches a limit of 1000bps while with control reaches 2000bps.

VI. Discussion

In this section, two main application are explored for the proposed Ca^{2+} control method, including: prevention of neurodegenerative diseases and molecular communication. We

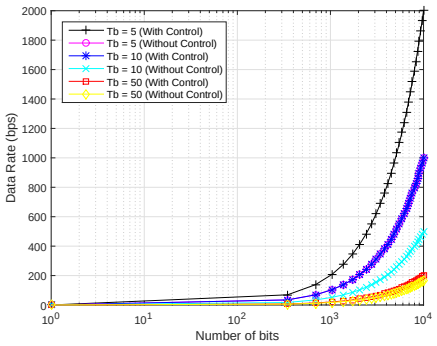

Fig. 10: Data rate performance of a Ca^{2+}-signalling molecular communication system with Tb values ($5s$, $10s$, $50s$). We compare the performance when the *feed-forward feedback* control technique is applied against the system with no control technique that has to wait for longer refractory periods.

believe that a significant impact will be expected from the utilization of the proposed method on those topics.

A. Prevention of Neurodegenerative Diseases

Approximately 24 million people worldwide suffer from dementia or neurodegenerative diseases with an annual cost of approximately $226 billion in the U.S. alone [30], [31]. Causes of such remains unknown and only conventional symptomatic treatment are available for improving the patients' health. This is achieved with drugs that target the symptoms alone, neither treating the underlying disease or at best delaying its progression. However, as they progress, brain cells die and connections among cells are lost, causing the disease symptoms to worsen [32].

A major issue with drug delivery techniques to the brain is the numerous protective barriers that encapsulates the central nervous system, and one of this example is blood-brain barrier [32]. Overcoming the blood-brain barrier can be achieved through biotechnology, synthetic biology, as well as nanotechnology, and this can lead to efficient and directed therapeutic tools. The control model proposed in this paper, can be developed from a combination of nanoparticles that are used to control the Ca^{2+} signalling, as well as synthetic biology. In the case of synthetic biology, programming of cells can be achieved that can also lead to stable levels of Ca^{2+} ions, preventing fluctuations that may lead to diseases. There are a number of works that have investigated mechanisms to use synthetic biology to engineer neurons to prevent neurological diseases. One example is optogenetics where neurons are programmed to be sensitive to light at a certain wavelength, providing a new alternative for externally controlled neural stimulation.

B. Molecular Communication

The low performance data rate is a natural characteristic of molecular communication systems due to many factors including stochastic propagation delay as well as excessive noise in the environments. These are due to the natural biological processes that result in poor communication performance. Therefore, integration of engineered processes will be required to counter these natural processes that can affect the performance. This engineering process will usually come through integration of nanotechnology through components and materials to control the biological process, or through manipulation of cell using techniques from synthetic biology.

In Section V-D, we showed how the proposed control technique is beneficial to limit the refractory period in order to increase the data rate. However, the proposed control approach is not limited to improving the data rate performance, but also can be extended to perform other communication functionalities that will improve the performance, such as modulation and noise cancellation. Recent work has proposed a modulation techniques for a Ca^{2+}-signalling based molecular communication system [38]. Digital modulator such as *On-Off Shift-Keying* (*OOK*) was used in conjunction with few error control techniques. In [29], noise in Ca^{2+}-signalling molecular communication was studied and quantified showing that its high concentration can negatively affect the communication system performance. The noise will emanate at the transmitter as the Ca^{2+} waves are stimulated, along the path as the waves are propagated, and at the receiver as they stimulate Ca^{2+} ions to receive digital bits. Therefore, based on this scenario, and also how we showed that noise can be limited through our technique, the control model can be engineered into the cells of the tissue to cancel noise as they propagate along the channel. This can be achieved by limiting the quantity of IP_3 for each cell that represent the transmitter, along the propagation path, as well as the receiver.

VII. Conclusion

In recent years, nanotechnology has brought together a number of different disciplines including synthetic biology and engineering, where the objective is to develop novel health care solutions to detect, prevent and cure diseases. This includes the field of molecular communication, where its aim is to model and construct biological communication systems for inter and intracellular cellular signalling. This new area of research aims to develop new approaches for detecting and preventing diseases that can emerge from impairments in the communication process, as well as create artificial communications that connect a network of nanomachines. This paper investigated one specific type of molecular communication that utilises Ca^{2+} signalling between astrocyte cells and pre and post-synaptic neurons. This three-way communication process is known as tripartite synapse. In particular, we focus on applying a feed-forward feedback control technique to main stability of Ca^{2+} levels as intercellular signalling is conducted between the cells. The application of the control model is two folds: firstly, the regulation of Ca^{2+} concentration from the signalling is demonstrated to maintain a stable level in order

to minimise any fluctuations that can result in neurodegenerative diseases, and secondly, application to improve the data rate performance for molecular communication using Ca^{2+}-signalling that are triggered from astrocyte cells. Previous studies have shown that Ca^{2+}-signalling in cellular tissue can lead to large quantity of noise within the environment, impairing the data rate performance. However, applying the control model led to reduction in the refractory period of the Ca^{2+}-signalling which resulted in smaller time-slot for bit transmissions. The control model proposed in this paper can pave the way for novel techniques for disease prevention, as well as mechanisms to improve the performance of molecular communication systems. The proposed technique can also integrate techniques for synthetic biology to program the cells to integrate this control function.

REFERENCES

[1] Y. Chahibi, M. Pierobon, S. O. Song, and I. F. Akyildiz, "A molecular communication system model for particulate drug delivery systems," *IEEE Transactions on Biomedical Engineering*, vol. 60, no. 12, pp. 3468–3483, Dec 2013.

[2] Y. Chahibi, M. Pierobon, and I. F. Akyildiz, "Pharmacokinetic modeling and biodistribution estimation through the molecular communication paradigm," *IEEE Transactions on Biomedical Engineering*, vol. 62, no. 10, pp. 2410–2420, Oct 2015.

[3] BBC, "Tissue engineering: Grow your own smart organs," [Online]. Available: http://www.bbc.com/future/story/20131016-smart-organs-for-everyone

[4] R. Langer and J. P. Vacanti, "Tissue engineering," *Science*, vol. 260, no. 5110, pp. 920–926, 1998.

[5] R. Skalak and C. F. Fox, *Tissue Engineering*. Alan R. Liss, 1988.

[6] I. Akyildiz, M. Pierobon, S. Balasubramaniam, and Y. Koucheryavy, "The internet of bio-nano things," *IEEE Communications Magazine*, vol. 53, no. 3, pp. 32–40, March 2015.

[7] B. Atakan, S. Balasubramaniam, and O. B. Akan, "Body area nanonetworks with molecular communications in nanomedicine," *IEEE Communications Magazine*, vol. 50, pp. 28–34, 2012.

[8] I. Akyildiz, F. Fekri, R. S. C. R. Forest, and B. K. Hammer, "Monaco: fundamentals of molecular nano-communication networks," *IEEE Wireless Communications*, vol. 19, no. 5, pp. 12–18, 2012.

[9] F. Mesiti, M. Veletć, P. A. Floor, and I. Balasingham, "Astrocyte-neuron communication as cascate of equivalent circuits," *Nano Communication Networks*, 2015.

[10] E. A. Newman, "New roles for astrocytes: Regulation of synaptic transmission," *Trends in Neuronscience*, vol. 36, no. 10, pp. 536–542, 2003.

[11] P. F. Pinsky and J. Rinzel, "Intrinsic and network rhythmogenesis in a reduced traub model for ca3 neurons," *Journal of Computational Neuroscience*, vol. 1, no. 1-2, pp. 39–60, 1994.

[12] S. Nadkarni and P. Jung, "Dressed neurons: modeling neuralglial interactions," *Physical Biology*, vol. 1, no. 1, p. 35, 2004.

[13] Q.-S. LIU, Q. XU, J. KANG, and M. NEDERGAARD, "Astrocyte activation of presynaptic metabotropic glutamate receptors modulates hippocampal inhibitory synaptic transmission," *Neuron Glia Biology*, vol. 1, pp. 307–316, 11 2004.

[14] C. Luscher and R. C. Malenka, "Nmda receptor-dependent long-term potentiation and long-term depression (ltp/ltd)," *Cold Spring Harbor Perspectives in Biology*, vol. 4, no. 6, p. a005710, 2012.

[15] M. M. Halassa, T. Fellin, and P. G. Haydon, "The tripartite synapse: roles for gliotransmission in health and disease," *Trends in Molecular Medicine*, vol. 13, no. 2, pp. 54 – 63, 2007.

[16] C. C. Rudy, H. C. Hunsberger, D. S. Weitzner, and M. N. Reed, "The role of the tripartite glutamatergic synapse in the pathophysiology of alzheimer's disease," *Aging and Disease*, vol. 6, no. 2, p. 131, 2015.

[17] A. Araque and M. Navarrete, "Glial cells in neuronal network function," *Philosophical Transactions of the Royal Society B: Biological Sciences*, vol. 365, no. 1551, pp. 2375–2381, 2010.

[18] G. Perea, M. Navarrete, and A. Araque, "Tripartite synapses: astrocytes process and control synaptic information," *Trends in Neurosciences*, vol. 32, no. 8, pp. 421 – 431, 2009.

[19] R. Antonelli, J. Harmand, J.-P. Steyer, and A. Astolfi, "Set-point regulation of an anaerobic digestion process with bounded output feedback," *IEEE Transactions on Control Systems Technology*, vol. 11, no. 4, pp. 495–504, July 2003.

[20] P. Raul, S. Manyam, P. Pagilla, and S. Darbha, "Output regulation of nonlinear systems with application to roll-to-roll manufacturing systems," *IEEE/ASME Transactions on Mechatronics*, vol. 20, no. 3, June 2015.

[21] M. Pitta, M. Goldberg, V. Volman, H. Berry, and E. Ben-Jacob, "Glutamate regulation of calcium and ip3 oscillating and pulsating dynamics in astrocytes," *Journal of Biological Physics*, vol. 35, pp. 383–411, 2009.

[22] S. Hussain, L. C. J. Thomassen, I. Ferecatu, M. Borot, K. Andreau, J. A. Martens, J. Fleury, A. Baeza-Squiban, F. Marano, and S. Boland, "Carbon black and titanium dioxide nanoparticles elicit distinct apoptotic pathways in bronchial epithelial cells," *Particle and Fibre Toxicology*, vol. 7, no. 10, pp. 1–17, 2010.

[23] R. Janicek, M. Hotka, J. A. Zahradnkov, A. Zahradnkov, and I. Zahradnk, "Quantitative analysis of calcium spikes in noisy fluorescent background," *PLoS ONE*, vol. 8, no. 5, p. e64394, 05 2013.

[24] M. P. Mattson and S. L. Chan, "Neuronal and glial calcium signaling in alzheimers disease," *Cell Calcium*, vol. 34, no. 45, pp. 385 – 397, 2003, neuronal Calcium Toxicity.

[25] A. Gaur, A. Midha, and A. L. Mbatia, "Applications of nanotechnology in medical sciences," *Asian Journal of Pharmaceutical Sciences*, vol. 2, pp. 80–85, 2008.

[26] S. Orrenius and P. Nicotera, "The calcium ion and cell death," *Journal of Neural Transmission. Supplementa*, vol. 43, pp. 1–11, 1994.

[27] F. M. LaFerla, "Calcium dyshomeostasis and intracellular signalling in alzheimer's disease," *Nature Reviews Neuroscience*, vol. 3, pp. 862–872, 2002.

[28] M. T. Barros, S. Balasubramaniam, and B. Jennings, "Comparative end-to-end analysis of ca2+ signaling-based molecular communication in biological tissues," *IEEE Transactions on Communications*, vol. PP, no. 99, pp. 1–1, 2015.

[29] M. T. Barros, S. Balasubramaniam, B. Jennings, and Y. Koucheryavy, "Transmission protocols for calcium signaling based molecular communications in deformable cellular tissues," *IEEE Transactions on Nanotechnology*, vol. 13, no. 4, pp. 779–788, 2014.

[30] A. Association, "Alzheimers disease facts and figures." [Online]. Available: https://www.alz.org/facts/downloads/facts_figures_2015.pdf

[31] C. P. Ferri, M. Prince, C. Brayne, and et al., "Global prevalence of dementia: A delphi consensus study," *Lancet*, vol. 366, pp. 2112–2117, 2005.

[32] G. Modi, V. Pillay, and Y. E. Choonara, "Advances in the treatment of neurodegenerative disorders employing nanotechnology," *Annals of the New York Academy of Sciences*, vol. 1184, pp. 154–172, 2010.

[33] K. Kostarelos and A. Miller, "Synthetic, self-assembly abcd nanoparticles; a structural paradigm for viable synthetic non-viral vectors," *Chemical Society Reviews*, vol. 34, pp. 970–994, 2005.

[34] P. GBorn and D. Muller-Schulte, "Nanoparticles in drug delivery and environmental exposure: same size, same risks?" *Nanomedicine*, vol. 1, pp. 235–249, 2006.

[35] Z. P. Xu, Q. Zeng, G. Lu, and A. Yu, "Inorganic nanoparticles as carriers for efficient cellular delivery," *Chemical Engineering Science*, vol. 61, pp. 1027–1040, 2007.

[36] C. Foged and H. Nielsen, "Cell-penetrating peptides for drug delivery across membrane barriers," *Expert Opinion on Drug Delivery*, vol. 5, pp. 1435–1342, 2008.

[37] S. Leary, C. Liu, and M. Apuzzo, "Toward the emergence of nanoneurosurgery: Part iii nanomedicine: Targeted nanotherapy, nanosurgery, and progress toward the realization of nanoneurosurgery," *Neurosurgery*, vol. 58, pp. 1009–1026, 2006.

[38] M. T. Barros, S. Balasubramaniam, and B. Jennings, "Error control for calcium signaling based molecular communications," in *47th Annual Asilomar Conference on Signals, Systems, and Computers*, 2013.

Michael Taynnan Barros (S'14) was born in Campina Grande, Brazil. He is currently a post-graduate researcher working towards his Ph.D degree in Telecommunication Software at the Telecommunications Software and Systems Group (TSSG) and the Waterford Institute of Technology (WIT). He received his M.Sc. degree in Computer Science at the Federal University of Campina Grande (UFCG) and B.Tech. degree in Telematics at the Federal Institute of Education, Science and Technology of Paraiba (IFPB). His experience concentrates on Dynamic Optical Networks, Vehicular Ad Hoc Networks, Routing, IP Traffic Classification, QoS-DiffServ Aware Networks and Molecular Communications, publishing more than 30 papers in international journals and conferences. He is also a reviewer for many journals and participated as technical program committee and reviewer for various international conferences. His research interests include Nano Networks, Molecular Communications and Bio-Inspired Techniques.

Subhrakanti Dey (M'96 - SM'06) was born in India in 1968. He received the B.Tech. and M.Tech. degrees from the Department of Electronics and Electrical Communication Engineering, Indian Institute of Technology, Kharagpur, in 1991 and 1993, respectively, and the Ph.D. degree from the Department of Systems Engineering, Research School of Information Sciences and Engineering, Australian National University, Canberra, in 1996. He is currently a Professor with the Department of Engineering Sciences in Uppsala University, Sweden. Prior to this, he was a Professor with the Department of Electrical and Electronic Engineering, University of Melbourne, Parkville, Australia, from 2000 until early 2013. From September 1995 to September 1997, and September 1998 to February 2000, he was a Postdoctoral Research Fellow with the Department of Systems Engineering, Australian National University. From September 1997 to September 1998, he was a Postdoctoral Research Associate with the Institute for Systems Research, University of Maryland, College Park. His current research interests include networked control systems, wireless communications and networks, signal processing for sensor networks, and stochastic and adaptive estimation and control. Professor Dey currently serves on the Editorial Board of the IEEE TRANSACTIONS ON SIGNAL PROCESSING and Elsevier SYSTEMS AND CONTROL LETTERS. He was also an Associate Editor for the IEEE TRANSACTIONS ON SIGNAL PROCESSING during 20072010 and the IEEE TRANSACTIONS ON AUTOMATIC CONTROL during 20042007

Sasitharan Balasubramaniam (SM'14) received his Bachelor (Electrical and Electronic Engineering) and Ph.D. degrees from the University of Queensland in 1998 and 2005, respectively, and Masters (Computer and Communication Engineering) degree in 1999 from the Queensland University of Technology. He is currently an Academy of Finland Research Fellow at the Nano Communication Centre, Department of Electronic and Communication Engineering, Tampere University of Technology, Finland. Previously, Sasitharan was a research fellow at the Telecommunication Software & Systems Group, Waterford Institute of Technology, Ireland, where he worked on a number of Science Foundation Ireland projects. He has published over 90 papers and actively participates in a number of technical programme committee for various conferences. Sasitharan was the General co-chair of ACM NANOCOM 2015 and TPC co-chair for ACM NANOCOM 2014 and IEEE MoNaCom 2011, both conferences which he co-founded. He is currently an editor for the IEEE Internet of Things journal, Elsevier Nano Communication Networks, Elsevier Swarm and Evolutionary Computation, and Elsevier Digital Communication and Networks. His current research interests includes bio-inspired communication networks, as well as molecular communications. Sasitharan is an IEEE Senior member.

Chapter 9

Discussion

The research presented in this thesis has applied common theories from communication engineering (e.g., characterisation of capacity, delay, noise of the channel) as well as communication networking protocols (e.g., transmission protocols), and tools from data analysis (e.g., inference process) to Ca^{2+}-signalling-based molecular communication systems. The major challenge of this research is mapping these theories that are taking from conventional communication systems, adapting them, and applying to the physical layer communication process using Ca^{2+} ions. This chapter will summarise these contributions and in particular discuss the insights from the results of the multi-disciplinary research of this thesis.

9.1 Communication-by-Silence in a Tissue

The thesis has analysed the noise that results from the Ca^{2+} signalling molecular communication systems, and how there are different types of noise depending on the location along the tissue. This noise dramatically impacts on the subsequent bits that are to be transmitted through the channel, and was discussed extensively in Chapter 5. While there are noise in wireless networks, the major challenge is selecting the protocol from conventional networks that suits the nature of the noise found in Ca^{2+}-signalling-based molecular communication

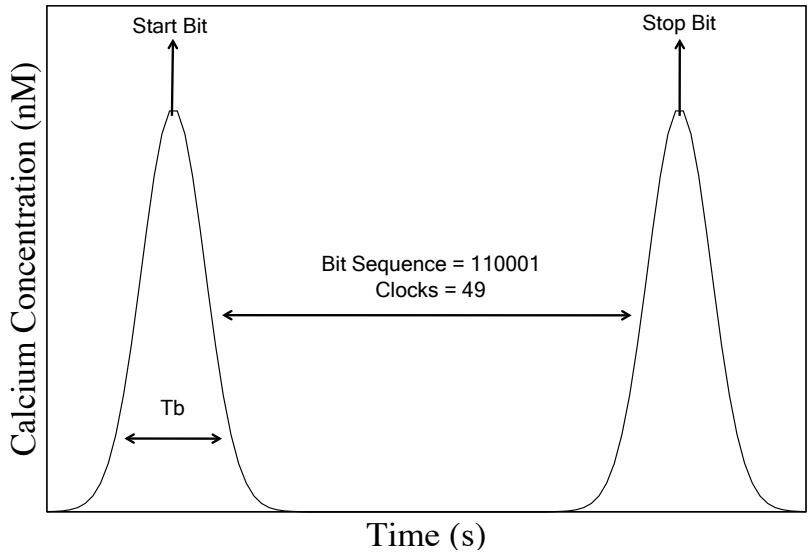

Fig. 9.1 Illustration of the communication-by-silence technique.

systems. The main difference is the time-variations, where in wireless networks, this is in the order of micro to milliseconds, while in the case of Ca^{2+} signalling-based molecular communication systems the noise in the channel can last up to a few sections. This means that the channel is highly sensitive, and any protocol selected to improve the channel capacity needs to minimise any additional transmissions that will lead to reflective noise. Therefore, the solution taken by this thesis is to push all the computational load for improving the performance into the transmitter and receiver nanomachine itself. By doing this, will minimise the additional transmissions. Therefore, the most appropriate approach was to use communication-by-silence that was proposed for wireless networks [106], and was also proposed for diffusion-based molecular communication [33].

In communication-by-silence, the *silence* period between successive signals is itself used to convey information. The communication process only requires two signals to be transmitted, which meets the objective of minimising any transmission along the channel. Figure 9.1 illustrates the described process.

The communication-by-silence technique improved data rate by 40 times compared to the conventional communication encoding process for Ca^{2+}-signalling-based molecular

communication using OOK. The significant improvement of data rate is based on the number of bits for transmission, total transmission duration, and the quantity of compression in the tissue deformation. However, the question remains as to how this could be realised with the current technologies for developing nanomachines to have counting capabilities and also synchronised clocks. Although synthetic biology has provided means to program cells into computing devices, the current engineering methodologies are far from achieving the clock rate of silicon technologies. However, one approach to realise this is through the silicon chip that can be embedded into the cells to represent transmitters and receivers [107].

9.2 Molecular Nanonetwork Inference Process

Numerous research efforts in recent years have been dedicated to technologies that enable *Tissue Engineering*. Tissue Engineering combines methodologies from engineering and life science to control and design tissues for organ construction [108; 109]. This technology provides an alternative treatment for patients that suffer from organ and tissue failure or shortage of organ donors [108; 110]. The naturally flexible structure of cells usually leads to them dynamically changing shapes under strain and forces, where numerous diseases are linked to the changes in the tissues structures. Therefore, detecting and inferring the tissue deformation is very appealing, where more precise diagnosis of tissue-related diseases can be achieved. This factor motivated the need to utilize Ca^{2+} signalling-based molecular communication to infer and detect the state of the tissue, and this as achieved through the *Molecular Nanonetwork Inference Process*.

Figure 9.2 shows the results for the inference accuracy for different tissue types. Mutual information, mutual information with generalized entropy and information distance were compared and analysed. The highest accuracy is achieved by the generalized entropy with $\alpha = 10$ for a five-node star topology. The mutual information $I(X;Y)$, on the other hand, resulted in the worst performance. This is attributed to the low divergent probability

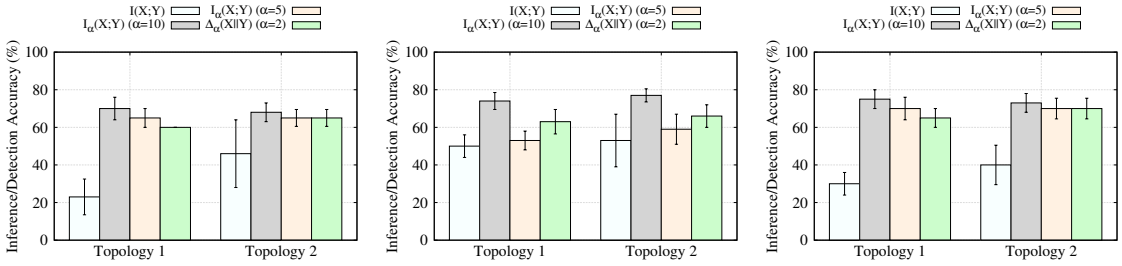

(a) Average for all compressing types.

(b) Tissue with a *one-side* compression.

(c) Tissue with a *S type* compression.

Fig. 9.2 Accuracy of inferring the type of deformation for a five-node star topologies.

distribution function, which results in the mutual information suffering from poor accuracy. Therefore, this result confirms the fact that the accuracy of the generalized entropy with high values of α performs better compared to other approaches. However, the presented techniques can also be improved for more accurate inferencing processes with more complex machine learning algorithms.

Embedding nanonetworks into the organs constructed from tissue engineering could provide new dimensions for advanced patient care. Langer [111], commented that the use of sensors embedded into tissues for monitoring and detecting illnesses can lead to *Smart Organs*. This allows the usage of multiple transmitter nanomachine sending data to a common receiver nanomachine. The collected monitoring data can also be transferred externally to the human body through an interface compatible with the IoBNT. In this case, there is a possibility of performing intense data processing based on external resources outside the human body, such as the cloud. Many diagnosis, treatment, and prevention of diseases tools can be explored and developed in the future using this proposed infrastructure.

9.3 Performance Comparison Between Ca^{2+} Signalling in Different Cellular Tissue Types

The performance comparison of the three tissue was investigated for four different metrics, which includes spatio-temporal Ca^{2+} dynamics, molecular delay, molecular gain, information capacity and intracellular interference. The analysis was concentrated on the following properties of the cells in the tissues: diffusion velocity as ions pass through the gap junction, the size, shape of the cell and their connectivity, and the gap junction behaviour for each cell type. The difference in this comparative analysis compared to previous works on Ca^{2+} signalling-based molecular communications is integration of these properties and analysing their relationships and its impact on the communication performance. Previous works have only selected a single or a few properties to generalise the property of a tissue, which is not realistic compared to the study conducted in this thesis.

In the literature for Ca^{2+} signalling, no comparison has been found to date for different cellular tissue types that uses these ions for communication between the cells. This comparison is very important for the characterization of the cellular tissues properties in cell types including excitable, non-excitable and hybrid cells. In particular since majority of the cells on the body uses Ca^{2+} signalling as their communication model. This ranges from cells found with the heart such as cardiomyocytes to epithelial cells of the skin. This motivated the comparative study in order to demonstrate to the communication engineering community how different cell types that communicate through the same signalling mechanism can lead to different communication performance. This comparative analysis is highly beneficial for the field of: 1) *Biotechnology*: This can lead to design of new therapeutic drugs that can address diseases resulting from impaired Ca^{2+} signalling; and 2) *Nanotechnology*: design of transmitter and receiver nanomachines that suit the channel characteristics and tissue environments.

9.4 Feed-forward Feedback Control Technique for Regulation of Intracellular Ca^{2+} Signalling in Astrocytes

Providing reliable Ca^{2+}-signalling-based molecular communication requires the increase of Ca^{2+} concentration that is being transmitted. However, molecular communication engineers have not take into account that high Ca^{2+} concentration can be hazardous to the tissue. This increase in the concentration can lead to cellular tissue diseases, as well as the death of cells. One example is the uncontrollable tissue growth with cancerous cells that is linked to high Ca^{2+} concentration. Another example is neurodegenerative diseases, which is related to the quality of the synapses in neuronal communication. However, a major challenge is selecting the most appropriate control technique that is suitable for the behaviour of Ca^{2+} signalling and its impact on the gliotransmitters. The control technique that was selected was the feed-forward feedback model. The impact of the feed-forward feedback control technique on the oscillatory Ca^{2+} behaviour is shown in the following, Fig 9.3. The proposed technique can efficiently maintain Ca^{2+} concentration levels throughout the time period shown. This positive result demonstrates the effectiveness and the potential of utilising the control technique to stabilise the excessive Ca^{2+} concentration.

Control theory has been used extensively in systems biology, and in particular to study the performance of metabolic pathways and regulations from intracellular signalling within the cells. However, very little attention has been paid to intercellular signalling. This is the motivating factor of studying and incorporating control theory to improve the performance of Ca^{2+} signalling-based molecular communication systems, but at the same time also to relate this to prevention of neurodegenerative disease. Since synthetic biology as a field is gaining popularity with new improved technologies to help engineer various types of cells, this could be used to engineer astrocytes to incorporate genetic circuits that represent the control required to maintain stable Ca^{2+} signalling.

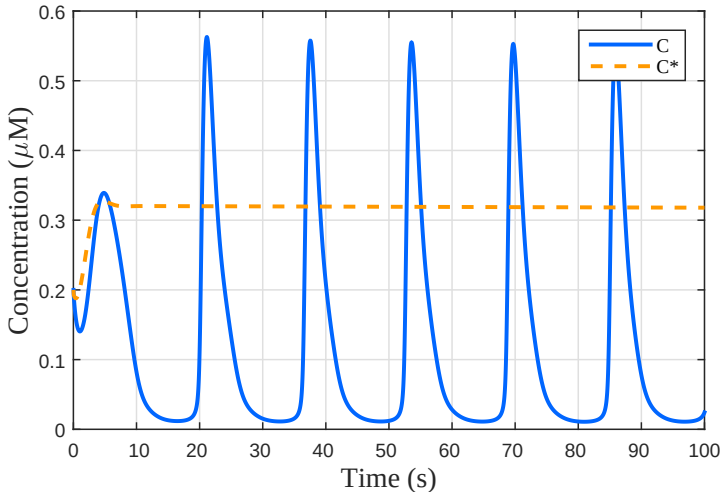

Fig. 9.3 Elimination of Ca^{2+} oscillation using the proposed feedback and feed-forward control technique. Regular Ca^{2+} oscillations C (straight lines) is compared to a controlled Ca^{2+} level C^* (dashed line).

Chapter 10

Conclusion

Nanotechnology and biotechnology advancements allow intense development in diagnosis, treatment and prevention of diseases that contributes to the field of nanomedicine. One of the enablers that will see the success of nanomedicine application as well as open further opportunities in the future is molecular communication. This communication can play a role at the nanoscale where molecules interact with the nanomachine as part of the reaction process with the environments (e.g., enzymes produced from diseased cells), or between nanomachines to cooperate and increase their capabilities. The latter can lead to new communication and networking paradigm at the nano and molecular scale, such as new forms of sensing and actuation. These communication and networking of nanomachines is a small subset of the vision of Internet of Bio-Nano Things, which will see engineered nanomachines made from cells that can communicate to the outside world. The impact of this vision will revolutionize healthcare systems by bringing low cost solutions for the wider population, as well as improved accuracy in diagnosis that will improve life quality and expectancy.

This thesis concentrated on Ca^{2+}-signalling-based molecular communication systems. The Ca^{2+} signalling is a short range natural communication process between cells. In particular, the focus of the thesis is in proposing a communication system for nanomachine that are constructed from engineered cells. The communication process is achieved by having

the transmitter nanomachine encode the information into the concentration of Ca^{2+} ions that will propagate over the tissue, and get decoded at a receiver nanomachine.

Research contribution of this thesis are as follows:

A framework for Ca^{2+}-signalling-based molecular communication system, that analyses the capacity, molecular delay, and molecular gain for three different types of cells. The cells include excitable cells (smooth muscle cells), non-excitable cells (epithelial cells), as well as hybrid cells (astrocyte cells). The analysis for these metrics, considered the type of signalling, which may be due to pure electrical, chemical, as well as a combination, the gap junction behaviour for each type of cells, their connectivity, as well as their physiological shapes. The main modulation type that was investigated was On-Off Keying, where the stimulation of Ca^{2+} ions will represent a digital bit and a digital zero is an absence of any stimulation. The contribution from this work is the communication performance analysis that will enable future design of nanomachines, or nanonetwork applications, to created tailored systems that suit specific type of applications.

Cells are subject to deformity and can affect the flow of ions that propagate through the tissue, which means that it can affect the communication performance. This is on top of the excessive amount of noise that emanate from stimulation of Ca^{2+} when digital bits are transmitted. In order to counter this, the thesis explored transmission protocols that are currently used in noisy environments of wireless networks. The specific protocol explored was communication-by-silence, which is based on transmitting two bits (Start and Stop) between a transmitter and a receiver, and utilizing a synchronised clock to count the values that are to be sent. This form of modulation was most appropriate due to the noise within the environment. At the same time, enhancements were made to incorporate dynamic time-slots for each bit transmission depending on the compression of the tissue.

While the deformity exists, and the dynamic time-slots can be used to enhance the data rate performance, there is a need for the transmitter nanomachines to know the state of the

tissue to tune the time-slot duration. For this, the thesis proposed the use of an inference process that will allow the transmitters to collect the data from the Ca^{2+} and infer the type and quantity of deformation, locations with respect to the receiver, as well as the concentration of Ca^{2+} ions transmitted. The Molecular Nanonetwork Inference Process is a technique based on a machine learning algorithm that incorporates information metrics and a classification process. In order to utilise this inference process, the thesis also considered an algorithm that adapts the time-slots depending on the accuracy of the inference process to allow the nanomachines to improve its data rate performance.

Since Ca^{2+} signalling can at time lead to disease due to the excessive quantity that are propagated between the cells, the thesis explored the use of control theory to stabilise the concentration for intracellular signalling. A feed-forward feedback control model was proposed for tripartite synapse that exist between the astrocyte cells that communicate with neurons (pre and post synaptic). Two applications of the control model were investigated, which included preventive of neurodegenerative diseases, as well as improving the data rate for Ca^{2+}-signalling-based molecular communication system. In the first case, the control model was used to maintain the concentration of intracellular signalling and preventing it from reaching either extreme high or low, which in the second case, the control model was used to limit the refractory process in order for the time-slots to be shorted and enable improved data rate.

In the following section, the future work will be discussed where further research can be built from the work that has been investigated and proposed in this thesis.

10.1 Future Work

Since the field of molecular communication is still in its infancy, and in particular Ca^{2+} signalling, there are a number of works that can be investigated in the future. This section will outline a number of possible topics for the future research.

10.1.1 Validation and Wet lab

The natural further step after the development of a theoretical framework is its validation. Wet lab experiments of the proposed Ca^{2+}-signalling-based molecular communication system needs to be carried to ensure that the proposed theoretical work can lead to novel applications of the future. This will involve close collaboration with molecular biologists working in the area of Ca^{2+} signalling, synthetic biologists that can program cells into a computing element that represent (transmitter and receivers), as well as researchers from the field of nanotechnology who work on embedded chips that can be placed into the cells (this is for the case where the transmitter and receiver are electronic chips that communicate through interfacing the cells to stimulate Ca^{2+} ions).

10.1.2 Bio-computing using Ca^{2+}-signalling-based Molecular Communication System

Bio-computation has been largely studied in bacteria and mammalian cells using transcription-based boolean logic gates and circuits [112]. However, those techniques often take hours to days in order to become active as the transcription machinery dictates the speed of transcriptional-based logic operators. Trying to decrease the processing time of such biological computation, a multicellular system can be used based on enzyme-computation. Multicellular computation is also required due to reliability purposes and can be achieved through intercellular communication that can give an output on a hour-time scale. Thus, a Bio-computing using Ca^{2+}-signalling-based molecular communication system can be appropriate approach. This will lead to molecular computing systems that are embedded into the tissue.

10.1.3 Tissue Engineering

Numerous research efforts in recent years have been dedicated to technologies that enable tissue engineering. Tissue engineering combines methods of engineering and life science in the control and design of tissues that can lead to organ construction [108][109]. This technology provides an alternative treatment for patients with organ and tissue failure, treatments that can alleviate issues relating to increasing costs of current treatments and the shortage of organ donors [108][110]. Embedding nanonetworks into the organs constructed from tissue engineering, could provide new dimensions for advanced patient care. Langer [111], commented that the use of sensors embedded into tissues for monitoring and detecting illnesses can lead to new generation of *Smart Organs*.

10.1.4 Prevention of Neurodegenerative Diseases

A major issue with drug delivery techniques to the brain is the numerous protective barriers that encapsulates the central nervous system, and one of this example is blood-brain barrier [113]. Overcoming the blood-brain barrier can be achieved through biotechnology, synthetic biology, as well as nanotechnology, and this can lead to efficient and directed therapeutic tools. The control model proposed in the thesis, can be developed from a combination of nanoparticles that are used to control the Ca^{2+} signalling, as well as synthetic biology. In the case of synthetic biology, programming of cells can be achieved that can also lead to stable levels of Ca^{2+} ions, preventing fluctuations that may lead to diseases. There are a number of works that have investigated mechanisms to use synthetic biology to engineer neurons to prevent neurological diseases. One example is optogenetics where neurons are programmed to be sensitive to light at a certain wavelength, providing a new alternative for externally controlled neural stimulation. In this way, the extension of the proposed model is going to be developed for measuring the gain in synapse transmission while controlling the Ca^{2+} signalling in astrocytes, and preventing neurodegenerative diseases.

Bibliography

[1] J.-M. Lu, X. Wang, C. Marin-Muller, H. Wang, P. H. Lin, Q. Yao, , and C. Chen, "Current advances in research and clinical applications of plga-based nanotechnology," *Expert Review of Molecular Diagnostics*, vol. 9, no. 4, pp. 325–341, 2009.

[2] W. H. D. Jong and P. J. A. Borm, "Drug delivery and nanoparticles: Applications and hazards," *International Journal of Nanomedicine*, vol. 3, no. 2, pp. 133–149, 2008.

[3] M. Ciutan, C. Sasu, and M. Skiba, "Nanomedicine - the future medicine," *Management in Health*, vol. 14, no. 1, p. e218, 2010.

[4] T. Nakano and M. Moore, "Molecular communication paradigm overview," *Journal of Next Generation Information Technology*, vol. 2, pp. 9–16, 2011.

[5] T. Nakano, M. J. Moore, F. Wei, A. V. Vasilakos, and J. Shuai, "Molecular communication and networking: Opportunities and challenges," *IEEE Transactions on NanoBioscience*, vol. 11, pp. 135 –148, 2012.

[6] T. Nakano, T. Suda, Y. Okaie, M. J. Moore, and A. V. Vasilakos, "Molecular communication among biological nanomachines: A layered architecture and research issues," *IEEE Transactions on NanoBioscience*, vol. 13, pp. 169–197, Sept 2014.

[7] M. Gregori and I. Akyildiz, "A new nanonetwork architecture using flagellated bacteria and catalytic nanomotors," *IEEE Journal on Selected Areas in Communications*, vol. 28, no. 4, pp. 612–619, 2010.

[8] I. F. Akyildiz, F. Brunetti, and C. Blazquez, "Nanonetworks: A new communication paradigm," *Computer Networks*, vol. 52, pp. 2260–2279, 2008.

[9] M. Pierobon and I. F. Akyildiz, "A physical end-to-end model for molecular communication in nanonetworks," *IEEE Journal on Selected Areas in Communications*, vol. 28, pp. 602–611, 2010.

[10] I. Llatser, E. Alarcon, and M. Pierobon, "Diffusion-based channel characterization in molecular nanonetworks," in *IEEE Conference on Computer Communications Workshops*, 2011.

[11] I. Llatsera, I. Pascual, N. Garralda, A. Cabellos-Aparicio, M. Pierobon, E. Alarcon, and J. Sole-Pareta, "Exploring the physical channel of diffusion-based molecular communication by simulation," in *IEEE Global Telecommunications Conference*, 2011.

[12] N. Garralda, I. Llatser, A. Cabellos-Aparicio, E. Alarcón, and M. Pierobon, "Diffusion-based physical channel identification in molecular nanonetworks," *Nano Communication Networks*, vol. 2, no. 4, pp. 196 – 204, 2011.

[13] I. Llatser, A. Cabellos-Aparicio, M. Pierobon, and E. Alarcon, "Detection techniques for diffusion-based molecular communication," *IEEE Journal on Selected Areas in Communications*, vol. 31, no. 12, pp. 726–734, 2013.

[14] Y. Lin, W. Lin, C. Lee, and P. Yeh, "Asynchronous threshold-based detection for quantity-type-modulated molecular communication systems," *IEEE Transactions on Molecular, Biological and Multi-Scale Communications*, vol. PP, no. 99, pp. 1–1, 2015.

[15] D. Kilinc and O. Akan, "Receiver design for molecular communication," *Selected Areas in Communications, IEEE Journal on*, vol. 31, no. 12, pp. 705–714, 2013.

[16] L.-S. Meng, P.-C. Yeh, K.-C. Chen, and I. Akyildiz, "On receiver design for diffusion-based molecular communication," *IEEE Transactions on Signal Processing*, vol. 62, no. 22, pp. 6032–6044, 2014.

[17] A. Noel, K. C. Cheung, and R. Schober, "Optimal receiver design for diffusive molecular communication with flow and additive noise," *IEEE Transactions on NanoBioscience*, vol. 13, no. 3, pp. 350–362, 2014.

[18] M. Pierobon and I. F. Akyildiz, "Diffusion-based noise analysis for molecular communication in nanonetworks," *IEEE Transactions on Signal Processing*, vol. 59, pp. 2532–2547, 2011.

[19] M. Pierobon and I. F. Akyildiz, "Noise analysis in ligand-binding reception for molecular communication in nanonetworks," *IEEE Transactions on Signal Processing*, vol. 59, p. 4168?4182, 2011.

[20] M. Pierobon and I. F. Akyildiz, "A statistical-physical model of interference in diffusion-based molecular nanonetworks," *IEEE Transactions on Communications*, vol. 62, pp. 2085–2095, June 2014.

[21] A. Aijaz and A.-H. Aghvami, "Error performance of diffusion-based molecular communication using pulse-based modulation," *IEEE Transactions on NanoBioscience*, vol. 14, pp. 146–151, Jan 2015.

[22] A. Noel, K. C. Cheung, and R. Schober, "Joint channel parameter estimation via diffusive molecular communication," *CoRR*, vol. abs/1410.4252, 2014.

[23] M. Pierobon and I. F. Akyildiz, "Information capacity of diffusion-based molecular communication in nanonetworks," in *IEEE INFOCOM*, 2011.

[24] M. Pierobon and I. F. Akyildiz, "Capacity of a diffusion-based molecular communication system with channel memory and molecular noise," *IEEE Transactions on Information Theory*, vol. 59, no. 2, pp. 942–954, 2013.

[25] A. Ahmadzadeh, A. Noel, A. Burkovski, and R. Schober, "Amplify-and-forward relaying in two-hop diffusion-based molecular communication networks," *CoRR*, vol. abs/1504.03738, 2015.

[26] L. C. Cobo and I. F. Akyildiz, "Bacteria-based communication in nanonetworks," *Nano Communication Networks*, vol. 1, p. 244?256, 2010.

[27] P. Lio and S. Balasubramaniam, "Opportunistic routing through conjugation in bacteria communication nanonetwork," *Nano Communication Networks*, vol. 3, p. 36?45, 2012.

[28] S. Balasubramaniam and P. Lio', "Multi-hop conjugation based bacteria nanonetworks," *IEEE Transactions on NanoBioscience*, vol. 12, no. 1, pp. 47–59, 2013.

[29] N. Michelusi and U. Mitra, "Capacity of electron-based communication over bacterial cables: the full-csi case," *IEEE Transactions on Molecular, Biological and Multi-Scale Communications*, vol. PP, no. 99, pp. 1–1, 2015.

[30] A. O. Bicen, C. M. Austin, I. F. Akyildiz, and C. R. Forest, "Efficient sampling of bacterial signal transduction for detection of pulse-amplitude modulated molecular signals," *IEEE Transactions on Biomedical Circuits and Systems*, vol. 9, pp. 505–517, Aug 2015.

[31] N. Islam and S. Misra, "Collision bottleneck throughput in bacterial conjugation-based nanonetworks," *IEEE Transactions on NanoBioscience*, vol. 14, pp. 112–120, Jan 2015.

[32] B. Krishnaswamy and R. Sivakumar, "Source addressing and medium access control in bacterial communication networks," in *Proceedings of the Second Annual International Conference on Nanoscale Computing and Communication*, NANOCOM' 15, pp. 1:1–1:6, 2015.

[33] B. Krishnaswamy *et al.*, "When bacteria talk: Time elapse communication for super-slow networks," in *IEEE International Conference on Communications*, 2013.

[34] B. Krishnaswamy, C. Austin, J. Bardill, D. Russakow, G. Holst, B. Hammer, C. Forest, and R. Sivakumar, "Time-elapse communication: Bacterial communication on a microfluidic chip," *IEEE Transactions on Communications*, vol. 61, pp. 5139–5151, December 2013.

[35] C. Lo, G. Wei, and R. Marculescu, "Towards autonomous control of molecular communication in populations of bacteria," in *Proceedings of the Second Annual International Conference on Nanoscale Computing and Communication*, NANOCOM' 15, pp. 29:1–29:6, 2015.

[36] Y. Okaie, T. Nakano, T. Hara, and S. Nishio, "Distributing nanomachines for minimizing mean residence time of molecular signals in bionanosensor networks," *IEEE Sensors Journal*, vol. 14, pp. 218–227, Jan 2014.

[37] Y. Okaie, T. Nakano, T. Hara, T. Obuchi, K. Hosoda, Y. Hiraoka, and S. Nishio, "Cooperative target tracking by a mobile bionanosensor network," *IEEE Transactions on NanoBioscience*, vol. 13, pp. 267–277, Sept 2014.

[38] Y. Okaie, T. Nakano, T. Hara, and S. Nishio, "Autonomous mobile bionanosensor networks for target tracking: A two-dimensional model," *Nano Communication Networks*, vol. 5, no. 3, pp. 63 – 71, 2014.

[39] A. Bicen and I. Akyildiz, "System-theoretic analysis and least-squares design of microfluidic channels for flow-induced molecular communication," *IEEE Transactions on Signal Processing*, vol. 61, pp. 5000–5013, Oct 2013.

[40] A. Bicen and I. Akyildiz, "End-to-end propagation noise and memory analysis for molecular communication over microfluidic channels," *IEEE Transactions on Communications*, vol. 62, pp. 2432–2443, July 2014.

[41] A. Bicen and I. Akyildiz, "Interference modeling and capacity analysis for microfluidic molecular communication channels," *IEEE Transactions on Nanotechnology*, vol. 14, pp. 570–579, May 2015.

[42] S. Wirdatmadja, D. Moltchanov, P. Bolcos, J. Väliaho, J. Kreutzer, P. Kallio, and Y. Koucheryavy, "Data rate performance of droplet microfluidic communication system," in *Proceedings of the Second Annual International Conference on Nanoscale Computing and Communication*, NANOCOM' 15, pp. 5:1–5:6, 2015.

[43] M. Moore, A. Enomoto, T. Nakano, R. Egashira, T. Suda, A. Kayasuga, H. Kojima, H. Sakakibara, and K. Oiwa, "A design of a molecular communication system for nanomachines using molecular motors," in *Fourth IEEE International Conference on Pervasive Computing and Communications Workshops*, 2006.

[44] M. J. Moore, A. Enomoto, S. Watanabe, K. Oiwa, and T. Suda, "Simulating molecular motor uni-cast information rate for molecular communication," in *43rd Annual Conference on Information Sciences and Systems*, 2009.

[45] A. Enomoto, M. J. Moore, T. Suda, and K. Oiwa, "Design of self-organizing microtubule networks for molecular communication," *Nano Communication Networks*, vol. 2, no. 1, pp. 16 – 24, 2011.

[46] Y. Chahibi and I. Balasingham, "Channel modeling and analysis for molecular motors in nano-scale communications," in *Proceedings of the Second Annual International Conference on Nanoscale Computing and Communication*, NANOCOM' 15, pp. 3:1–3:6, 2015.

[47] L. Felicetti, M. Femminella, G. Reali, and P. Lio, "Applications of molecular communications to medicine: A survey," *Nano Communication Networks*, Aug 2015.

[48] Y. Chahibi, M. Pierobon, S. O. Song, and I. F. Akyildiz, "A molecular communication system model for particulate drug delivery systems," *IEEE Transactions on Biomedical Engineering*, vol. 60, pp. 3468–3483, Dec 2013.

[49] Y. Chahibi, M. Pierobon, and I. F. Akyildiz, "Pharmacokinetic modeling and biodistribution estimation through the molecular communication paradigm," *IEEE Transactions on Biomedical Engineering*, vol. 62, pp. 2410–2420, Oct 2015.

[50] Y. Chahibi, I. F. Akyildiz, S. Balasubramaniam, and Y. Koucheryavy, "Molecular communication modeling of antibody-mediated drug delivery systems," *IEEE Transactions on Biomedical Engineering*, vol. 62, pp. 1683–1695, July 2015.

[51] Y. Chahibi and I. F. Akyildiz, "Molecular communication noise and capacity analysis for particulate drug delivery systems," *IEEE Transactions on Communications*, vol. 62, pp. 3891–3903, Nov 2014.

[52] I. F. Akyildiz and J. M. Jornet, "The internet of nano-things," *IEEE Wireless Communications*, vol. 17, pp. 58–63, 2010.

[53] I. Akyildiz, M. Pierobon, S. Balasubramaniam, and Y. Koucheryavy, "The internet of bio-nano things," *IEEE Communications Magazine*, vol. 53, pp. 32–40, March 2015.

[54] M. J. Berridge, M. D. Bootman, and H. L. Roderick, "Calcium signalling: dynamics, homeostasis and remodelling.," *Nature Reviews Molecular Cell Biology*, vol. 4, pp. 517–529, 2003.

[55] M. T. Barros, S. Balasubramaniam, and B. Jennings, "Error control for calcium signaling based molecular communications," in *47th Annual Asilomar Conference on Signals, Systems, and Computers*, 2013.

[56] M. T. Barros, S. Balasubramaniam, and B. Jennings, "Using information metrics and molecular communication to detect cellular tissue deformation," *IEEE Transactions on Nanobioscience*, vol. 13, no. 3, pp. 278–288, 2014.

[57] S. Ruediger, "Stochastic models of intracellular calcium signals," *Physics Report*, vol. 534, no. 2, pp. 39–87, 2007.

[58] M. T. Barros, S. Balasubramaniam, and B. Jennings, "Adaptive transmission protocol for molecular communications in cellular tissues," in *The IEEE Conference on Communications*, 2014.

[59] I. Akyildiz, F. Fekri, R. S. C. R. Forest, and B. K. Hammer, "Monaco: fundamentals of molecular nano-communication networks," *IEEE Wireless Communications*, vol. 19, no. 5, pp. 12–18, 2012.

[60] T. Nakano and J.-Q. Liu, "Design and analysis of molecular relay channels: An information theoretic approach," *IEEE Transactions on NanoBioscience*, vol. 9, pp. 213–221, 2010.

[61] A. Goldbeter, G. Dupont, and M. J. Berridge, "Minimal model for signal-induced ca2+ oscillations and for their frequency encoding through protein phosphorylation," *Proceedings of the Natinoal Academy of Science USA*, vol. 87, pp. 1461–1465, 1990.

[62] L. Leybaert and M. J. Sanderson, "Intercellular ca2+ waves: mechanisms and functions," *Physiology Review*, vol. 92, pp. 1359–1392, 2012.

[63] J. Harris and Y. Timofeeva, "Intercellular calcium waves in the fire-diffuse-fire framework: Green's function for gap-junctional coupling," *Physical Review*, vol. 82, no. 1, p. 051910, 2010.

[64] M. T. Barros, S. Balasubramaniam, B. Jennings, and Y. Koucheryavy, "Transmission protocols for calcium signaling based molecular communications in deformable cellular tissues," *IEEE Transactions on Nanotechnology*, vol. 13, no. 4, pp. 779–788, 2014.

[65] S. Orrenius and P. Nicotera, "The calcium ion and cell death," *Journal of Neural Transmission. Supplementa*, vol. 43, pp. 1–11, 1994.

[66] J. P. Keener and J. Sneyd, *Mathematical Physiology: I: Cellular Physiology (Interdisciplinary Applied Mathematics)*. Springer, 2008.

[67] A. M. Hofer and E. M. Brown, "Extracellular calcium sensing and signalling," *Nature Reviews Molecular Cell Biology*, vol. 4, pp. 530–538, 2003.

[68] S. E. Webb and A. L. Miller, "Calcium signalling during embryonic development," *Nature Reviews Molecular Cell Biology*, vol. 4, pp. 539–551, 2003.

[69] S. Orrenius, B. Zhivotovsky, and P. Nicotera, "Regulation of cell death: the calcium-apoptosis link," *Nature Reviews Molecular Cell Biology*, vol. 4, pp. 522–565, 2003.

[70] D. H. MacLennan and E. G. Kranias, "Phospholamban: a crucial regulator of cardiac contractility," *Nature Reviews Molecular Cell Biology*, vol. 4, pp. 566–577, 2003.

[71] M. J. Berridge, "Elementary and global aspects of calcium signalling," *Journal of Physiology*, vol. 499, pp. 291–306, 1997.

[72] E. Carafoli, "Calcium signaling: a tale for all seasons," *Proceedings of the National Academy of Sciences*, vol. 99, pp. 1115–1122, 2002.

[73] M. J. Berridge, "The am and fm of calcium signalling," *Nature*, vol. 386, pp. 759–760, 1997.

[74] M. J. Berridge, P. Lipp, and M. D. Bootman, "The versatility and universality of calcium signalling," *Nature Reviews Molecular Cell Biology*, vol. 1, pp. 11–21, 2000.

[75] R. W. Tsien and R. Y. Tsien, "Calcium channels, stores, and oscillations," *Annual Review of Cell Biology*, vol. 6, pp. 715–760, 1990.

[76] E. Scemes and C. Giaume, "Astrocytes calcium waves: what they are and what they do," *Glia*, vol. 54, pp. 716–725, 2006.

[77] E. Scemes, S. O. Saudicani, G. Dahl, and D. C. Spray, "Connexin and pannexin mediated cell-cell communication," *Neuron Glia Biology*, vol. 3, pp. 199–208, 2007.

[78] A. C. Charles, S. K. Kodali, and R. F. Tyndale, "Intercellular calcium waves in neurons," *Molecular and Cellular Neuroscience*, vol. 7, no. 5, pp. 337–353, 1996.

[79] K. Motoyama, I. E. Karl, M. W. Flye, D. F. Osborne, and R. S. Hotchkiss, "Effect of Ca2+ agonists in the perfused liver: determination via laser scanning confocal microscopy," *American Journal of Physiology*, vol. 276, pp. R575–R585, 1999.

[80] L. D. Robb-Gaspers and A. P. Thomas, "Coordination of Ca2+ signalling by intercellular propagation of Ca2+ waves in the liver," *The Journal of Biological Chemistry*, vol. 270, pp. 8102–8107, 1995.

[81] P. Gomes, S. P. Srinivas, J. Vereecke, and B. Himpens, "Gap junctional intercellular communication in bovine corneal endothelial cells," *Experimental Eye Research*, vol. 83, no. 5, pp. 1225–1237, 2006.

[82] N. Halidi, F.-X. Boittin, J.-L. Beny, and J.-J. Meister, "Propagation of fast and slow intercellular Ca2+ waves in primary cultured arterial smooth muscle cells," *Cell Regulation*, vol. 50, no. 5, pp. 459–467, 2011.

[83] S. O. Suadicani, M. J. Vink, and D. C. Apray, "Slow intercellular Ca2+ signalling in wild-type and Cx43-null neonatal mouse cardiac myocytes," *American Journal of Physiology - Heart and Circulatory Physiology*, vol. 279, pp. H3076–H3088, 2000.

[84] L. D. Gaspers and A. P. Thomas, "Calcium signaling in liver," *Cell Calcium*, vol. 38, pp. 329–342, 2005.

[85] N. R. Jorgensen, "Short-range intercellular calcium signaling in bone," *Acta Pathologica, Microbiologica et immunologica scandinava - supplementum*, pp. 5–36, 2005.

[86] T. Kono, T. Nishikori, H. Kataoka, Y. Uchio, M. Ochi, and K. Enomoto, "Spontaneous oscillation and mechanically induced calcium waves in chondrocytes," *Cell Biochemistry and Function*, vol. 24, pp. 103–111, 2006.

[87] J. P. Peterdi, "Calcium wave of tubuloglomerular feedback," *American Journal of Physiology - Renal Physiology*, vol. 291, pp. F473–F480, 2006.

[88] K. Enomoto, K. Furuya, S. Yamagishi, and T. Maeno, "Mechanically induced electrical and intracellular calcium responses in normal and cancerous mammary cells," *Cell Calcium*, vol. 13, pp. 501–511, 1992.

[89] Y. Osipchuk and M. Cahalan, "Cell-to-cell spread of calcium signals by atp receptors in mast cells," *Nature*, vol. 359, pp. 241–244, 1992.

[90] D. I. Yule, E. Stuenkel, and J. A. Williams, "Intercellular calcium waves in rat pancreatic acini: mechanisms of coactivation," *American Journal of Physiology - Cell Physiology*, vol. 271, pp. C1285–C1294, 1996.

[91] S. Koizumi, K. Fujisjita, K. Inoue, Y. Shigemoto-Mogami, and M. Tsuda, "Ca2+ waves in keratinocytes are transmitted to sensory neurons: the involvement of extracelllular ATP and P2Y2 receptor activation," *Biochemistry Journal*, vol. 380, pp. 329–338, 2004.

[92] T. Masselter and T. Speck, "Quantitative and qualitative changes in primary and secondary stem organization of aristolochia macrophylla during ontogeny: functional growth analysis and experiments," *Journal of Experimental Botany*, vol. 59, no. 11, pp. 2955–2967, 2008.

[93] N. M. Kumar and N. B. Gilula, "The gap junction commmunication channel," *Cell*, vol. 84, pp. 381–388, 1997.

[94] W. R. Loewenstein, "Junctional intercellular communication: the cell-to-cell membrane channel," *Physiology Review*, vol. 61, pp. 829–913, 1981.

[95] P. P. Mehta, A. Hotz-Wagenblatt, B. Rose, D. Showlloway, and W. R. Loewenstein, "Incorporation of the gene for a cell-cell channel protein into transformed cells leads to normalization of growth.," *Journal of Physical Chemistry*, vol. 124, pp. 207–225, 1991.

[96] T. Nakano, T. Suda, M. Moore, R. Egashira, A. Enomoto, and K. Arima, "Molecular communication for nanomachines using intercellular calcium signaling," in *5th IEEE Conference on Nanotechnology*, 2005.

[97] T. Nakano, T. Suda, T. Koujin, T. Karaguchi, and Y. Hiraoka, "Molecular communication through gap junction channels: System, design, experiment, and modelling," in *Proc. 2nd International Conference on Bio-Inspired Models of Network, Information and Computing Systems (BIONETICS 2007)*, pp. 139–146, 2007.

[98] F. Walsh, N. T. Boyle, A. Mardinoglu, A. D. Chiesa, D. Botvich, A. Prina-Mello, and S. Balasubramaniam, "Artificial backbone neuronal network for nano scale sensors," in *IEEE Conference on Computer Communications Workshops*, 2011.

[99] S. Balasubramaniam, N. T. Boyle, A. Della-Chiesa, F. Walsh, A. Mardinoglu, D. Botvich, and A. Prina-Mello, "Development of artificial neuronal networks for molecular communication," *Nano Communication Networks*, vol. 2, pp. 150–160, 2011.

[100] A. S. Cacciapuoti, M. Caleffi, and A. Piras, "Neuronal communication: Presynaptic terminals as transmitter array," in *Proceedings of the Second Annual International Conference on Nanoscale Computing and Communication*, NANOCOM' 15, pp. 12:1–12:5, 2015.

[101] H. Ramezani and O. B. Akan, "Synaptic channel model including effects of spike width variation," in *Proceedings of the Second Annual International Conference on Nanoscale Computing and Communication*, NANOCOM' 15, pp. 11:1–11:6, 2015.

[102] F. Mesiti, M. Veletć, P. A. Floor, and I. Balasingham, "Astrocyte-neuron communication as cascate of equivalent circuits," *Nano Communication Networks*, 2015.

[103] A. Araque and M. Navarrete, "Glial cells in neuronal network function," *Philosophical Transactions of the royal society*, vol. 365, no. 1551, pp. 2375–2381, 2010.

[104] D. Kilinc and O. B. Akan, "An information theoretical analysis of nanoscale molecular gap junction communication channel between cardiomyocytes," *IEEE Transactions on Nanotechnology*, vol. 12, pp. 129–136, March 2013.

[105] T.-C. Shih, J.-H. Chen, D. Liu, K. Nie, L. Sun, M. Lin, D. Chang, O. Nalcioglu, , and M.-Y. Su, "Computational simulation of breast compression based on segmented breast and fibroglandular tissues on magnetic resonance images," *Physics in medicine and biology*, vol. 55, no. 14, pp. 4153–4168, 2010.

[106] Y. Zhu and R. Sivakumar, "Challenges: Communication through silence in wireless sensor networks," in *ACM International Conference on Mobile Computing and Networking (MOBICOM)*, 2005.

[107] R. Gomez-Martinez, A. M. Hernandez-Pinto, M. Duch, P. Vazquez, K. Zinoviev, E. J. de la Rosa, J. Esteve, T. Suarez, and J. A. Plaza, "Silicon chips detect intracellular pressure changes in living cells," *Nature Nanotechnology*, vol. 8, pp. 517–521, 2013.

[108] B. Mason, J. Califano, and C. Reinhart-King, "Matrix stiffness: A regulator of cellular behavior and tissue formation," in *Engineering Biomaterials for Regenerative Medicine* (S. K. Bhatia, ed.), pp. 19–37, Springer New York, 2012.

[109] R. Skalak and C. F. Fox, *Tissue Engineering*. Alan R. Liss, 1988.

[110] R. Langer and J. P. Vacanti, "Tissue engineering," *Science*, vol. 260, no. 5110, pp. 920–926, 1998.

[111] BBC, "Tissue engineering: Grow your own smart organs."

[112] B. D. Unluturk, A. O. Bicen, and I. F. Akyildiz, "Genetically engineered bacteria-based biotransceivers for molecular communication," *IEEE Transactions on Communications*, vol. 63, pp. 1271–1281, April 2015.

[113] G. Modi, V. Pillay, and Y. E. Choonara, "Advances in the treatment of neurodegenerative disorders employing nanotechnology," *Annals of the New York Academy of Sciences*, vol. 1184, pp. 154–172, 2010.